UNIVERSITÀ DI PISA

Scuola di Dottorato in Ingegneria "Leonardo da Vinci"

Corso di Dottorato di Ricerca in
Ingegneria dell'Informazione

Tesi di Dottorato di Ricerca

Distributed Power Control Techniques Based on Game Theory for Wideband Wireless Networks

Autore:

Giacomo Bacci _____

Relatore:

Prof. Marco Luise _____

Anno 2008

Manuscript received February 29, 2008

Accepted March 11, 2008

Sommario

In questa tesi, viene effettuata un'analisi teorica destinata allo sviluppo di algoritmi distribuiti (decentralizzati) per il controllo di potenza, progettati per reti wireless ad elevato throughput che utilizzano la tecnologia ultrawideband (UWB). In questo contesto, viene fatto uso della teoria dei giochi, la quale si rivela particolarmente utile per derivare tecniche di controllo di potenza che siano distribuite, scalabili ed efficienti dal punto di vista energetico, e pertanto particolarmente indicate per terminali mobili operanti in uno scenario multipath. Più nel dettaglio, il problema del controllo di potenza è modellato come un gioco noncooperativo, nel quale ciascun utente decide il livello di potenza in trasmissione in modo da massimizzare la sua utilità, definita come il rapporto tra throughput e potenza trasmessa. Sebbene sia noto che uno schema di controllo distribuito (noncooperativo) sia subottimo nei confronti di una soluzione centralizzata (cooperativa), mediante un'analisi di tipo large-system viene evidenziato che la degradazione dell'algoritmo basato sull'equilibrio di Nash risulta trascurabile rispetto allo schema centralizzato. Il modello teorico sviluppato in questa tesi è in grado di analizzare le prestazioni di altri sistemi wireless a larga banda, tra cui le reti che fanno uso dell'accesso multiplo a suddivisione di codice (code division multiple access, CDMA). In particolare, è possibile dimostrare che la tecnologia UWB fornisce prestazioni leggermente superiori rispetto al CDMA in termini di utilità all'equilibrio di Nash.

Abstract

This thesis describes a theoretical framework for the design and the analysis of distributed (decentralized) power control algorithms for high-throughput wireless networks using ultrawideband (UWB) technologies. The tools of game theory are shown to be expedient for deriving scalable, energy-efficient, distributed power control schemes to be applied to a population of battery-operated user terminals in a rich multipath environment. In particular, the power control issue is modeled as a noncooperative game in which each user chooses its transmit power so as to maximize its own utility, which is defined as the ratio of throughput to transmit power. Although distributed (noncooperative) control is known to be suboptimal with respect to the optimal centralized (cooperative) solution, it is shown via large-system analysis that the game-theoretic distributed algorithm based on Nash equilibrium exhibits negligible performance degradation with respect to the centralized socially optimal configuration. The framework described here is general enough to also encompass the analysis of code division multiple access (CDMA) systems and to show that UWB slightly outperforms CDMA in terms of achieved utility at the Nash equilibrium.

Acknowledgments

I am deeply grateful to my advisor, Prof. Marco Luise, for his valuable encouragement, support, and experience. I began cooperating with Marco Luise when I wrote my B.E. thesis, and since then it has been a real honor to keep working under his guidance and exploiting his enthusiasm.

I would like to thank all my colleagues at the DSP Communication Lab for their precious help and the pleasant atmosphere they created. I am particularly indebted to Dr. Fabio Principe, Francesca Zanier, Marilena Maiolo, Antonio D. Fittipaldi and Gabriele Boccolini, not just in terms of technical support, but also because they became good friends of mine through these years. I want to thank Dr. Luca Giugno, Dr. Cosimo Saccomando and Marco Della Maggiora, who welcomed me in the lab in the early days of my Ph.D. program, and Pamela Cologna, for her valuable support. I am also grateful to all the B.E. and M.E. students I supervised in these years, for their cooperative spirit and their precious comments.

A considerable part of this thesis has been developed during my stay at Princeton University, Dept. Electrical Engineering. I am sincerely indebted to Prof. H. Vincent Poor, who gave me the opportunity of living this great experience and helped me with his outstanding guidance and encouragement. Working with Vince Poor and learning from him has been a true privilege. I want also to thank Prof. Antonia M. Tulino, who gave me better understanding of some crucial aspects of this thesis.

I am very grateful to all my colleagues in the ISS group at Princeton, not only for their professional support, but also for the kind hospitality they offered. I would like to thank Sharon M. Betz, whose comments and suggestions both clarified and strengthened may points of my work. Moreover, Sharon's potluck dinners were occasions for me to get closer to all my officemates and their families: Yury Polyanskiy and his wife Olga, Dr. Olympia Hadjiliadis and her husband Iannis, Dr. Simon Pun, Dr. Siu Wai Ho, Jiaping Liu, Dr. Hai Jiang and Dr. Yingbin Liang.

I am also really thankful to the Italian "community" in Princeton for spending many enjoyable nights together and making me feel closer to home. In particular, I would like to thank Francesco Cellarosi and his wife Elisa, Alfonso Sorrentino, Lorenzo Sironi, Adriano Basso and Gabriele Neretti. I am particularly grateful to Jason C. Pedicone and his family and to Kent Gordon and his family, who accepted me as a close friend and shared with me special moments such as Thanksgiving and Christmas during my stay in the United States.

Most importantly of all, I would like to thank my mum Marisa, my dad Stefano, my sister Alice and my grandparents for supporting me every day of my life. It is through their encouragement and their love that I could have reached this point in life. Finally, my most heartfelt gratitude goes to Valentina, who always lovingly supported me and enriched both my life and my dreams.

Pisa, April 2008 Giacomo Bacci

Contents

List of Figures

List of Tables

List of Acronyms

ACM	adaptive coding and modulation
AP	access point
aPDP	averaged power delay profile
ARake	all-Rake
a.s.	almost surely
AWGN	additive white Gaussian noise
BER	bit error rate
BPSK	binary phase-shift keying
BRPC	best-response power-control
CDMA	code division multiple access
DS	direct sequence
DSL	digital subscriber line
ECC	Electronic Communications Committee
EIRP	equivalent isotropically radiated power
FCC	Federal Communications Commission
GPS	global positioning system
i.i.d.	independent and identically distributed
IR	impulse radio
MAC	medium access control
MAI	multiple access interference
MC	multi-carrier
MF	matched filter
MIMO	multiple input multiple output

MMSE	minimum mean square error
MRC	maximal ratio combining
MUD	multiuser detector
NPCG	noncooperative power control game
NE	Nash equilibrium
nmse	normalized mean square error
NP	nondeterministic polynomial-time
OSI	open systems interconnection
PPM	pulse position modulation
PRake	partial-Rake
PSD	power spectral density
PSR	packet success rate
QoS	quality of service
RCDMA	random code division multiple access
RRM	radio resource management
RV	random variable
SC	single-carrier
SI	self-interference
SINR	signal-to-interference-plus-noise ratio
SNR	signal-to-noise ratio
SO	social optimum
SP	signal part
SS	spread spectrum
SSIR	signal-to-self-interference ratio
SU	single user
TH	time hopping
USB	universal serial bus
UWB	ultrawideband
WPAN	wireless personal area network

List of Symbols and Operators

cross product	$\times$
Hadamard (element-wise) product	$\circ$
floor function (rounding downward)	$\lfloor \cdot \rfloor$
absolute value	$\lvert \cdot \rvert$
vector norm	$\lvert\lvert \cdot \rvert\rvert$
conjugate transposition	$(\cdot)^H$
transposition	$(\cdot)^T$
pure strategy of player k	$a_k \in \mathcal{A}_k$
pure strategy of player k at the Nash equilibrium	$a_k^* \in \mathcal{A}_k$
Pareto-optimal pure-strategy of player k	$\tilde{a}_k \in \mathcal{A}_k$
pure-strategy profile	$\mathbf{a} = [a_1, \ldots, a_K]$
pure-strategy profile at the Nash equilibrium	$\mathbf{a}^* = [a_1^*, \ldots, a_K^*]$
Pareto-optimal pure-strategy profile	$\tilde{\mathbf{a}} = [\tilde{a}_1, \ldots, \tilde{a}_K]$
matrix of fading coefficient of user k	$\mathbf{A}_k$
pure-strategy space of player k	$\mathcal{A}_k$
joint set of pure-strategy spaces	$\boldsymbol{\mathcal{A}} = \times_k \mathcal{A}_k$
information symbol transmitted by user k	$b_\ell^{(k)}$
matrix of combining weights of the Rake receiver for user k	$\mathbf{B}_k$
nth TH chip of user k	$c_n^{(k)}$
TH sequence of user k	$\mathbf{c}_k = \{c_1^{(k)}, \cdots, c_{N_f}^{(k)}\}$

matrix for large-system analysis of the path coefficients of the kth user	$\mathbf{C}_k^{\alpha}$
matrix for large-system analysis of the combining weights of the kth Rake receiver	$\mathbf{C}_k^{\beta}$
circularly symmetric complex Gaussian RV	$\mathcal{CN}$
distance between user k and the AP	d_k
nth polarity chip of user k	$d_n^{(k)}$
polarity code of user k	$\mathbf{d}_k = \{d_0^{(k)}, \cdots, d_{N_f-1}^{(k)}\}$
number of information bits in a packet	D
diagonal matrix for the standard deviation of path coefficients of the kth user	$\mathbf{D}_k^{\alpha}$
diagonal matrix for the standard deviation of combining weight of the kth Rake receiver	$\mathbf{D}_k^{\beta}$
expectation of a random variable X	$\mathbb{E}[X]$
efficiency function of user k	$f(\gamma_k)$
PSR of user k	$f_s(\gamma_k)$
processing matrix of the Rake receiver	$\mathbf{G}$
game	$\mathcal{G}$
proper subgame of a game $\mathcal{G}$	$\mathcal{G}'$
channel gain of user k	h_k
term due to the MAI of user j for user k	$h_{kj}^{(\mathrm{MAI})}$
term due to the SI for user k	$h_k^{(\mathrm{SI})}$
term due to the SP for user k	$h_k^{(\mathrm{SP})}$
player k's opponents	$\backslash k$
number of players	K
set of players	$\mathcal{K}$
number of channel paths	L
number of fingers of the Rake receiver	L_P
number of total bits in a packet	M
nmse of estimated achieved utility of user k at the Nash equilibrium	$\mathrm{nmse}(u_k^*)$

set of natural numbers	$\mathbb{N}$
spreading factor (processing gain)	$N = N_c \cdot N_f$
number of slots per UWB frame	N_c
number of UWB frames per bit period	N_f
transmit power of terminal k	$p_k \in \mathcal{P}_k$
transmit power of terminal k at step m of the BRPC algorithm	$p_k^{(m)}$
minimum allowable transmit power of user k	$\underline{p}_k$
maximum allowable transmit power of user k	$\overline{p}_k$
transmit power of terminal k at the Nash equilibrium	p_k^*
transmit power of terminal k at the Nash equilibrium using an ARake receiver	$p_{k_A}^*$
transmit power of terminal k at the social optimum	$\tilde{p}_k$
vector of transmit powers	$\mathbf{p} = [p_1, \ldots, p_K]$
vector of transmit powers at step m of the BRPC algorithm	$\mathbf{p}^{(m)}$
vector of transmit powers at the Nash equilibrium	$\mathbf{p}^* = [p_1^*, \ldots, p_K^*]$
probability of having at least one user transmitting at the maximum power	P_o
transmit power set of user k	$\mathcal{P}_k$
joint set of transmit power s	$\boldsymbol{\mathcal{P}} = \times_k \mathcal{P}_k$
product of the transmit power times the SP term at the Nash equilibrium	q
complementary cumulative distribution function of a standard normal RV	$Q(\cdot)$
ratio of the number of Rake fingers to the number of channel paths	$r = L_P/L$
best response to an opponents' profile $\mathbf{a}_{\setminus k}$	$r_k\left(\mathbf{a}_{\setminus k}\right)$
vector of best responses	$\mathbf{r}(\mathbf{p}) = [r_1(\mathbf{p}), \ldots, r_K(\mathbf{p})]$
set of real numbers	$\mathbb{R}$

transmission rate of user k	R_k
transmitted signal from user k	$s_{tx}^{(k)}(t)$
nth chip of the spreading sequence of user k	$s_n^{(k)}$
spreading sequence of user k	$\mathbf{s}^{(k)}$
amount of information delivered by user k	t_k
throughput of user k	T_k
bit period	$T_b = N_f \cdot T_f$
UWB pulse duration	T_c
period of a UWB frame	T_f
trace operator	$\mathrm{Tr}(\cdot)$
step function	$u[\cdot]$
utility of player k	$u_k(\mathbf{a})$
utility of terminal k at the Nash equilibrium	u_k^*
utility of terminal k at the Nash equilibrium in a CDMA-based network	$u_{k_C}^*$
utility of terminal k at the Nash equilibrium in a UWB-based network	$u_{k_U}^*$
utility of terminal k at the Nash equilibrium using an ARake receiver	$u_{k_A}^*$
variance of a random variable X	$\mathbb{V}\mathrm{ar}[X]$
unit-energy UWB pulse (monocycle)	$w_{tx}(t)$
unit-variance vector of fading coefficients of user k	$\mathbf{w}^{(k)}$
transmitting cost of user k	z_k
fading coefficient of the lth path of user k	$\alpha_l^{(k)}$
vector of fading coefficient of user k	$\boldsymbol{\alpha}_k = [\alpha_1^{(k)}, \ldots, \alpha_L^{(k)}]^T$
weight of the lth finger of the Rake receiver for user k	$\beta_l^{(k)}$
vector of combining weights of the Rake receiver for user k	$\boldsymbol{\beta}_k = [\beta_1^{(k)}, \ldots, \beta_L^{(k)}]^T$
SSIR of user k	$\gamma_{0,k} = h_k^{(\mathrm{SP})}/h_k^{(\mathrm{SI})}$
SINR of user k	γ_k

SINR of user k at step m of the BRPC algorithm	$\gamma_k^{(m)}$
SINR of user k at the Nash equilibrium	γ_k^*
SINR of user k at the Nash equilibrium in the flat-fading scenario	$\overline{\gamma}^* = \Gamma(\infty)$
dependency of the SINR at the Nash equilibrium γ_k^* on the SSIR $\gamma_{0,k}$	$\Gamma(\gamma_{0,k})$
Dirac's delta function	$\delta(t)$
random variable to model τ_k	Δ_k
difference between $\nu_0(\Lambda, r)$ and $\nu(\Lambda, r, \rho)$	$\Delta\nu(\Lambda, r, \rho)$
ratio of the MAI terms to the SP terms for user k	ζ_k
mean value of the quantity q	η_q
random variable for large-system analysis of the SI term	$\theta_k(l, i)$
weight of the kth utility for the social-optimum solution	λ_k
aPDP decay constant	Λ
large-system analysis term proportional to MAI for a PRake receiver	$\mu(\Lambda, r)$
large-system analysis term proportional to MAI for an ARake receiver	$\mu_A(\Lambda)$
large-system analysis term proportional to SI for a PRake receiver	$\nu(\Lambda, r, \rho)$
large-system analysis term proportional to SI for a PRake receiver in a CDMA-based network	$\nu_0(\Lambda, r)$
large-system analysis term proportional to SI for an ARake receiver	$\nu_A(\Lambda, \rho)$
mixed strategy of player k	$\xi_k \in \Xi_k$
mixed-strategy space of player k	Ξ_k
joint set of mixed-strategy spaces	$\boldsymbol{\Xi} = \times_k \Xi_k$
channel response experienced by user k	$\pi_k(t)$
load factor of the network	$\rho = N_c/L$

output variance of the ambient AWGN	σ^2
variance of the first fading coefficient of user k	$\sigma_k^2 = \sigma_{k_1}^2$
variance of the lth fading coefficient of user k	$\sigma_{k_l}^2$
variance of the quantity q	σ_q^2
propagation delay of user k	τ_k
coefficient for $h_k^{(\mathrm{SI})}$	ϕ_l
matrix operator for the large-system analysis of the Nash equilibrium	$\varphi(\cdot)$
matrix of coefficients for $h_k^{(\mathrm{SI})}$	$\mathbf{\Phi}$
random variable for large-system analysis of MAI terms	χ_l
performance loss of a PRake receiver with respect to an ARake receiver	Ψ
performance loss of a CDMA network with respect to a UWB network (linear scale)	ω
performance loss of a CDMA network with respect to a UWB network (logarithmic scale)	Ω

Introduction

Motivations

Since the early days of wireless communications, the importance of radio resource management (RRM) has emerged as a key issue in network design. A typical example of RRM is represented by *power control*, whose principal purpose is to provide each signal in the network with adequate quality without causing unnecessary interference to other users in the system. Cochannel interference, which is due to the shared nature of the wireless medium, represents in fact a major impairment to the performance of wireless communications.

The first schemes that aim to achieve this goal in the field of spread spectrum (SS) satellite communications were the signal-to-interference-plus-noise ratio (SINR)-balancing algorithms (also called power balancing algorithms), proposed in the early 1970s by Aein [1] and Meyerhoff [86]. Until mid-1990s, power control techniques were primarily focused on voice communications systems [2, 58, 94, 95, 139, 140]. In this context, distributed schemes such as the one proposed by Foschini and Miljanic [46], have proved to achieve excellent performance. For this kind of applications, SINR-balancing schemes are in fact particularly suitable, since voice users are usually indifferent to small changes in their SINRs. In other words, the level of satisfaction perceived by each user shows a simple, threshold-like zero-one relationship with the level of SINR measured at the receiver. Hence, the optimum power control scheme for wireless telephone networks is the algorithm that maximizes the number of conversations that can simultaneously achieve a certain quality of service (QoS) target.

With the advent of the third-generation cellular networks, high-speed data services have become available to the mobile population and the spectacular success of wireless data applications in the last few years has produced an ever-increasing demand for reliable high-speed data services. These market drivers have generated a number of

new technologies that provide multiple access capability and possibly interference mitigation. Ultrawideband (UWB) communication has emerged as a possible solution for next-generation short-range high-speed data transmission, due to its large spreading factor (which implies large multiuser capacity) and low power spectral density (which allows coexistence with incumbent systems in the same frequency bands).

The main difference with respect to conventional narrowband or wideband networks thoroughly studied in the literature is represented by the frequency selectivity of the wireless channel, which is due to the extremely high temporal resolution of the transmitted signals. This motivates us to study the effect of such frequency selectivity when applying power control schemes to UWB-based networks.

Unlike voice applications, data communications are intolerant of errors and require a larger SINR. Higher SINRs lead to a lesser number of retransmissions, which translates into a larger amount of information correctly delivered at the receiver. As a consequence, the level of satisfaction achieved by each user is a continuous function of the SINR [55]. Throughout this thesis, we focus on *energy efficient* criteria for power control, which aim at maximizing the number of transmitted bits per energy unit rather than the pure maximization of the throughput of the link. This is mainly due to the presence of battery-powered mobile terminals in the network, which calls for careful management of the energy consumption. This goal can be achieved through application of a *noncooperative game* wherein the users are allowed to choose their transmit powers according to a utility-maximization criterion, where the *utility* is defined as the ratio of throughput to transmit power.

Recently, *game theory* has been used as an effective tool to study distributed power control in data networks. An important feature of the game-theoretic approach is the inherent decentralization of the algorithms for power control, which allows each user to individually choose its own transmit power through a simple noncooperative scheme. Distributed (noncooperative) solutions are in general suboptimal with respect to those obtained via a centralized (cooperative) approach, but they are particularly well suited to a largely populated network due to their intrinsic *scalability*. The centralized approach is often characterized by NP-hard problems, whose solutions cannot be reasonably computed (or even approximated) in real-time.

The prominent characteristic of the game-theoretic approach, which justifies its widespread range of applications, is its capability of distributing decision-making processes among "rational" users [77], once benefits and drawbacks of the actions

they are allowed to choose are quantified. Even though game theory was originally developed to predict the outcome of interactions among economic agents, it is apparent that this framework also fits the situation of resource competition in wireless networks.

There is a substantial literature on power control techniques based on noncooperative game theory, mostly focused on code division multiple access (CDMA) wireless communication networks [5, 36, 55, 71, 85, 110, 122, 134]. In this thesis, we will address the problem of game-theoretic power control for wideband wireless communication systems operating in a frequency selective scenario, which include both UWB-based and CDMA-based networks.

Main contributions

This thesis is focused on the application of noncooperative game theory to power control in the uplink of (ultra)wideband infrastructure wireless communication networks. Due to the large bandwidths of the transmitted signals, the channel fading is assumed to be frequency selective, and a set of Rake receivers at the access point is employed. By posing the energy efficiency of the power control algorithm as the key requirement of the system, we devise a game-theoretic model for the distributed power control scheme. This analysis is general enough to also encompass the study of CDMA systems.

In this context, the contributions of this thesis are as follows:

- the derived framework extends the results available in the literature for energy-efficient approaches in flat-fading scenarios;
- the existence and the uniqueness of the solution of the noncooperative power control game (the Nash equilibrium) are proved by means of the analytical tools of game theory and distributed control theory;
- an iterative and distributed algorithm for reaching the Nash solution of the power control scheme is derived, and its convergence is studied theoretically and validated by numerical examples;
- the effects of self-interference and multiple-access interference are characterized in terms of the relevant parameters of the network through a large-system

analysis; the results are derived for a general channel model, which includes both large- and small-scale statistics, and are independent of the single channel realizations;

- system design criteria, such as the minimum spreading factor of the network and the performance loss of partial-Rake receivers with respect to all-Rake receivers, are proposed;
- the performance of the distributed solution (the Nash equilibrium) is compared with the centralized (social-optimal) solution, showing that the difference between these two approaches is not significant for typical networks;
- the performance of UWB-based networks is compared to CDMA-based networks, showing that UWB slightly outperforms CDMA in terms of achieved utility at the Nash equilibrium.

Outline

The remainder of this thesis is structured as follows.

In Chapter 1, we introduce the fundamental tools of noncooperative game theory. In particular, we outline the basic concepts of static and dynamic games. We then provide motivating examples for the application of noncooperative game theory to power control problems, and we review the literature on game-theoretic power control in wireless networks.

In Chapter 2, we describe the system considered throughout the thesis. After a brief introduction of UWB technology, we present the analytical models for transmitter side, wireless channel and receiver side, respectively. We then discuss the relevant features of the described system and we identify why effective power control techniques are particularly desirable in this scenario.

In Chapter 3, we formally introduce the power control problem for UWB-based wireless networks as a noncooperative game. After discussing the main advantages of distributed solutions, we formulate the power control scheme using an energy-efficient approach. We then study the existence and the uniqueness of the Nash equilibrium of the proposed game, and we describe an iterative algorithm to reach the Nash solution in a distributed fashion.

In Chapter 4, we identify the main properties of the Nash solution of the power control game. To derive explicit expressions for the relevant quantities of the system, namely transmit powers and achieved utilities, we propose a large-system analysis of the network. This framework allows us to obtain a theoretical description of both the self-interference and the multiple-access interference, which are independent of the particular channel realization. Using these asymptotical values, we measure the performance indexes and we derive some system design criteria. We also show the results of extensive simulations that validate the proposed analysis.

In Chapter 5, we compare the distributed (noncooperative) solution (the Nash equilibrium) with the centralized (cooperative) solution (the social optimum) in terms of achieved utilities. Using the large-system analysis developed in Chapter 4, we measure the performance loss of the distributed approach. We then compare this theoretical analysis with the numerical results, and we draw some conclusions about advantages and flaws of the noncooperative solution.

In Chapter 6, we adapt the game-theoretic framework described in the previous chapters to the case of a wideband wireless network using CDMA as the multiple access technique. We then perform a comparison between UWB-based and CDMA-based networks. Performance of the two access methods is evaluated in both the frequency-selective and in the flat-fading scenario. By means of both theoretical and numerical results, we show that the UWB technology slightly outperforms CDMA in terms of achieved utilities.

In Chapter 7, we draw some conclusions for this thesis and we discuss open issues and further perspectives for this research field.

Chapter 1

Basics of noncooperative game theory

Game theory is a broad field of applied mathematics aimed at describing and analyzing interactive decision processes. In particular, it provides the analytical tools to predict the outcome of complex interactions among rational entities, where rationality calls for strict adherence to a strategy based on perceived or measured results [98]. Economists have long used game theory as a framework for examining the actions of economic agents such as firms in a market. In recent years, it has been extensively used to address many optimization problems in the field of communication engineering and computer science.

This chapter contains an introduction to the fundamental tools of noncooperative game theory. After a brief chronology of game theory, given in Sect. 1.1, the basic concepts of static and dynamic games are outlined in Sects. 1.2 and 1.3, respectively. Finally, Sect. 1.4 provides a survey of the relevant applications of noncooperative game theory to the problem of power control in wireless network.

1.1 Historical notes

The first studies of games in the economics literature were the papers by Cournot (1838) [32], Bertrand (1883) [19], and Edgeworth (1897) [35] on oligopoly pricing and production.[1] However, these contributions were seen as special models that

[1] Although these works are commonly acknowledged as the first problems stated in a game-theoretic framework, similar approaches in the context of card games can be found in the 18th

did little to change the way economists thought about most problems. The idea of a general theory of games can be dated to 1928, when von Neumann set forth the basis for this discipline as a unique field [128], and culminated in 1944, when von Neumann and Morgenstern published their famous book *"Theory of Games and Economic Behavior"* [129], which proposed that most economic questions should be analyzed as games.

Noncooperative game theory is a branch of game theory which studies interactions among agents that are not able to form binding commitments. Hence, it analyzes the behavior of agents in any situation in which each agent's optimal choice may depend on his/her forecast of the choices of his/her opponents. Before 1950, limitations in the mathematical framework of noncooperative game theory made it applicable only under special and limited conditions.[2] In this period, the research was primarily focused on *cooperative* game theory, which analyzes optimal strategies for groups of individuals, assuming that they can enforce agreements among themselves.

Seminal contributions to both cooperative and noncooperative game theory were given in 1950-53 by Nash [90–93]. In the context of noncooperative game theory, in 1950 Nash proposed what came to be known as the *Nash equilibrium* as a way of extending game theory analyses to non-zero-sum games [91]. The Nash equilibrium requires that each player's strategy in the game be a payoff-maximizing response to the strategy that he/she forecasts that his/her opponents will use, and further that each player's forecast be correct. This is a natural generalization of the equilibria studied in specific models by Cournot and Bertrand, and it is the starting point for most economic analyses.

Since then, game theory has been a subject of considerable study, so that several concepts were deeply studied and understood. Among the others, Selten (1965) [113] and Harsanyi (1967-68) [61] introduced concepts that have been widely used in recent years. Selten argued that in games where the player choose contingent plans, not all the Nash equilibria are equally reasonable, because some of them may rely on the ability of players to make contingent plans that would not in fact be optimal

century [18]. Oddly enough, Aumann and Maschler showed that a recommendation given by the Babylonian Talmud (0-500 A.D.) anticipates some of the results of modern game theory [9].

[2] In [129], von Neumann and Morgenstern showed that a solution (the minmax solution) exists in a special class of strictly noncooperative games, the two-player zero-sum games, in which the interests of the players are directly opposed, with no common interests at all.

to carry out. Selten introduced his concept of subgame perfection to rule out the equilibria that rely on this kind of threats. Harsanyi proposed a way to use standard game-theoretic techniques to model situations where the players are unsure of one another's payoff. His Bayesian Nash equilibrium represents the cornerstone of many game-theoretic analyses.

Traditionally, the main areas of application have been economics, political science, biology, and sociology. Since the early 1990s, engineering and computer science have been added to the list. Recently, game theory has also been widely used in telecommunications and wireless communications [8, 39, 76].

The remainder of this chapter contains a brief description of the main tools to analyze game-theoretic problems. A comprehensive treatment of basic and advanced topics in noncooperative game theory can be found in [48, 53, 98]. For a detailed analysis of cooperative game theory, please refer to [98].

1.2 Static games

In the game-theoretic context, a *game* can be defined as "a description of strategic interaction that includes the constraints on the actions that the players take and the players' interests" [98]. In this scenario, the basic entity is represented by the *player*, who can be thought of as an individual or as a group of individuals making a decision. If the actions taken by each player are chosen *individually*, then the game is referred to as *noncooperative*. Alternatively, if the actions of each *group* of players are chosen *jointly*, then the game is referred to as *cooperative*. As motivated later in the text, throughout this thesis we will focus on noncooperative games only.

The existence of many possible formulations of a game can easily be argued from the general definition provided above. The simpler type of a game is represented by the *static game*, which follows this form: first, the players simultaneously choose their actions; and then, the players receive their own payoffs that depend on the combination of actions just chosen by *all* players.[3] Within the class of such static (or simultaneous-move) games, we restrict attention to games of *complete information*. The concept of complete information implies that each player's *payoff function* (the

[3] Actually, a static game does not imply that the parties necessarily act simultaneously: as better stated in Sect. 1.3, it suffices that each player chooses his/her own action without knowledge of the others' choices.

function that determines the player's payoff from the combination of actions chosen by all the players) is common knowledge between all the players. Games of incomplete information, also called Bayesian games, are not considered in this thesis.

1.2.1 Strategic-form representation

A game in *strategic* (or *normal*) *form* consists of three components:

(1) a set of players;

(2) a set of actions (strategies) available to each player;

(3) the payoff received by each player for each combination of strategies that could be chosen by the players.

In its mathematical formulation, a K-player game can be represented as follows [53]:

Definition 1 *The* strategic-form representation *of a game can be denoted by* $\mathcal{G} = [\mathcal{K}, \{\mathcal{A}_k\}, \{u_k(\mathbf{a})\}]$*, where:*

(1) $\mathcal{K} = \{1, \ldots, K\}$ *is the finite set of players;*

(2) $\mathcal{A}_k$ *is the set of* pure strategies *(actions) available to player* k*; and*

(3) $u_k(\mathbf{a})$ *is the* utility *(payoff) for player* k*.*

The set of pure strategies $\mathcal{A}_k$ (often referred to as player k's *pure-strategy space*) represents the space of all the possible strategies that player k can choose. Based on the nature of the pure-strategy space, two different types of game can be identified:

- *finite games*, i.e., games where the joint set of strategy space $\boldsymbol{\mathcal{A}} = \mathcal{A}_1 \times \ldots \times \mathcal{A}_K$ is finite, or, equivalently, where the number of actions is countable;
- *infinite games*, i.e., games where the number of actions is uncountable.

For the ease of presentation, the examples provided in the following involve finite games. However, as can be seen in the next chapters, the major results of this thesis focus on infinite games.

The strategy chosen by player k can be expressed as $a_k \in \mathcal{A}_k$. When considering a pure-strategy space, there exists a *deterministic* relationship that assigns each player

k a certain strategy a_k. The set of strategies chosen by all players in the game constitutes the *pure-strategy profile* $\mathbf{a} = [a_1, \ldots, a_K]$.

This approach can be extended by resorting to a *mixed strategy* $\xi_k \in \Xi_k$, where Ξ_k is the mixed-strategy space, and ξ_k is a probability distribution over player k's pure strategy. In other words, ξ_k is a probability distribution that assigns a probability $\xi_k(a_k)$ to each action a_k. Note that the set of mixed strategies contains the pure-strategy space, as degenerate probability distributions are included. In fact, a_k can be simply obtained when ξ_k assigns zero probability to all actions but a_k. As can be better seen in the next chapters, this thesis is primarily focused on pure-strategy games. As a consequence, mixed strategies are not discussed in the remainder of this section. However, it should be noted that mixed strategies play a key role in all game-theoretic aspects, as will be clearly stated in Sect. 1.2.2. For a detailed discussion, please refer to [48, 98].

The utility achieved by each player is a function that measures his/her level of satisfaction. Clearly, the utility $u_k(\mathbf{a})$ achieved by player k depends not only on his/her own strategy a_k, but also on the actual strategies chosen by all the other players, referred to as player k's *opponents*[4] and denoted by $\backslash k \triangleq \mathcal{K} \setminus \{k\}$. As a consequence, $u_k(\mathbf{a})$ depends on the pure-strategy profile $\mathbf{a}$, whose definition can also be restated as $\mathbf{a} = \left[a_k, \mathbf{a}_{\backslash k}\right]$, where obviously $\mathbf{a}_{\backslash k} \triangleq [a_1, \ldots, a_{k-1}, a_{k+1}, \ldots, a_K] \in \mathcal{A}_{\backslash k}$. Hence, player k's utility is $u_k(\mathbf{a}) = u_k\left(a_k, \mathbf{a}_{\backslash k}\right)$.[5]

Definition 2 *A game with* complete information *is a game in which each player knows the game* $\mathcal{G} = [\mathcal{K}, \{\mathcal{A}_k\}, \{u_k(\mathbf{a})\}]$*, notably the set of players* $\mathcal{K}$*, the set of strategies* $\{\mathcal{A}_k\}$ *of each player, and the payoff functions* $\{u_k(\mathbf{a})\}$ *of each player.*

To illustrate the concepts above introduced, it is worth resorting to a classic two-player example, which goes by the name of *Prisoner's dilemma*. The Prisoner's dilemma was originally framed by M. Flood and M. Dresher at RAND Corporation in 1950. The story that currently accompanies the game, along with its name, was

[4] To avoid misunderstanding, it is worth emphasizing that this terminology does not mean that the other players are trying to "beat" player k. Rather, each player's objective is to maximize his/her own payoff function, and this may involve "helping" or "hurting" the other players.

[5] In the case of mixed strategies, player's k payoff is a polynomial function of the mixed strategies of all players in the game [48].

originally formalized by A. W. Tucker, who wanted to make Flood and Dresher's idea more accessible to an audience of Stanford psychologists, as follows [126]:

> "Two men, charged with a joint violation of law, are held separately by the police. Each is told that
>
> (1) if one confesses and the other does not, the former will be given a reward of one unit and the latter will be fined two units,
>
> (2) if both confess, each will be fined one unit.
>
> At the same time each has good reason to believe that
>
> (3) if neither confesses, both will go clear."

In this game, the number of players (the prisoners) is $K = 2$, and thus $\mathcal{K} = \{1, 2\}$. For both players, the (finite) set of allowed strategies (which implies that the Prisoner's dilemma is a finite game) is represented by the space $\mathcal{A}_1 = \mathcal{A}_2 = \{\text{confess}, \text{not confess}\}$. The Prisoner's dilemma, as well as all strategic-form games, can conveniently be studied using the *payoff matrix* presented in Fig. 1.1. Prisoner 1's actions are identified by the rows and prisoner 2's by the columns. The pair of numbers in the box represents the utility $(u_1(a_1, a_2), u_2(a_1, a_2))$ achieved by the players. As an example, if prisoner 1 chooses not to confess and prisoner 2 chooses to confess, then prisoner 1 receives a payoff of -2 (representing a fine of two units) and prisoner 2 receives the payoff $+1$ (representing a reward of one unit).

1.2.2 Nash equilibrium

As stated in Sect. 1.2, a game describes the constraints on the players' actions and interests, but does not specify the actions that the players *do* take [98]. Once the game is expressed in its strategic form, it is interesting to *solve* it. Solving a game means predicting the strategy each player will choose. To predict the outcome of a static game, it is fundamental to assume that:

i) the game is of complete information, i.e., all players know the structure of the strategic form, and know that their opponents know it, and know that their opponents know that they know, and so on ad infinitum;

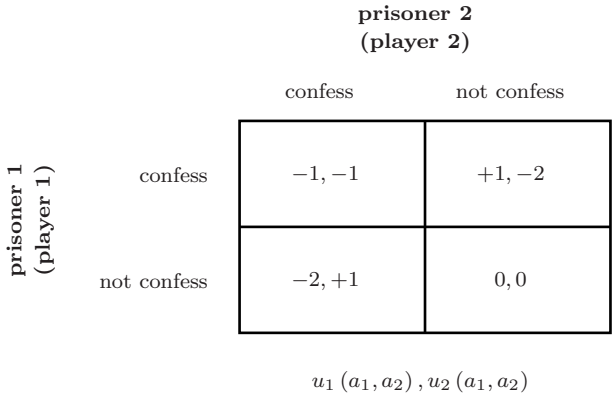

Figure 1.1: *Payoff matrix for the Prisoner's dilemma.*

ii) all players are *rational*, i.e., they are aware of their alternatives, form expectations about any unknowns, have clear preferences, and choose their action deliberately after some process of optimization.

The rational behavior reflects in the fact that a rational player will not play a strictly dominated strategy, defined as follows:

Definition 3 *In the strategic-form game* $\mathcal{G} = [\mathcal{K}, \{\mathcal{A}_k\}, \{u_k(\mathbf{a})\}]$*, a strategy* a_k'' *is* strictly dominated *by strategy* a_k' *if*

$$u_k\left(a_k'', \mathbf{a}_{\setminus k}\right) < u_k\left(a_k', \mathbf{a}_{\setminus k}\right), \quad \forall \mathbf{a}_{\setminus k} \in \mathcal{A}_{\setminus k}. \tag{1.1}$$

It is straightforward to understand that a rational player does not choose a strictly dominated strategy, since the payoff achieved by playing it is always lower than that provided by another action irrespective of the opponents' strategies. Coming back to the Prisoner's dilemma in Fig. 1.1, if one prisoner is going to confess, then the other would prefer to confess and so to receive a fine of one unit, rather than not to confess and so to receive a fine of two units ($-2 < -1$). Similarly, if one prisoner is going not to confess, then the other would prefer to confess and get a reward of one unit, rather than not to confess and go clear ($0 < 1$). Thus, for prisoner k, playing "not confess" is dominated by playing "confess" — for each strategy that the other prisoner could choose, the payoff of prisoner k from not confessing is less than the payoff from

confessing. As a consequence, in the Prisoner's dilemma a rational player will choose "confess", so (confess, confess) will be the outcome reached by two rational players, even though (confess, confess) results in worse payoffs for both players than would (not confess, not confess).

More generally, the solution of a strategic-form game can be found by iteratively eliminating strictly dominated strategies. Such method goes by the name of *iterated strict dominance* [53]. Unfortunately, many if not most games of practical interest are not solvable by iterated strict dominance. In contrast, the concept of a Nash equilibrium solution produces much tighter predictions in a very broad class of games. This notion captures a steady-state of the play of a strategic game in which each player holds the correct expectation about the other players' behavior and acts rationally.[6]

Definition 4 *A pure-strategy profile* $\mathbf{a}^* = \left[a_k^*, \mathbf{a}_{\setminus k}^*\right]$ *is a pure-strategy* Nash equilibrium *of the strategic-form game* $\mathcal{G} = [\mathcal{K}, \{\mathcal{A}_k\}, \{u_k(\mathbf{a})\}]$*, if, for all players* $k \in \mathcal{K}$*,*

$$u_k\left(a_k^*, \mathbf{a}_{\setminus k}^*\right) \geq u_k\left(a_k, \mathbf{a}_{\setminus k}^*\right), \quad \forall a_k \in \mathcal{A}_k, \tag{1.2}$$

where $\mathbf{a}_{\setminus k}^* = \left[a_1^*, \ldots, a_{k-1}^*, a_{k+1}^*, \ldots, a_K^*\right]$.

The definition of the Nash equilibrium can easily be extended to mixed-strategy profiles [48]. Analogously to pure strategies, pure-strategy Nash equilibria are degenerated mixed-strategy Nash equilibria.

The Nash equilibrium offers a stronger solution concept than iterated elimination of strictly dominated strategies, in the sense that the players' strategies in a Nash equilibrium always survive iterated elimination of strictly dominated strategies, but the converse is not true [53]. As an example of the first part of this statement, it is easy to check that the solution obtained by iterated strict dominance, (confess, confess), is a Nash equilibrium in the Prisoner's dilemma represented in Fig. 1.1.

By inspecting Definition 4, it is clear that a Nash equilibrium represents a stable outcome of the noncooperative game in which multiple agents (players) with (in general) conflicting interests compete through self-optimization and reach a point where no player has any incentive to *unilaterally* deviate. The Nash equilibrium can be seen from another point of view. In a noncooperative game, the strategy chosen

[6] It is worth stating that the concept of Nash equilibrium does not attempt to examine the process by which a steady state is reached.

by a rational self-optimizing player constitutes a *best response* to the actions chosen by the other players. Formally, player k's best-response function $r_k : \mathcal{A}_{\setminus k} \to \mathcal{A}_k$ is the correspondence that assigns each opponents' profile $\mathbf{a}_{\setminus k} \in \mathcal{A}_{\setminus k}$ the set

$$\begin{aligned} r_k\left(\mathbf{a}_{\setminus k}\right) &= \arg\max_{a_k \in \mathcal{A}_k} u_k\left(a_k, \mathbf{a}_{\setminus k}\right) \\ &= \left\{a_k \in \mathcal{A}_k : u_k\left(a_k, \mathbf{a}_{\setminus k}\right) \geq u_k\left(a'_k, \mathbf{a}_{\setminus k}\right) \quad \text{for all } a'_k \in \mathcal{A}_k\right\}. \end{aligned} \tag{1.3}$$

With the notion of a player's best response, the Nash equilibrium can be restated as follows:

Definition 5 *The pure-strategy profile* $\mathbf{a}^*$ *is a pure-strategy Nash equilibrium of the game* $\mathcal{G} = [\mathcal{K}, \{\mathcal{A}_k\}, \{u_k(\mathbf{a})\}]$ *if and only if*

$$a_k^* \in r_k\left(\mathbf{a}_{\setminus k}^*\right), \quad \textit{for all } k \in \mathcal{K}. \tag{1.4}$$

Theorem 1 (Nash, [91]) *In the strategic-form game* $\mathcal{G} = [\mathcal{K}, \{\mathcal{A}_k\}, \{u_k(\mathbf{a})\}]$*, if* K *is finite and* $\mathcal{A}_k$ *is finite for every* k *(i.e., in a finite game), then there exists at least one Nash equilibrium, possibly involving mixed strategies.*

The proof makes use of the Brouwer-Kakutani fixed-point theorem and can be found in [48, 53].

This theorem is of crucial importance in game theory, since it establishes the existence of (at least) one steady state solution for *every* finite game. In fact, although characterizing the set of equilibria is in general difficult in many interesting games, this result allows the properties of these equilibria to be studied without funding them explicitly and without taking the risk that we are studying the empty set.

The existence of at least one (possibly mixed-strategy) Nash equilibrium implies that a strategic-form finite game may have no pure-strategy equilibria, one pure-strategy equilibrium, or multiple pure-strategy equilibria. It is interesting to note that Theorem 1 represents a special case of the following theorem, which considers infinite games (i.e., games with an uncountable number of strategies) with continuous payoffs:

Theorem 2 (Debreu, [33]; Glicksberg, [54]; Fan, [37]) *Consider a game* $\mathcal{G}$ *in strategic form, in which the pure-strategy spaces* $\mathcal{A}_k$ *are nonempty compact convex*

subsets of a Euclidean space. If the utility functions $u_k(\mathbf{a})$ *are continuous in* $\mathbf{a}$ *and quasi-concave*[7] *in* a_k*, there exists a pure-strategy Nash equilibrium in* $\mathcal{G}$*.*

The proof, similar to that of Theorem 1, can be found in [48].

As can be seen in the following chapters, this result is of particular interest for the scope of this thesis, since it establishes the existence of (at least) one pure-strategy Nash-equilibrium in infinite strategic-form games, provided that the hypotheses of Theorem 2 are met.

1.2.3 Pareto optimality

So far, no considerations about the efficiency of the outcome of the game have been done. In general, there is no guarantee that a Nash equilibrium is a desirable outcome for the players. Intuitively, this is motivated by the distributed approach between the players, which could be expected to be less *efficient* than a possible strategy profile obtained through *cooperation* between the players and/or as a result of a centralized optimization. This is apparent in the Prisoner's dilemma depicted in Fig. 1.1, where the concept of Nash equilibrium leads both players to choose the strategy pair (confess, confess), which provides a utility of -1, rather than the pair (not confess, not confess), which yields a utility of 0. In this particular example, the paradoxical conclusion is due to the lack of trust between the players, which is implicit in the formulation of all noncooperative static games.

Two important concepts to investigate the efficiency of the solution(s) of strategic-form games are the Pareto dominance and the Pareto optimality. A strategy profile is said to be more efficient (or *Pareto-dominant*) if it is possible to increase the utility of some of the players without hurting any other player. A formal definition is as follows:

Definition 6 *A strategy profile* $\tilde{\mathbf{a}}$ Pareto-dominates *another vector* $\mathbf{a}$ *if, for all* $k \in \mathcal{K}$*,* $u_k\left(\tilde{a}_k, \tilde{\mathbf{a}}_{\setminus k}\right) \geq u_k\left(a_k, \mathbf{a}_{\setminus k}\right)$*, and, for some* $k \in \mathcal{K}$*,* $u_k\left(\tilde{a}_k, \tilde{\mathbf{a}}_{\setminus k}\right) > u_k\left(a_k, \mathbf{a}_{\setminus k}\right)$*.*

It is worth noting that the players might need to change their strategies simultaneously to reach the Pareto-dominant strategy profile $\tilde{\mathbf{a}}$. Based on the concept of Pareto dominance, it is possible to identify the most efficient strategy profile(s):

[7] A function $u_k(\mathbf{a}) : \mathcal{A}_k \to \mathbb{R}^1_+$ defined on the convex set $\mathcal{A}_k$ is quasi-concave in a_k if and only if $u_k\left(\lambda a_k + (1-\lambda)a'_k, \mathbf{a}_{\setminus k}\right) \geq \min\left\{u_k\left(a_k, \mathbf{a}_{\setminus k}\right), u_k\left(a'_k, \mathbf{a}_{\setminus k}\right)\right\}$ for all a_k, $a'_k \in \mathcal{A}_k$ and $\lambda \in [0,1]$.

Definition 7 *A strategy profile* $\tilde{\mathbf{a}}$ *is* Pareto-optimal *if there exists no other strategy profile* $\mathbf{a}$ *such that* $u_k\left(a_k, \mathbf{a}_{\setminus k}\right) \geq u_k\left(\tilde{a}_k, \tilde{\mathbf{a}}_{\setminus k}\right)$ *for all* $k \in \mathcal{K}$ *and* $u_k\left(a_k, \mathbf{a}_{\setminus k}\right) > u_k\left(\tilde{a}_k, \tilde{\mathbf{a}}_{\setminus k}\right)$ *for some* $k \in \mathcal{K}$.

In other words, in a Pareto-optimal strategy profile, it is not possible to increase the payoff of one player without decreasing that of at least one other player. Furthermore, it can be shown in general that there exists no mixed-strategy profile that Pareto-dominates any pure-strategy profile, because any mixed strategy of a player k is a linear combination of his/her own pure strategies with positive coefficients that sum up to 1 [39].

The game can have several Pareto-optimal strategy profiles and the set of these profiles is called the *Pareto frontier*. It is important to emphasize that a Pareto-optimal strategy profile is not necessarily a Nash equilibrium. Moreover, a Pareto-optimal strategy profile *does not* necessarily Pareto-dominate *all* other strategy profiles.

The Prisoner's dilemma confirms the previous statements. In fact, it is easy to verify that:

- the strategy profile (confess, confess) is a Nash equilibrium, but not Pareto-optimal;
- the strategy profiles (not confess, not confess), (confess, not confess), and (not confess, confess) (which constitute the Pareto frontier) are Pareto-optimal, but not Nash equilibria;
- any Pareto-optimal strategy Pareto-dominates the Nash equilibrium, which is said to be *inefficient*;
- any Pareto-optimal strategy profile does not Pareto-dominate another Pareto-optimal profile.

As will be better stated in the remainder of this thesis, the efficiency of the outcome of a noncooperative game must seriously be taken into account. In fact, although noncooperative approaches show many appealing features due to their inherent decentralization scheme, a significant inefficiency of their outcome(s) could make them inapplicable to practical scenarios.

1.3 Dynamic games

The class of static games of complete information[8] presented in Sect. 1.2 considers situations in which the players choose their actions simultaneously, without being allowed to reconsider their plans of action after some events in the game have been unfolded. Much of the recent interest in many fields of applications of game theory, including wireless engineering, has been in *dynamic games*, i.e., situations with an important dynamic structure. In other words, players are allowed to have a *sequential* interaction, meaning that the move of one player is conditioned by the previous moves in the game.

If at each move in the game the player with the move knows the full history of the play of the game thus far, then the game is said to be of *perfect information*. Alternatively, if the player with the move does not know the full history of the game, the game is defined of *imperfect information*. This is the case of games in which some players make simultaneous moves, thus having imperfect information about the unfolding of the game. Static games represent a special class of dynamic games of imperfect information with only one stage.

Dynamic games can also be classified according to whether the number of stage is finite or infinite. In the first hypothesis, *finite-horizon games* are considered. In the case of an infinite number of stages, games are said to be *infinite-horizon games*.

The remainder of this section briefly describes the main tools to study dynamic problems. Since the main focus of this thesis is on static games,[9] most concepts are not thoroughly expanded.

1.3.1 Extensive-form representation

In the strategic-form representation it is usually assumed that the players make their moves simultaneously. In the case of dynamic games, in which the players choose their move sequentially, a more convenient representation is provided by the extensive form. However, it is worth emphasizing that any (static or dynamic) game can be

[8] As already stated in Sect. 1.2, we restrict our attention to games of complete information only. For games of incomplete information, please refer to [48, 53, 98].

[9] More precisely, the games discussed in this thesis are actually a special case of dynamic games. However, as is better detailed in the following chapters, the main definitions and theoretical results lie in the field of static games.

represented in both strategic and extensive form, since the two representations are completely equivalent.

Definition 8 *A game in* extensive form *consists of:*

(1) *a set of players;*

(2a) *the order of moves – i.e., who moves when;*

(2b) *what the players' choices are when they move;*

(2c) *what each player knows when he/she makes his/her choices;*

(3) *the payoff received by each player for each combination of strategies that could be chosen by the players.*

In the extensive form, a finite game is represented as a tree, which is a collection of ordered nodes. The start of the game is the root of the tree, whereas each *stage* of the game is represented by one level of the tree. The player with the move is represented as a label on the node. For infinite games, the extensive form presents graphical but non conceptual difficulties in describing continuous action spaces. For further details on extensive-form representation, please refer to [48, 53].

As the numbering conventions in the definitions of the strategic and extensive form suggest, there is a close connection between a player's feasible strategies (item 2) given in the strategic form and the description of when a player moves, what he/she can do, and what he/she knows (items 2a, 2b, and 2c) in the extensive form. To illustrate the equivalence between the two representations, Fig. 1.2 reports the extensive form of the Prisoner's dilemma given in Fig. 1.1. The dotted line connecting the two decision nodes represents player 2's ignorance about player 1's move.

To represent this kind of ignorance of previous moves in an extensive-form game, it is worth introducing the following concept:

Definition 9 *An* information set *for a player is a collection of decision nodes satisfying the following conditions:*

i) the player has the move at every node in the information set; and

ii) when the play of the game reaches a node in the information set, the player with the move does not know which node in the information set has (or has not) been reached.

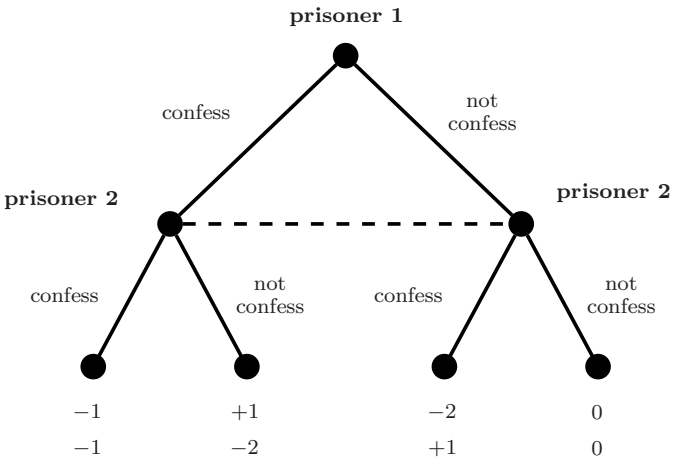

Figure 1.2: *Extensive-form representation for the Prisoner's dilemma.*

In Fig. 1.2, the dotted line indicates player 2's information set, whose interpretation is: when prisoner 2 gets the move, all he/she knows is that the information set has been reached (i.e., that prisoner 1 has moved), not which node has been reached (i.e., what prisoner 1 did).

1.3.2 Games of perfect information

In a sequential decision-making interaction, players may or may not have a perfect knowledge of all previous moves in the game at any moment they are with the move. The concepts introduced in Sect. 1.3.1 are useful to formally define the concept of perfect information for the class of games of complete information [48].

Definition 10 *A dynamic game is of* perfect information *if every information set is a singleton (i.e., players move one at time, and each players knows all previous moves when making his/her decisions).*

As stated in Sect. 1.3.1 for the general case of dynamic games, any finite game of perfect information can be described by its strategic-form representation. Analogously to static games, it is possible to use the tools presented in Sect. 1.2 to obtain the Nash equilibria of the game. However, not every outcome of a finite game of perfect

information can be considered "reasonable" [48]. A central issue in all dynamic games is in fact *credibility*. In other words, certain Nash equilibria are strategies that can be thought of as *empty* (or *noncredible*) *threats*, in that they seem not to consider the previous history of the game and then not to choose the optimal strategy.

In dynamic games of perfect information, equilibria based on empty threats can be eliminated using the technique of *backward induction*. This method is so called because it starts by solving for the optimal choice of the last mover for each possible situation he/she might face, and then work backwards to compute the optimal choice for the player before.[10] In other words, this technique assumes that the players can reliably forecast the behavior of other players and that they believe that the other can do the same. Hence, each player can compute his/her own best response. By iterating this procedure, it is possible to derive the *backward-induction outcome* of the game. Note that backward induction is similar to the technique of iterated strict dominance in strategic-form games. However, it is worth emphasizing that this argument might be less appealing for longer extensive-form games due to the complexity of prediction.

1.3.3 Games of imperfect information

As seen in Sect. 1.3.2, many practical situations are described by a game considered as a sequence of stages, with the moves in all previous stages observed before the next stage begins. However, sometimes it is interesting to allow the players to move simultaneously in the same stage. Dynamic games of this kind are termed games of *imperfect information* [53]. A subclass of these games, in which players move simultaneously in every stage, is often referred to as the class of *multi-stage games with observed actions* [48].

A more formal definition of imperfect information can be given in the case of games of complete information as follows:

Definition 11 *A dynamic game is of* imperfect information *if there is at least one non-singleton information set.*

Backward induction does not apply to games of imperfect information, since a non-singleton information sets implies that at this point there are many last movers, and

[10] Such description is intuitive for the case of finite games with a finite horizon. Nonetheless, backward induction can also be extended to games with infinite horizon and to infinite games by using the analysis provided in [48].

each of them must know the moves of the others to compute his/her own optimal choice (best response). In other words, the presence of a simultaneous-move stage involves solving a real game rather than solving a single-person optimization problem as in Sect. 1.3.2.

This impairment is somewhat analogous to that of static games that cannot be solved by iterated strict dominance. A way out of this impasse is offered by the tools described in Sect. 1.3.4.

1.3.4 Subgame-perfect Nash equilibrium

Seminal contributions to the study of dynamic games of complete information were given by Selten, who overcame the difficulties described in Sect. 1.3.3 by introducing the concepts of *subgame perfection* and *subgame-perfect Nash equilibrium*. More specifically, the subgame-perfect Nash equilibrium extends the idea of backward induction to extensive games where players move simultaneously in several periods [113].

A key role for this formulation is played by the concept of proper subgame, defined as follows:

Definition 12 *The game $\mathcal{G}'$ is a* proper subgame *of an extensive-form game (with both perfect and imperfect information) if:*

i) $\mathcal{G}'$ begins at a decision node n that is a singleton information set;

ii) $\mathcal{G}'$ includes all the decision and the terminal nodes following node n in the game tree (but no nodes that do not follow node n); and

iii) $\mathcal{G}'$ does not cut any information sets.

Thorough motivations for defining proper subgames can be found in [48, 53]. For the scope of this thesis, it suffices to mention that the conditions above mentioned guarantee that, in a proper subgame $\mathcal{G}'$, the complete history of the game thus far is common knowledge between all the players. It is easy to verify that there are no proper subgames in any simultaneous-move (including static) games.

Given the general definition of a proper subgame, it is possible to formally define the concept of subgame perfection. This definition reduces to backward induction in finite games with perfect information.

Definition 13 (Selten, [113]) *A (mixed-strategy) profile* **a** *is a* subgame perfect Nash equilibrium *of an extensive-form game $\mathcal{G}$ if it is a Nash equilibrium of any proper subgame $\mathcal{G}'$ of the original game $\mathcal{G}$.*

It is immediate to show (by construction) that any finite game of complete information has a subgame-perfect Nash equilibrium, perhaps in mixed strategies [53]. In the case of finite games of complete and perfect information, it is possible to prove that there exists (at least) one pure-strategy subgame-perfect Nash equilibrium [72, 98].

Because any proper subgame is a game itself, a subgame-perfect Nash equilibrium is necessarily a Nash equilibrium. In other words, subgame-perfect Nash equilibria are a subset of Nash equilibria. The importance of the concept of subgame-perfect Nash equilibrium lies in its capability of eliminating Nash equilibria that rely on empty threats.

Furthermore, a subgame-perfect Nash equilibrium represents a collection of strategies (a complete plan of action) for each player in response to any possible unfolding of the game. Nevertheless, subgame perfection has been often criticized, mostly with arguments based on equilibrium selection [48].

1.3.5 Repeated games

Repeated games represent a subclass of dynamic games, in which the players face the same single-stage (static) game in every period. Repeated games can be classified according to the time horizon. If the time horizon is finite, the games are said to be *finite-horizon* or, equivalently, *finitely repeated games*. Similarly, if the time horizon is infinite, the games are termed *infinite-horizon* or, equivalently, *infinitely repeated games*.

In some cases, the objective of the players in a repeated game can be to maximize their own payoffs only for the next stage (i.e., as if they played a static game). These games are referred to as *myopic games*, as the players are short-sighted optimizers. Alternatively, in some situations the player's payoff is a weighted average of the payoffs in each stage. These games constitute the class of *long-sighted games*.

In both cases, the players' actions are observed at the end of each stage. This involves the concepts of "reputation" and "punishment" between the players in the game [76]. In fact, when players participate in repeated interactions, they must consider the effects that their chosen strategies in any stage of the game may have on

opponents' strategies in subsequent rounds. As a consequence, it becomes possible for the players to condition their play on the past play of their opponents, which can lead to equilibrium outcomes that do not arise when the game is played only once (i.e., when the game is static). As a conclusion, the repeated interaction between the players may induce a sort of "cooperation" between them [98].

When considering long-sighted games (with both finite and infinite time horizon), the concept of *discount factor* is of particular interest, since it allows the decrease of the value for future payoffs to be described mathematically. In the economic context, the discount factor represents the ratio between the present value of an amount of money and the amount of money received one stage later and is related to the positive interest rate per stage. This formulation is also applicable to the wireless and networking context, since terminals in a network want to exchange information as soon as possible. A fundamental result in this context is provided by the so-called *folk theorems* [47, 98].

1.4 Game theory in wireless networks

As stated in Sect. 1.1, game theory has been profitably applied to wireless networks since the mid-1990s. To exploit the analytical tools of game theory, the abstract concepts introduced in the previous sections should be properly adapted to wireless networks. Sect. 1.4.1 contains some toy examples that are expedient to understand how a simplified power control problem can be modeled as a noncooperative game [13]. Sect. 1.4.2 provides a brief overview of current research in the field of power control for wireless networks based on the noncooperative game-theoretic framework [82].

1.4.1 Motivating examples

To illustrate the intuitive meaning of these concepts, we consider a trivial example of a static noncooperative game, called the *near-far effect game*. Two wireless terminals (player 1 and player 2) transmit to a certain access point (AP) in a code division multiple access (CDMA) network. Player 1 is located close to the AP, whilst player 2 is much farther away, as is depicted in Fig. 1.3. Hence, $K = 2$ and $\mathcal{K} = \{1, 2\}$. Each user is allowed either to transmit at a certain power level $p_k = p$, or to wait ($p_k = 0$). This translates into $\mathcal{A}_k = \mathcal{P}_k = \{0, p\}$. Each terminal achieves a degree

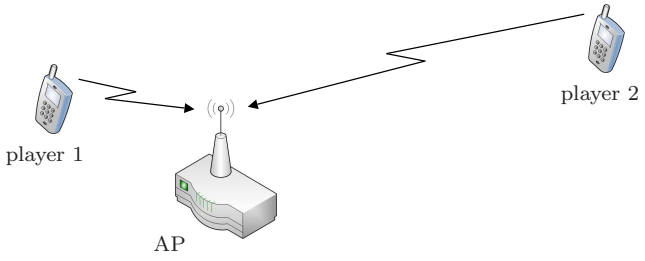

Figure 1.3: *The network scenario in the near-far effect game.*

of satisfaction which depends on the outcome of the transmission and on the cost due to the energy spent for transmitting at power p_k. Mathematically, this translates into an adimensional utility $u_k(\mathbf{a}) = u_k(p_1, p_2) = t_k - z_k$, where $t_k = 1$ if the transmission is successful and $t_k = 0$ otherwise; also, the cost is $z_k = z \ll 1$ if the player chooses to transmit, and $z_k = 0$ otherwise. Due to the near-far effect, sketched in Fig. 1.3, whenever the near player (player 1) chooses to transmit, his/her transmission is successful irrespective of the action of the far player (player 2). In particular, if $p_1 = p$, player 1 can deliver his/her information, thus receiving a utility $u_1(p, p_2) = 1 - z$ (irrespective of p_2). If $p_1 = 0$ (player 1 is idle), his/her utility is $u_1(0, p_2) = 0$ (irrespective of p_2 again). Let us now focus on player 2. Because of the interference caused by player 1, player 2 transmits successfully only when player 1 is idle ($p_1 = 0$). In this case, $u_2(0, p) = 1 - z$. If both players play $p_k = p$, due to the near-far effect, player 2's transmission fails and $u_2(p, p) = -z$. Similarly to player 1, $u_2(p_1, 0) = 0$ when player 2 is idle.

The near-far effect game is summarized in the strategic-form matrix depicted in Fig. 1.4. By inspecting the payoff matrix, it is apparent that player 1's best strategy is represented by $p_1 = p$ whatever p_2 is, since $1 - z > 0$ under the assumption $z \ll 1$. This is known to player 2 as well. Hence, to "limit damage", he/she rationally chooses to play $p_2 = 0$. As a conclusion, the near-far effect game has only one pure-strategy Nash equilibrium, represented by the strategy $\mathbf{a} = (p, 0)$ (the same conclusion follows from Definition 4).

By applying Definition 7, this game can be shown to have two Pareto-optimal solutions, namely $(p, 0)$ and $(0, p)$. Hence, the (only) pure-strategy Nash equilibrium is also Pareto-optimal. However, our solution $(p, 0)$ is highly unsatisfactory for player

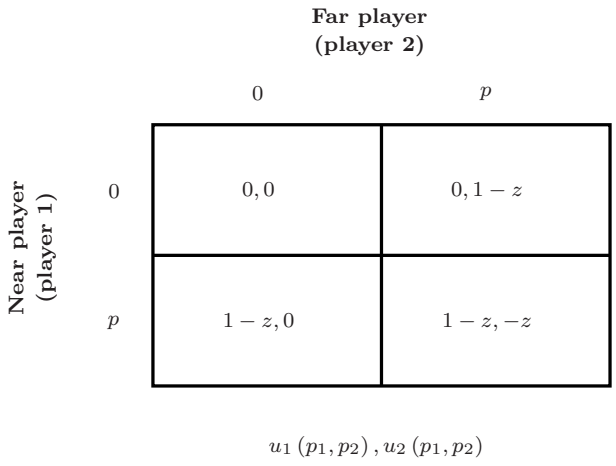

Figure 1.4: *Payoff matrix for the near-far effect game.*

2 since he/she does not show to convey any information to the AP. We take this apparent need for *fairness* as our motivation to introduce power control.

Let us provide our near-far effect game with a naive form of *power control*. Assume now that each terminal is allowed to transmit choosing between two different levels of transmit power: either a certain amount p, or a reduced level ηp, where η, $0 < \eta < 1$. The power control factor η is such that the received power for both players is the same when the far player uses p and the near player uses ηp. Hence, $\mathcal{A}_k = \mathcal{P}_k = \{\eta p, p\}$. Similarly to the previous game with no power control, $u_k(p_1, p_2) = t_k - z_k$, where $t_k = 1$ if the transmission for player k is successful, and $t_k = 0$ otherwise, and where z_k is proportional to the consumed energy, i.e., $z_k = z$ if $p_k = p$, and $z_k = \eta z$ if $p_k = \eta p$. As before, due to the near-far effect, player 1 can successfully transmit irrespective of p_2, whereas player 2 can correctly reach the receiver only if $p_2 > p_1$. The payoff matrix for this game is shown in Fig. 1.5. Since $1 - \eta z > 1 - z$, player 1's best strategy is $p_1 = \eta p$. Consequently, player 2 plays $p_2 = p$. This game has thus one pure-strategy Nash equilibrium, which is also the only Pareto-optimal solution.

This power control technique seems to compensate for the near-far effect, since both players are now able to transmit. However, this scenario does not actually model real data networks. The main inaccuracy lies in the over-simplified utility

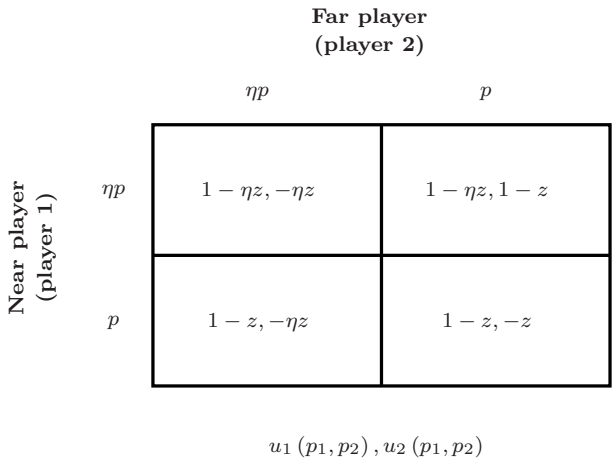

Figure 1.5: *Payoff matrix for the near-far effect game with power control and zero-one utility.*

function. Our "go/no-go" utility is suitable only for those applications for which the acceptable quality of a connection is specified by a maximum tolerable bit error rate (BER), which turns into a minimum signal-to-interference-plus-noise ratio (SINR) requirement. This is the typical case for voice networks, in which the voice user is usually indifferent to small changes in its SINR [55]. In a data network, higher SINRs lead to a larger amount of transmitted information. This implies that the utility for a data terminal is a continuous function of its SINR. To account for this different point of view, the term t_k should be a function of the amount of information that is actually delivered to the receiver. Focusing on player 1, if $p_1 = p$, the (normalized) amount of information (we may call it the throughput) is equal to $t_1 = t \gg z$. If player 1 uses a lower power $p_1 = \eta p$, then $t_1 = \lambda t$, with $\eta < \lambda \lesssim 1$.[11] Considering player 2, $t_2 = 0$ if $p_2 \leq p_1$, and $t_2 = \lambda t$ if $p_2 > p_1$, since the received power for player 2 is equal to that of player 1 with $p_1 = \eta p$.

The payoff matrix for this game is shown in Fig. 1.6. Similarly to the near-far effect game without power control, player 1's best strategy is represented by $p_1 = p$

[11] Note that $\eta < \lambda$ in all practical scenarios, since the performance in terms of correct detection does not show a linear dependence on the transmit power.

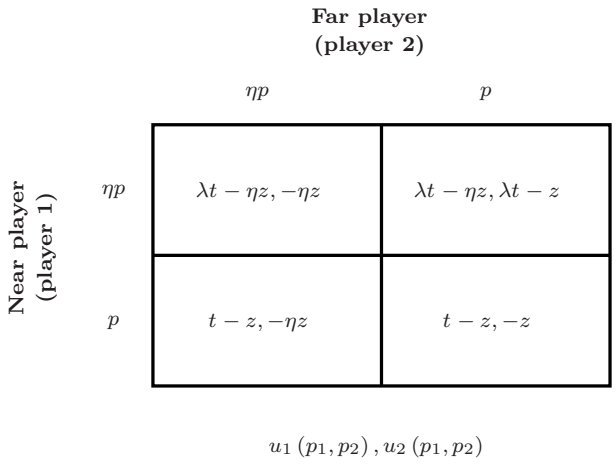

Figure 1.6: *Payoff matrix for the near-far effect game with power control and variable throughput.*

whatever p_2 is, since $t - z > \lambda t - \eta z$ under the assumption $t \gg z$. As a consequence, player 2 rationally chooses to play $p_2 = \eta p$. The pure-strategy Nash equilibrium is represented by the strategy $(p, \eta p)$, whereas the Pareto-optimal solutions are $(p, \eta p)$ and $(\eta p, p)$. We appear to be back to the original situation we had without power control, since at the Nash equilibrium player 2 is unable to transmit.

The inefficiency of this scheme can be measured in terms of *social optimality*. Although formally different from the Pareto-optimal solution, the social-optimal solution is strongly connected with the efficiency of a certain strategy in terms of the overall performance of the network. In other words, the social-optimal solution provides a measure of the maximal revenue of the network as a whole assuming that the terminals act according to a cooperative scheme rather than choose their action selfishly. As can be seen in the next chapters, we will use this notion to measure the inefficiency of the outcome of distributed schemes. In the specific case of the near-far effect game with variable throughput, a solution is socially optimal if the overall utility $u_{\text{network}}(p_1, p_2) = u_1(p_1, p_2) + u_2(p_1, p_2)$ is a maximum. We see that $(p, \eta p)$, in spite of being Pareto-optimal, does not represent the best solution for the network as a whole, since the overall utility is $u_{\text{network}}(p, \eta p) = t - (1 + \eta) z < 2\lambda t - (1 + \eta) z =$

$u_{\text{network}}(\eta p, p)$. Hence, the Nash equilibrium is not desirable in a social sense.

We can make this situation considerably better by resorting to a dynamic game. It is easy to see that $(p, \eta p)$ is the best strategy for player 1 in a one-move (static) game only. If the near-far effect game of Fig. 1.6 is played with several moves, player 1 will choose the strategy $p_1 = \eta p$. To see the motivation for this, assume that $1/\lambda$ is an integer for the sake of simplicity (the same conclusions hold even when such assumption is not verified). If the players play $(\eta p, p)$ for $1/\lambda$ times, player 1 achieves a total utility $(\lambda t - \eta z)/\lambda = t - \eta z/\lambda$, which is greater than $t - z$ due to $\eta < \lambda$. The only disadvantage is an increased transmission time, which is not necessarily a negative feature (it actually is only for delay-sensitive applications, which call for different utility functions).

1.4.2 Applications to power control

In the last two decades, game theory has been extensively applied to many resource allocation issues, that span all the layers of the open systems interconnection (OSI) reference stack [68]. Since this thesis is mainly focused on power control techniques, this subsection will provide an overview of the relevant noncooperative game-theoretic approaches to power control in the context of wireless communication networks. The interested reader may refer to [8, 38, 65, 76, 96, 107, 116] for a survey on game-theoretic approaches in other resource allocation issues.

The need for *power control* in wireless communications emerged since the pioneering works on spread spectrum (SS) satellite communications [1, 86]. Until mid-1990s, power control techniques were primarily focused on voice communications systems [46, 58, 95, 140]. For these applications, SINR-balancing schemes are particularly suitable, since voice users are usually indifferent to small changes in their SINRs.

With the advent of the third-generation cellular networks, high-speed data services became available to the mobile population. Since data communications are intolerant of errors, higher SINRs lead to a lesser number of retransmissions, which translates into a larger amount of information correctly delivered at the receiver. As a consequence, the level of satisfaction achieved by each user becomes a continuous function of the SINR [55].

Noncooperative game theory has shown to be particularly suitable to address the problem of power allocation for wireless data networks. The game-theoretic frame-

work was originally proposed in the context of voice traffic in 1998 by Ji and Huang in [69], in which the mobile terminals in a cellular network competing for the uplink channels are modeled as noncooperative players in a strategic-form game.

In [36, 114], Shah *et al.* extended this framework to data traffic, formulating an effective utility function to focus power control on the *energy efficiency* of the terminal. To properly capture the tradeoff between achieving a satisfactory QoS and prolonging battery life, the utility of each user is measured as the ratio of its throughput to its transmit power in the uplink of a CDMA infrastructure network using matched filter receivers. In other terms, this utility function measures the number of bits than can be correctly delivered at the receiver per joule of energy consumed. Using Yates' standard power control framework [137], the Nash equilibrium is shown to be reached when all the terminals achieve the same SINR target. However, although the proposed game-theoretic algorithm mimics a SINR-balancing power control scheme, the SINR target is chosen accordingly to the tradeoff between throughput and transmit power.

In [114], Shah *et al.* also proposed linear pricing techniques to improve the efficiency of the Nash equilibrium in terms of Pareto optimality. The formal proof of the convergence of the algorithm is provided by Saraydar *et al.* in [110], in which the properties of supermodular games [6, 123, 124] are applied to the power control game with pricing. This approach is extended by Hayajneh and Abdallah in [63] to arbitrary channels using statistical learning theory.

A different method to improve the Pareto efficiency of the Nash equilibrium is derived by Goodman and Mandayam in [56, 57]. A network-assisted power control algorithm is proposed, in which the SINR target is chosen by a central controller (typically, the base station) and broadcast to all users in the network. (A similar approach is proposed by MacKenzie and Wicker in [77], in which a repeated power control game is also derived.)

In the schemes described above, the main focus in on single-cell networks. In [109], Saraydar *et al.* extended the framework by Shah *et al.* to the case of a multi-cell network, proving the existence and uniqueness of a Nash equilibrium for the power control scheme and the convergence of the iterative algorithm. The energy-efficient approach to power control for infrastructure networks has been extended by Meshkati *et al.* in [79] to multicarrier CDMA systems.

A different pricing technique is employed by Feng *et al.* [40] to study the performance of distributed (noncooperative) algorithms with respect to a centralized (cooperative)

framework. While previous pricing schemes were based on transmit powers, here the pricing is based on throughputs to serve as a mediator between the user-centric and the network-centric approach. The algorithm is derived by using a Stackelberg (dynamic) game. This method is extended to multi-cell systems in [41].

The energy efficiency framework is also suitable to derive distributed schemes for infrastructure networks to jointly address power control and other aspects of the network design. In [85], Meshkati *et al.* studied the cross-layer design of joint power control and linear multiuser detection, showing that the transmit powers of the users are SINR-balanced at the Nash equilibrium. This approach is further generalized in [81] to a broader class of receivers, including nonlinear receivers (see also [24]). (Although with a layered approach, the effect of successive interference cancellation was studied also by St Jean and Jabbari in [117].)

The approach outlined in [85] is extended by Buzzi *et al.* in [22] considering the effects of distortion due to multipath propagation. In [23], the spreading code optimization is added to the joint power control and receiver design, also proposing a stochastic algorithm to the noncooperative game and extending the results to multi-cell systems [25, 26].

Another cross-layer approach using the energy-efficient formulation is proposed by Meshkati *et al.* in [83, 84] by considering QoS delay requirements in CDMA networks. The effects of modulation on energy efficiency have been analyzed in [80].

The game-theoretic formulation proposed in [114] for CDMA infrastructure networks is also suitable to study the performance of ad hoc networks. In [67], Ileri *et al.* studied a cross-layer design of power control and forwarding in a multihop ad hoc network using a Stackelberg model with pricing based on channel use and reimbursement for forwarding. In [20], Betz and Poor extended the results of joint power control and receiver design in [85] to multihop ad hoc networks.

In [133, 134], Xiao *et al.* reformulated the problem of distributed power control by proposing a *utility-based* scheme. The major criticisms to the energy efficiency framework outlined in [109, 110, 114] lie in the possible divergence of the energy-efficient algorithm in the absence of tight bounds for the transmit powers and the complexity of the updating mechanism. To address these problems, Xiao *et al.* focused on the downlink channel of a wireless data networks. In this scenario, they proposed an iterative algorithm to reach a Nash equilibrium of a static game (using [137] for the convergence) in which the player aim at maximizing the difference between a

utility function and a pricing function. Using concepts from the theory of neural networks, the proposed utility is a sigmoidal-shape function. It is worth stating that this function, although presenting some desirable properties, such as inherent admission control and convergence of the algorithm, is not related to any physical quantity, and thus a proper tuning of the algorithm is required.

The utility-based framework, originally developed for infrastructure networks, can be extended to ad hoc networks as well. In [43], Fittipaldi and Luise adopted the sigmoidal utility function to model the power control scheme of an ad hoc network, also proposing an alternative approach in which the SINR is replaced by the Shannon capacity to increase the average number of active links. In [66], Huang and Letaief used utility-based framework [134] to study the cross-layer problem of scheduling and power control for wireless single-hop ad-hoc networks.

In [122], Sung and Wang proposed a *capacity-maximizing* approach to the game-theoretic power control for wireless data CDMA networks. The objective of the distributed scheme is maximizing the difference between the Shannon capacity and a pricing function. Similarly to [114], pricing is introduced to improve the Pareto efficiency of the Nash solution, although the pricing parameter is normalized accordingly to the total interference at the base station and broadcast by the system. The Nash equilibrium of the proposed static game is achieved through an iterative algorithm (using [137] for the convergence) in the general case of users with different data rates.

A similar approach is described by Alpcan *et al.* in [5] for the uplink power control in a single-cell CDMA wireless network. The proposed static game aims at maximizing the difference between the Shannon capacity, properly scaled by a user-specific parameter, and the pricing function. Alpcan *et al.* proposed two different pricing strategies, namely the centralized scheme (with admission control), and the distributed (market-based) scheme. The convergence of the algorithm is studied in both the synchronous and asynchronous update mechanism. This framework is extended to a multi-cell system in [3], also using a broader class of pricing functions.

The results presented in [5] have been extended by Gunturi and Paganini in [59], in which maximum power constraints on the users are taken into account. The multi-cell scenario is also considered. A similar approach is used by Altman *et al.* in [7], in which a discrete power control for the uplink of a wireless network is studied. The distributed framework (suitable also for ad hoc and sensor networks) considers a discrete set of available power levels, including a limit on the average power. In [78],

Maillé considered the utility as the difference between Shannon capacity and pricing to address the problem of downlink power control in CDMA wireless networks with a variable number of users. The solution of this problem is obtained by resorting to an auction-based game.

In [4], Alpcan *et al.* modified the utility function to consider the outage probability of the system. The convergence of the algorithm is verified also in the case of a stochastic version of the update scheme to take into account the effects of estimation and quantization errors. In [64], Hayajneh and Abdallah used a capacity-maximizing criterion to address the problem of joint rate and power control for infrastructure networks. The game-theoretic algorithm is decoupled in a rate control game and a subsequent power control game. A similar approach is considered by Yuan *et al.* in [138], in which the power control represents a subproblem of a cross-layer optimization in the context of wireless mesh networks.

In [99], Palomar *et al.* studied the game-theoretic power allocation in multiple input multiple output (MIMO) systems. In this context, the utility function is represented by the mutual information, and several types of games are considered, namely pure- and mixed-strategy static games and Stackelberg (dynamic) games. In the case of unavailable statistics of the channels, the game-theoretic approach leads to a uniform power allocation, which is shown to be a robust solution of the problem. In [75], Liang and Dandekar extended this framework to MIMO ad hoc networks by modeling the power allocation in each link as a noncooperative game.

In [10], Baccarelli *et al.* used the game-theoretic framework to study the distributed joint power allocation and signal shaping in a MIMO ad hoc network. The strategies of the transmit/receive units are the covariance matrices, while the utility function is the conditional throughput. In [29], Chen *et al.* studied the uplink power control for a cellular MIMO system. Game theory is used to derive an iterative algorithm for adaptive power allocation, whose convergence is verified through simulations. The outcome of the iterative update scheme is compared with iterative waterfilling.

Opportunistic power allocation modeled as a noncooperative game is considered by Sun and Modiano in [119] for infrastructure wireless networks. The objective of the power allocation scheme is to maximize the throughput subject to a maximum average amount of consumed energy. This is achieved by selecting power levels that maximize the probability of successful reception based on the channel state. In [74], Leung and Sung considered an opportunistic game-theoretic algorithm for multi-cell networks.

The proposed utility is the difference between the square root of the SINR and a linear pricing function. The convergence of the algorithm is shown using the framework by Sung and Leung [120], also considering the simultaneous presence of SINR-balancing and opportunistic terminals in the network. The stability of the update scheme is verified even in the case of a soft handoff. The decentralization of the algorithm allows this approach to be applicable to ad hoc networks as well.

In [121], Sung and Leung studied the problem of joint distributed power and signature sequence control for CDMA systems. In particular, the conditions to ensure the existence of Nash equilibria are derived, and the Nash solution is obtained by separating the joint problem into two subproblems, namely sequence adaptation and power control. The solution of the joint power control and sequence adaptation problem is completely characterized in the case of synchronous single-cell system, whereas the multi-cell scenario remains unsolved.

In [60], Han and Liu analyzed the joint problem of power and rate allocation for an infrastructure wireless network. The joint allocation scheme is performed by means of two interrelated games, namely the power control at the user level, and the rate control at the system level.

Finally, a different approach to power control for infrastructure wireless networks (in both uplink and downlink) is considered by Koskie and Gajic in [71]. The major criticisms to the SINR-balancing schemes, such as the Foschini-Miljanic algorithm [46] and those resulting from the energy efficient approach derived in [110, 114], lie in the high power consumption required to achieve the SINR target and slow convergence of the algorithm. To reduce power levels while preserving an acceptable QoS, the proposed utility is proportional to the transmit power and the difference between achieved SINR and target SINR. The convergence of the distributed algorithm is ensured by Yates' framework.

Chapter 2

The ultrawideband network scenario

This chapter describes the system model considered throughout this thesis. After introducing the key points of UWB wireless networks in Sect. 2.1, Sect. 2.2 provides an analytical characterization of transmitter side, channel model, and receiver side, respectively. Finally, Sect. 2.3 motivates the use of power control techniques to improve the performance of this kind of networks.

2.1 Introduction

The increasing demand for reliable high-speed data services in wireless networks has generated a number of new technologies that provide multiple access capability with efficient resource allocation and possibly interference mitigation. UWB communication has emerged as a possible solution to satisfy these market drivers. As its name suggests, this technique makes use of extremely wide radio-frequency bandwidths to offer a wealth of attractive features for wireless communications, as well as for networking, radar, imaging and positioning systems [51, 88, 108, 136]. UWB has a history as old as wireless itself, as the pioneering work on wireless telegraphy of Guglielmo Marconi made use of spark-gap transmission devices [103, 136]. The first applications of "modern" UWB technology dates back to the late 1960s [17], when UWB radars were introduced in military applications, whilst UWB for commercial wireless communications gained prominence with the groundbreaking work on impulse radio (IR) by Win and Scholtz in the 1990s [111, 131, 132]. The final clearance of

UWB technology for commercial applications was ratified with the first rulemaking proposal in 2002, when the United States (US) frequency regulator, the Federal Communications Commission (FCC), allowed unlicensed UWB operation [31]. Currently, similar regulatory processes are under way in many other countries worldwide: for instance, Japan and Korea have already approved a preliminary emission policy [100], whereas in Europe, the Electronic Communications Committee (ECC) TG3 officially authorized the use of UWB technology in 2007 [97]. At present, UWB is spreading in the world of information technologies in two competing *de-facto* standards, either for wireless personal area networks (WPANs), or for high-speed connection of computer peripherals to main units – the so-called *wireless universal serial bus (USB).*

The physical layer of IR-UWB systems is based on the transmission of low-power ultra-short information-bearing pulses (commonly referred to as *monocycles*). This approach brings forth a number of distinctive features such as:

i) significant multiuser capability, due to the large bandwidth spreading factor;

ii) potential for extremely high data rates, thanks to the wide transmission bandwidth;

iii) enhanced capability to penetrate through obstacles, due to the concurrent presence of energy over a wide range of different frequencies;

iv) coexistence with incumbent systems in the same frequency bands, because of its low power spectral density; and

v) potential for small-size and low-powered mobile terminals, due to the small processing power required.

The list above represents the main motivations that led to the development of UWB technology as an access scheme for innovative high-speed data networks [27, 50, 89, 103]. However, the appealing features of UWB technology are not enough *per se* to comply with the current ever-increasing demand for larger network capacity. In the near future, wireless networks are expected to support a variety of applications with different QoS constraints. In addition, efficient resource allocation at the transmitter side is mandatory in any instances, due to the presence of mobile, battery-powered terminals. The goal of the system designer is thus to design wireless networks that use the available resources (namely, bandwidth and energy) as efficiently as possible,

while satisfying the QoS requirements of the users. Although a layered approach based on the OSI model is very successful for designing wired systems [34], this has proven to be quite inefficient for wireless networks [82]. This is especially true for large, dynamic networks with variable, possibly mobile nodes, whose control must be as adaptive and scalable as possible. The natural consequence is that the network design must follow a cross-layer approach that involves optimization and performance evaluation of both the physical and the data-link layer, as has been briefly sketched in Sect. 1.4.2.

2.2 System outline

UWB systems include all bandpass transmitting schemes with either large relative bandwidth (typically, larger than 20%), and all baseband systems with large absolute bandwidth (typically, larger than 500 MHz). To allow unlicensed operation over such wide ranges, radiation emissions must respect strict frequency regulations not to affect the performance of incumbent (possibly licensed) systems. Those "frequency masks" depend on the application and on the environment in which the devices operate.

As an example of the outputs of regulatory processes, Fig. 2.1 shows the spectral mask issued by the US FCC for indoor communications (solid line) in terms of equivalent isotropically radiated power (EIRP) [31]. As can be seen, a power spectral density (PSD) of -41.3 dBm/ MHz is allowed in the frequency band between 3.1 and 10.6 GHz. Outside of that band, no intentional emissions are allowed, and the admissible PSD for spurious emissions provides special protection for global positioning system (GPS) and cellular services. The dashed line shows the spectral mask as specified in the European Union (EU) [97]. As can be noticed, current EU regulations are stricter than those provided by the FCC.[1]

2.2.1 Transmitter side

Several technologies to implement UWB fulfill the regulations [31] and [97]. Depending on the spreading codes employed, these systems are termed time hopping (TH)-UWB [111], direct-sequence (DS)-UWB [44], or baseband single-carrier/multicarrier

[1] Fig. 2.1 reports the EU indoor spectral mask valid until the end of 2010. After 2010, the maximum EU EIRP emission levels in certain bandwidths will be even lower [97].

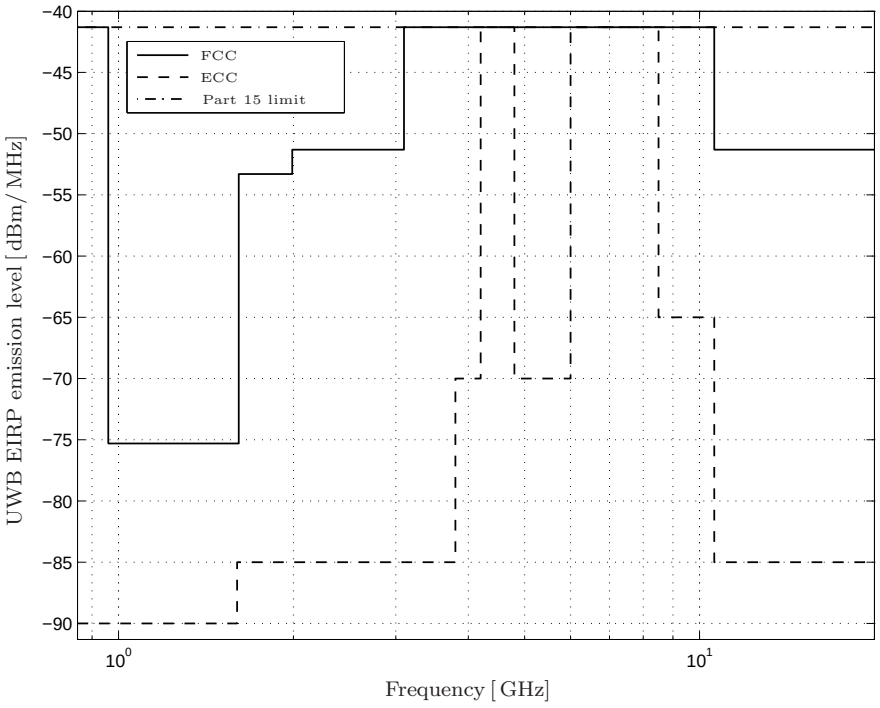

Figure 2.1: *UWB spectral mask for indoor commercial systems.*

(SC/MC)-UWB [130, 135], just to mention a few.

In this work, we will focus on TH systems, where the multiple access is performed by using a pseudo-random TH sequence for each user. The information is conveyed by either the position or the polarity of an ultrashort pulse, which correspond to pulse position modulation (PPM) and binary phase-shift keying (BPSK), respectively. Each pulse is called a "monocycle" and has a basic shape given by the time-derivative of a Gaussian waveform. In "classical" IR, the polarity of the monocycle is always the same [73, 132]. Alternatively, here we will consider polarity randomization [89] which reduces the multiple access interference (MAI) and optimizes the spectral shape according to FCC/ECC specifications. With this technique, each monocycle has a random polarity code in addition to data modulation.

Throughout our analysis, we consider the uplink of an infrastructure BPSK ran-

domized TH-IR system with K users sharing the same channel to communicate with a common AP. The transmitted signal from user k is [50]

$$s_{tx}^{(k)}(t) = \sqrt{\frac{p_k T_f}{N}} \sum_{n=-\infty}^{+\infty} d_n^{(k)} b_{\lfloor n/N_f \rfloor}^{(k)} w_{tx}(t - nT_f - c_n^{(k)} T_c), \tag{2.1}$$

where:

- $w_{tx}(t)$ is the unit-energy UWB pulse, whose duration T_c is on the order of tens or hundreds of nanoseconds;
- p_k is the transmit power of user k, whose maximum value is determined according to PSD regulations;
- T_f is the period of a *frame*, and N_f is the number of frames per bit period T_b ($T_b = N_f T_f$);
- N_c is the number of slots into which each frame is partitioned, representing the N_c possible positions of a pulse; the width of each time slot is T_c;
- as a consequence, $N = N_c \cdot N_f$ is the total spreading factor inherent in UWB signaling;
- the operator $\lfloor \cdot \rfloor$ indicates the integer part of its argument, so that $\lfloor n/N_f \rfloor$ represents the time index of each data bit;
- $b_{\lfloor n/N_f \rfloor}^{(k)} \in \{-1, +1\}$ is the information symbol transmitted by user k;
- $\mathbf{d}_k = \left\{ d_0^{(k)}, \cdots, d_{N_f-1}^{(k)} \right\}$ is the polarity code, where $d_n^{(k)} \in \pm 1$ with probability $1/2$; and
- $\mathbf{c}_k = \left\{ c_1^{(k)}, \cdots, c_{N_f}^{(k)} \right\}$ is the TH sequence, where $c_n^{(k)} \in \{0, 1, \cdots, N_c - 1\}$ with equal probability.

Fig. 2.2 illustrates a sample TH-IR signal as in (2.1), which conveys a single information symbol '+1'. In this simple example, we use $N_f = 3$ frames (thus corresponding to sending three monocycles for each information symbol) and $N_c = T_f/T_c = 5$ possible pulse positions. Hence, the spreading factor is $N = N_f \cdot N_c = 15$. As can be seen, the TH sequence is $\{1, 3, 0\}$, whereas the polarity code is $\{+1, -1, -1\}$. In practical systems, the numbers N_f and N_c are much larger.

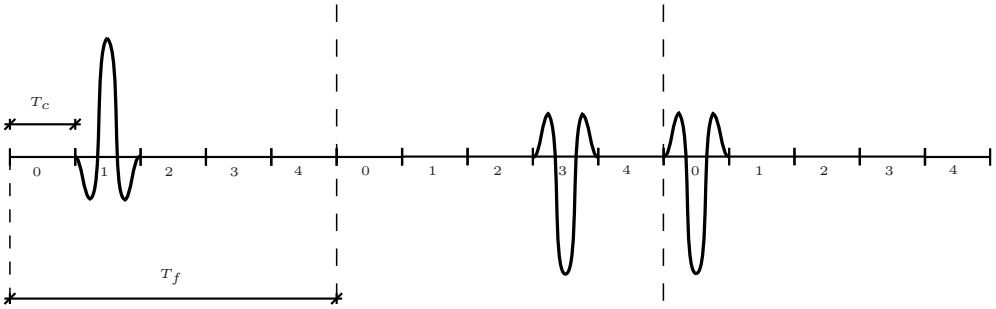

Figure 2.2: *Example of TH-IR signal with pulse-based polarity randomization.*

It is also of interest to highlight the relationship between our (randomized) IR-UWB and traditional random-CDMA (RCDMA) , that is, DS/SS signaling with long pseudo-random spreading codes. To this end, we introduce the *ternary* sequence $\mathbf{s}^{(k)} = \{s_n^{(k)}\}$, defined as

$$s_n^{(k)} = \begin{cases} d_{\lfloor n/N_c \rfloor}^{(k)}, & c_{\lfloor n/N_c \rfloor \cdot N_c}^{(k)} = n - \lfloor n/N_c \rfloor \cdot N_c, \\ 0, & \text{otherwise;} \end{cases} \tag{2.2}$$

which can cast (2.1) into

$$s_{tx}^{(k)}(t) = \sqrt{\frac{p_k T_f}{N}} \sum_{n=-\infty}^{+\infty} s_n^{(k)} b_{\lfloor n/N \rfloor}^{(k)} w_{tx}(t - nT_c). \tag{2.3}$$

Definition (2.2) is a formally correct but complicated way to state that the "chips" of the spreading sequence $s_n^{(k)}$ are 0 when no pulse is sent in the corresponding slot, and is equal to the pulse polarity (± 1) when the pulse is active. The resemblance with RCDMA is apparent. The main difference is that the spreading sequence is ternary rather than binary as in conventional DS/SS. Also, the binary chips of traditional spreading codes for DS/SS are approximately delta-correlated, while the values of the sequence $s_n^{(k)}$ have a correlation pattern dictated by the TH sequence. We have strict coincidence of IR-UWB and DS/SS only when $N_c = 1$ (no TH).

2.2.2 Channel model

Due to their extremely large bandwidths, UWB signals have a much higher temporal resolution than conventional narrowband or wideband signals. As a consequence, the multipath channel experienced by such signals is extremely "rich", i.e., crowded with hundreds of resolvable propagation paths in an indoor environment. Our channel model is a conventional tapped-delay line [52, 104]:

$$\pi_k(t) = \sum_{l=1}^{L} \alpha_l^{(k)} \delta(t - (l-1)T_c - \tau_k), \tag{2.4}$$

where L is the number of channel paths, and $\boldsymbol{\alpha}_k = [\alpha_1^{(k)}, \ldots, \alpha_L^{(k)}]^T$ are the fading coefficients. Our model also captures the different overall propagation delay τ_k of user k, that we suppose for simplicity to be an integer multiple of T_c: $\tau_k = \Delta_k T_c$, for every k, where Δ_k is uniformly distributed in $\{0, 1, \ldots, N-1\}$. We also assume that the channel characteristics remain unchanged over several symbol intervals [50].

2.2.3 Receiver side

Especially in indoor environments, multipath channels can have hundreds of multipath components due to the high resolution of UWB signals. In such cases, linear receivers such as matched filters (MFs), pulse-discarding receivers [42], and multiuser detectors (MUDs) [127] cannot provide good performance, since more collisions will occur through multipath components. To mitigate the effects of multipath, we consider an AP that uses K Rake receivers [102].[2] The Rake receiver for user k is characterized by the L coefficients collected into the vector $\boldsymbol{\beta}_k = \mathbf{G} \cdot \boldsymbol{\alpha}_k = [\beta_1^{(k)}, \ldots, \beta_L^{(k)}]^T$, which represent the combining weights for user k, and where the $L \times L$ matrix $\mathbf{G}$ depends on the type of Rake receiver employed. In particular, if $\mathbf{G}$ is a deterministic diagonal matrix, where

$$\{\mathbf{G}\}_{ll} = \begin{cases} 1, & 1 \le l \le r \cdot L, \\ 0, & \text{elsewhere}, \end{cases} \tag{2.5}$$

with $r \triangleq L_P/L$ and $0 < L_P \le L$, then this receiver is a partial Rake (PRake) with L_P fingers using maximal ratio combining (MRC). Note that, when $r = 1$, this receiver

[2] Since the focus of this thesis is on the interplay between power control and Rake receivers, perfect channel estimation is considered throughout the paper for ease of calculation.

becomes an all-Rake (ARake).

The SINR of the kth user at the output of the Rake receiver can be well approximated (for large N_f, typically, at least 5) by [50]

$$\gamma_k = \frac{h_k^{(\mathrm{SP})} p_k}{h_k^{(\mathrm{SI})} p_k + \sum\limits_{j=1, j\neq k}^{K} h_{kj}^{(\mathrm{MAI})} p_j + \sigma^2}, \tag{2.6}$$

where σ^2 is the output variance due to ambient additive white Gaussian noise (AWGN); $h_k^{(\mathrm{SP})}$ is the term due to the signal part (SP); $h_k^{(\mathrm{SI})}$ is the term due to the self-interference (SI), i.e., the effect of the cross-term that arises between the output of the propagation path $\alpha_l^{(k)}$ and the m-th Rake coefficient $\beta_m^{(k)}$, $m \neq l$; and $h_{kj}^{(\mathrm{MAI})}$ is the term due to the MAI of user $j \neq k$. These terms are expressed by [15, 50]

$$h_k^{(\mathrm{SP})} = \boldsymbol{\beta}_k^H \cdot \boldsymbol{\alpha}_k, \tag{2.7}$$

$$h_k^{(\mathrm{SI})} = \frac{1}{N} \frac{\left|\left| \boldsymbol{\Phi} \cdot \left(\mathbf{B}_k^H \cdot \boldsymbol{\alpha}_k + \mathbf{A}_k^H \cdot \boldsymbol{\beta}_k \right) \right|\right|^2}{\boldsymbol{\beta}_k^H \cdot \boldsymbol{\alpha}_k}, \tag{2.8}$$

$$h_{kj}^{(\mathrm{MAI})} = \frac{1}{N} \frac{\left|\left| \mathbf{B}_k^H \cdot \boldsymbol{\alpha}_j \right|\right|^2 + \left|\left| \mathbf{A}_j^H \cdot \boldsymbol{\beta}_k \right|\right|^2 + \left| \boldsymbol{\beta}_k^H \cdot \boldsymbol{\alpha}_j \right|^2}{\boldsymbol{\beta}_k^H \cdot \boldsymbol{\alpha}_k}, \tag{2.9}$$

respectively, where the matrices

$$\mathbf{A}_k = \begin{pmatrix} \alpha_L^{(k)} & \cdots & \cdots & \alpha_2^{(k)} \\ 0 & \alpha_L^{(k)} & \cdots & \alpha_3^{(k)} \\ \vdots & \ddots & \ddots & \vdots \\ 0 & \cdots & 0 & \alpha_L^{(k)} \\ 0 & \cdots & \cdots & 0 \end{pmatrix}, \tag{2.10}$$

$$\mathbf{B}_k = \begin{pmatrix} \beta_L^{(k)} & \cdots & \cdots & \beta_2^{(k)} \\ 0 & \beta_L^{(k)} & \cdots & \beta_3^{(k)} \\ \vdots & \ddots & \ddots & \vdots \\ 0 & \cdots & 0 & \beta_L^{(k)} \\ 0 & \cdots & \cdots & 0 \end{pmatrix}, \tag{2.11}$$

$$\boldsymbol{\Phi} = \mathrm{diag}\left\{ \phi_1, \ldots, \phi_{L-1} \right\}, \tag{2.12}$$

with

$$\phi_l = \sqrt{\frac{\min\{L-l, N_c\}}{N_c}}, \tag{2.13}$$

have been introduced for convenience of notation.

2.3 The need for power control techniques

Equation (2.6) is our starting point to motivate the need for resource allocation, in general, and for power control, in particular. Assume first that we have no multipath. The term $h_k^{(\mathrm{SI})} p_k$ disappears, and the SINR appears to improve. However, we still an MAI amount that is proportional to the interferers' power p_j, $j \neq k$. This is the classical scenario of CDMA, and the conclusions are pretty much the same [55, 79, 85, 109].

In the presence of the term $h_k^{(\mathrm{SI})}$ (i.e., in a frequency-selective scenario), the SI impacts system performance as well. In fact, p_k does appear not only in the numerator of (2.6), but also in the denominator, owing to the presence of multiple paths. Hence, the problem of an efficient resource allocation scheme becomes more challenging than in the case of a non-dispersive channel. To design scalable and reduced-complexity power control schemes, it is desirable to use distributed algorithms, which have many advantages. Just to mention a few, such algorithms do not present any limitations in terms of the network size, as they allow each terminal to choose its own transmit power via a linear relationship (centralized schemes are typically described by NP-hard problems); moreover, they reduce the resources needed for a return link,[3] since no centralized control is involved. A viable method for devising distributed power control algorithms is provided by game theory, as has been outlined in Sect. 1.4.

[3] An exchange of information between the user and the AP is demanded in distributed algorithms as well, yet the amount of communications is minimal.

Chapter 3

Game-theoretic power control

This thesis is specifically focused on the problem of power control, which is a key issue in data wireless networks based on wideband physical layer technologies, such as UWB and direct-sequence (DS) CDMA (here abbreviated CDMA). As seen in Sect. 2.2.1, a wideband wireless network based on CDMA can be seen as a special case of a network using UWB as the multiple access technique. As a consequence, it is possible to focus our analysis on multiuser UWB networks. The CDMA case will be detailed in Chapter 6, in which the two access schemes are compared in terms of achieved performance.

Sect. 3.1 illustrates the main reasons that motivate us to devise a distributed power control scheme in the context of wireless data networks using UWB as the multiple access technology. The game-theoretic formulation of the distributed power control problem is provided in Sect. 3.2. The noncooperative power control game is formally discussed in Sect. 3.3, in which the existence and the uniqueness of a pure-strategy Nash solution are shown by means of the analytical tools of game theory. Finally, Sect. 3.4 describes an iterative algorithm to reach the Nash equilibrium in a distributed fashion.

3.1 Motivations

As is apparent from the ever-increasing demand for wireless services, next-generation data communications call for extremely high data rates with QoS requirements. Due to the intolerance of errors of data transmissions, the level of satisfaction achieved by each user is proportional to the amount of information correctly delivered at the destination. Nevertheless, mobility of user terminals represents a mandatory feature of

modern wireless systems. As a consequence, energy consumption of battery-powered terminals should play a central role in designing wireless data networks.

Hence, although many formulations of the power control problem in wireless data networks do exist, as detailed in Sect. 1.4.2, these considerations motivate us to focus on *energy efficient* criteria. In a wireless network with (mostly) battery-powered mobile terminals, a primary goal is in fact the maximization of the number of transmitted bits per energy unit rather than the pure maximization of the throughput of the link. This goal can be achieved through application of a noncooperative game wherein the users are allowed to choose their transmit powers according to a utility-maximization criterion, where the *utility* is defined as the ratio of throughput to transmit power.

As already seen in Chapter 1, an important feature of the game-theoretic approach is the inherent de-centralization of the algorithms for power control, which allows each user to individually choose its own transmit power through a simple noncooperative scheme. The advantages of noncooperative (distributed) approaches with respect to a cooperative (centralized) approach are mainly due to the *scalability* of the network. Many of the problems to be solved in a communications system are in fact known to be NP-hard. As a consequence, real-time solution of these optimization problems in a centralized fashion becomes infeasible as the network size increases and as the number of users varies. The performance loss of distributed schemes with respect to centralized allocation is studied in Chapter 5.

The prominent characteristic of the game-theoretic approach, which justifies its widespread range of applications, is its capability of distributing decision-making processes among "rational" users, once benefits and drawbacks of the actions they are allowed to choose are quantified. Although game theory was originally developed to predict the outcome of interactions among economic agents, it is apparent that this framework also fits the situation of resource competition in wireless networks.

3.2 Formulation

The problem of energy-efficient power allocation in the uplink of the TH-UWB data network depicted in Chapter 2 can be addressed resorting to the game-theoretic framework described in Chapter 1.

In this network, every terminal is assumed to be rational, i.e., it locally and selfishly chooses its action to maximize its own utility. As is apparent from (2.6), the strategy

chosen by a user, i.e., his/her transmit power, affects the performance of the other users in terms of received SINR through MAI. Furthermore, since a realistic TH-UWB transmission takes place in frequency-selective multipath channels, the effect of SI cannot be neglected.

To pose the power control problem as a noncooperative game, a suitable definition of a utility function is needed to measure energy efficiency for wireless data applications. A tradeoff relationship exists between obtaining high SINR levels and consuming low energy. These issues can be quantified [114] by defining the utility function of the kth user to be the ratio of its throughput T_k to its transmit power p_k, i.e.

$$u_k(\mathbf{a}) = u_k(\mathbf{p}) = \frac{T_k}{p_k}, \tag{3.1}$$

where $\mathbf{p} = [p_1, \ldots, p_K]$ is the vector of transmit powers, with K denoting the number of users in the network.

Throughput, here referred to as the *goodput*, i.e., the net number of information bits that are received without error per unit time, can be expressed as

$$T_k = \frac{D}{M} R_k f_s(\gamma_k), \tag{3.2}$$

where D and M are the number of information bits and the total number of bits in a packet, respectively; R_k and γ_k are the transmission rate and the SINR for the kth user, respectively; and $f_s(\gamma_k)$ is the efficiency function representing the packet success rate (PSR), i.e., the probability that a packet is received without an error. Our assumption is that a packet will be retransmitted if it has one or more bit errors.

The PSR depends on the details of the data transmission, including its modulation, coding, and packet size [102]. To prevent the mathematical anomalies described in [55], we replace PSR with an *efficiency function* $f(\gamma_k)$ when calculating the throughput for our utility function. A useful example for the efficiency function is $f(\gamma_k) = \left(1 - \mathrm{e}^{-\gamma_k/2}\right)^M$, which serves as a reasonable approximation to the PSR for moderate-to-large values of M. The plot of this efficiency function is given in Fig. 3.1 with $M = 100$. The interested reader may refer to [106] for a detailed discussion of this efficiency function.

However, our analysis throughout this thesis is valid for any efficiency function that is increasing, S-shaped,[1] and continuously differentiable, with $f(0) = 0$, $f(+\infty) = 1$,

[1] An increasing function is S-shaped if there is a point above which the function is concave, and below which the function is convex.

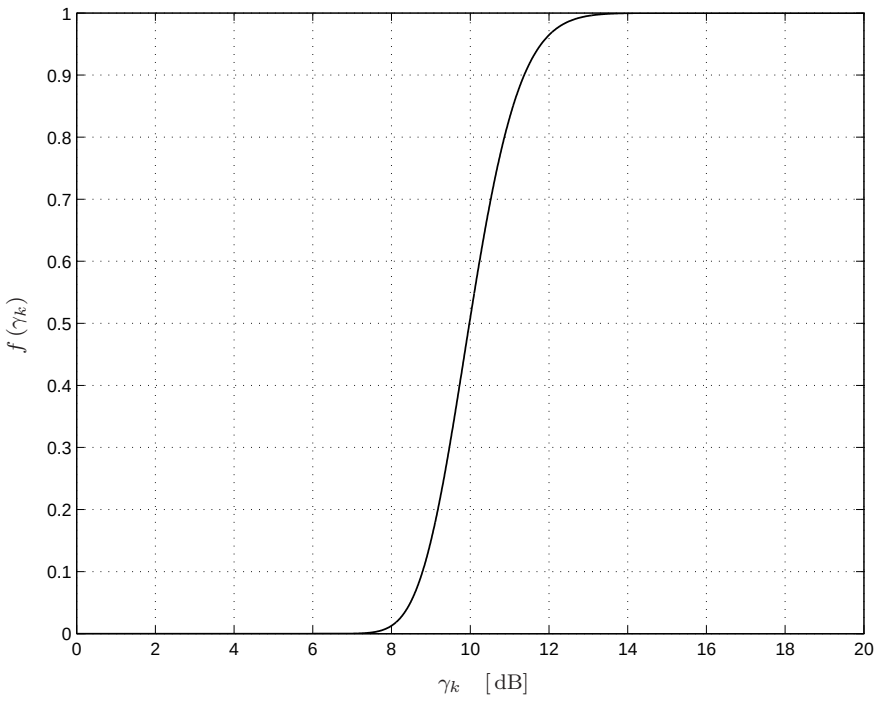

Figure 3.1: *Typical shape of the efficiency function ($M = 100$).*

and $f'(0) = df(\gamma_k)/d\gamma_k|_{\gamma_k=0} = 0$. These assumptions are valid in many practical systems. Furthermore, we assume that all users have the same efficiency function. Generalization to the case where the efficiency function is dependent on k is straightforward. Note that this formulation could be extended to capacity-maximizing approaches (e.g., those proposed by Sung and Wong [122], and by Alpcan *et al.* [5]) by replacing the throughput T_k in (3.2) with the Shannon capacity formula, provided that $u_k(\mathbf{p})$ in (3.1) is appropriately modified to ensure $u_k(\mathbf{p}) = 0$ when $p_k = 0$.

Combining (3.1) and (3.2), and replacing the PSR with $f(\gamma_k)$,

$$u_k(\mathbf{p}) = \frac{D}{M} R_k \frac{f(\gamma_k)}{p_k}. \tag{3.3}$$

This utility function, which has units of bits/Joule, represents the total number of data bits that are delivered to the destination without an error per Joule of energy

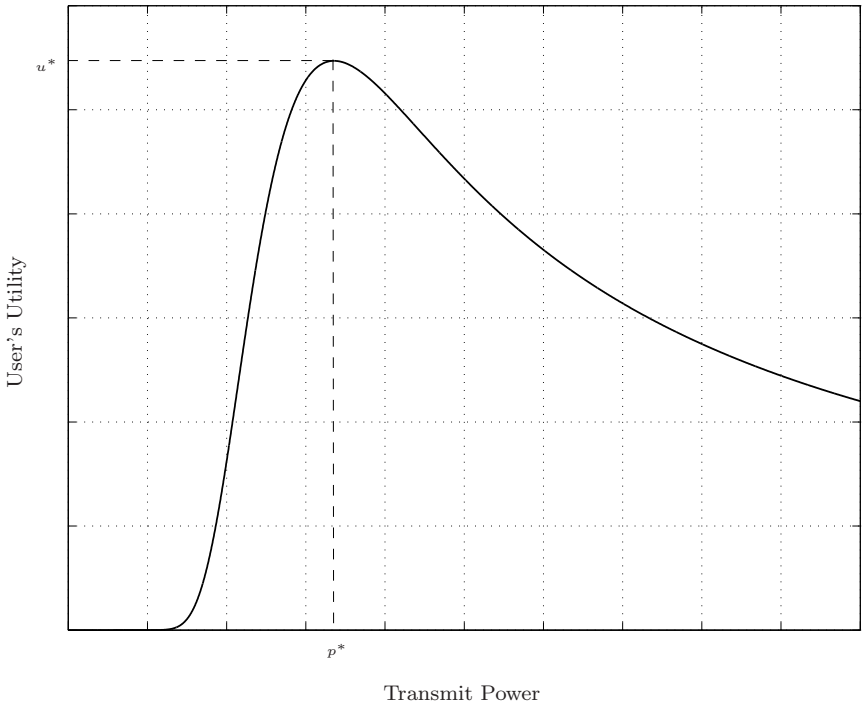

Figure 3.2: *User's utility as a function of transmit power for a fixed interference.*

consumed, capturing the tradeoff between throughput and battery life. For the sake of simplicity, we assume that the transmission rate is the same for all users, i.e., $R_1 = \cdots = R_K = R$. All the results obtained here can easily be generalized to the case of unequal rates. Fig. 3.2 shows the shape of the utility function in (3.3) as a function of transmit power keeping other users' transmit power fixed (the meaning of p^* and u^* will be provided in the remainder of this chapter).

3.3 The noncooperative power control game

In this section, we propose a noncooperative power control game (NPCG) in which every user seeks to maximize his/her own utility by choosing his/her transmit power.

Let $\mathcal{G} = [\mathcal{K}, \{\mathcal{P}_k\}, \{u_k(\mathbf{p})\}]$ be the proposed noncooperative strategic-form game where $\mathcal{K} = \{1, \ldots, K\}$ is the index set for the terminal users; $\mathcal{A}_k = \mathcal{P}_k = \left[\underline{p}_k, \overline{p}_k\right]$ is the pure-strategy set, with $\underline{p}_k$ and $\overline{p}_k$ denoting minimum and maximum power constraints, respectively; and $u_k(\mathbf{a}) = u_k(\mathbf{p})$ is the payoff function for user k [110]. Throughout this thesis, we assume $\underline{p}_k = 0$ and $\overline{p}_k = \overline{p} > 0$ for all $k \in \mathcal{K}$.

Formally, following the notation introduced in Sect. 1.2, the NPCG can be expressed as

$$\max_{p_k \in \mathcal{P}_k} u_k(\mathbf{p}) = \max_{p_k \in \mathcal{P}_k} u_k\left(p_k, \mathbf{p}_{\setminus k}\right), \qquad \text{for } k = 1, \ldots, K, \tag{3.4}$$

where $\mathbf{p}_{\setminus k}$ denotes the vector of transmit powers of all terminals except terminal k. The latter notation is used to emphasize that the kth user has control over its own power p_k only. Assuming equal transmission rate for all users, (3.4) can be rewritten as

$$\max_{p_k \in \mathcal{P}_k} \frac{f\left(\gamma_k\left(p_k, \mathbf{p}_{\setminus k}\right)\right)}{p_k}, \qquad \text{for } k = 1, \ldots, K, \tag{3.5}$$

where we have explicitly shown that γ_k is a function of $\mathbf{p}$, as expressed in (2.6).

3.3.1 Existence of pure-strategy Nash equilibria

The solution that is most widely used for noncooperative game theoretic problems is the *Nash equilibrium*, introduced in Definition 4. Formally, a power vector $\mathbf{p}^* = [p_1^*, \ldots, p_K^*]$ is a pure-strategy Nash equilibrium of $\mathcal{G} = [\mathcal{K}, \{\mathcal{P}_k\}, \{u_k(\mathbf{p})\}]$ if, for every $k \in \mathcal{K}$, $u_k\left(p_k^*, \mathbf{p}_{\setminus k}^*\right) \geq u_k\left(p_k, \mathbf{p}_{\setminus k}^*\right)$ for all $p_k \in \mathcal{P}_k$.

The Nash equilibrium concept offers a predictable, stable outcome of a noncooperative game where multiple agents with conflicting interests compete through self-optimization and reach a point where no player wishes to deviate. However, such a point does not necessarily exist. First, we investigate the existence of an equilibrium in the NPCG.

Theorem 3 *At least one pure-strategy Nash equilibrium exists in the NPCG* $\mathcal{G} = [\mathcal{K}, \{\mathcal{P}_k\}, \{u_k(\mathbf{p})\}]$. *Furthermore, the unconstrained maximization of the utility function occurs when each user* k *achieves an SINR* γ_k^* *that is a solution of*

$$f'(\gamma_k^*) \cdot \gamma_k^* \cdot (1 - \gamma_k^*/\gamma_{0,k}) = f(\gamma_k^*), \tag{3.6}$$

where

$$\gamma_{0,k} = \frac{h_k^{(SP)}}{h_k^{(SI)}} = N \cdot \frac{\left(\boldsymbol{\beta}_k^H \cdot \boldsymbol{\alpha}_k\right)^2}{\left|\left|\boldsymbol{\Phi} \cdot \left(\mathbf{B}_k^H \cdot \boldsymbol{\alpha}_k + \mathbf{A}_k^H \cdot \boldsymbol{\beta}_k\right)\right|\right|^2} \geq 1 \tag{3.7}$$

is the signal-to-self-interference ratio (SSIR), and $f'(\gamma_k^*) = df\left(\gamma_k\right)/d\gamma_k|_{\gamma_k=\gamma_k^*}$.

Proof The NPCG belongs to the category of infinite games, since the joint strategy set of transmit power $\boldsymbol{\mathcal{P}} = \times_k \mathcal{P}_k$ is infinite. Hence, the existence of pure-strategy Nash equilibria can be proven using Theorem 2, described in Sect. 1.2.2.

In particular, (at least) one pure-strategy Nash equilibrium exists in the noncooperative game $\mathcal{G} = [\mathcal{K}, \{\mathcal{P}_k\}, \{u_k(\mathbf{p})\}]$ if, for all $k = 1, \ldots, K$:

1. $\mathcal{P}_k$ is a nonempty, convex, and compact subset of some Euclidean space $\mathbb{R}^K$; and

2. $u_k(\mathbf{p})$ is continuous in $\mathbf{p}$ and quasi-concave in p_k.

Each user k has a strategy space that is defined by a minimum power $\underline{p}_k$ and a maximum power $\overline{p}_k$, and all power values in between. We also assume that $\overline{p}_k \geq \underline{p}_k$. Thus, the first condition is satisfied.

Since $p_k \geq 0$, it is apparent from (2.6) and (3.3) and that $u_k(\mathbf{p})$ is continuous in $\mathbf{p}$. To show that the utility function $u_k(\mathbf{p})$ is quasi-concave in p_k for all k in the NPCG, it is sufficient to prove that the local maximum of $u_k(\mathbf{p})$ is at the same time a global maximum [101, 105].

For a differentiable function, the first-order necessary optimality condition is given by $\partial u_k(\mathbf{p})/\partial p_k = 0$. Recalling (2.6) and (3.3), the partial derivative of $u_k(\mathbf{p})$ with respect to p_k is

$$\frac{\partial u_k(\mathbf{p})}{\partial p_k} = \frac{DR}{Mp_k^2}\left(f'(\gamma_k) \cdot \gamma_k \cdot (1 - \gamma_k/\gamma_{0,k}) - f(\gamma_k)\right), \tag{3.8}$$

where the SSIR $\gamma_{0,k}$ is defined as in (3.7) and $f'(\gamma_k) = df\left(\gamma_k\right)/d\gamma_k$. For the sake of simplicity, we do not explicitly show the dependence of γ_k on p_k.

Since $p_k \geq 0$ in $\mathcal{G}$, we examine only positive real numbers. Evaluating (3.8) at $p_k = 0$, we get $\partial u_k\left(p_k, \mathbf{p}_{-k}\right)/\partial p_k = 0$. Therefore, $p_k = 0$ is a stationary point and the value of utility at this point is $u_k(\mathbf{p}) = 0$. If we evaluate utility in the ε-neighborhood of $p_k = 0$, where ε is a small positive number, we notice that the utility is positive, which implies utility is increasing at $p_k = 0$. Hence, $p_k = 0$ cannot be a local maximum.

For nonzero values of the transmit power, we examine the values of $\gamma_k^* = \gamma_k(p_k^*)$ such that $\partial u_k\left(p_k, \mathbf{p}_{-k}\right)/\partial p_k|_{p_k=p_k^*} = 0$, thus satisfying the first-order necessary optimality condition.

In other words, we evaluate γ_k^* such that

$$\gamma_k^*\left(1-\gamma_k^*/\gamma_{0,k}\right) = f\left(\gamma_k^*\right)/f'(\gamma_k^*), \tag{3.9}$$

as shown in (3.6). We observe that the left-hand side of (3.9) is a concave parabola with its vertex in $\gamma_k = \gamma_{0,k}/2 > 0$, and $d\left(\gamma_k\left(1-\gamma_k/\gamma_{0,k}\right)\right)/d\gamma_k|_{\gamma_k=0} = 1$. The right-hand side is an increasing function, with $d\left(f\left(\gamma_k\right)/f'(\gamma_k)\right)/d\gamma_k|_{\gamma_k=0} = 1/\ell < 1$ when $f'(0) = 0$, where $\ell = \min\{n \in \mathbb{N} : d^n f\left(\gamma_k\right)/d\gamma_k^n|_{\gamma_k=0} \neq 0\}$. Furthermore, the equation is satisfied at $\gamma_k = 0$. Therefore, there is a single value γ_k^* that satisfies (3.6) for $\gamma_k > 0$. The second-order partial derivative of the utility with respect to the power reveals that this point is a local maximum and therefore a global maximum. Hence, the utility function of user k is quasi-concave in p_k for all k.

The same conclusion applies also if $p_k^* > \overline{p}_k$ for some k, even though γ_k^* cannot be achieved. In fact, by applying the previous considerations to (3.8), it is easy to verify that $u_k\left(p_k, \mathbf{p}_{\setminus k}\right)$ is strictly increasing in $\gamma_k \in [0, \gamma_k(p_k^*) = \gamma_k^*)$, which in turn, from (2.6), is strictly increasing in $p_k \in [0, p_k^*)$. Since $p_k \in [\underline{p}_k, \overline{p}_k]$, which is a subset of $[0, p_k^*)$, $u_k\left(p_k = \overline{p}_k, \mathbf{p}_{\setminus k}\right)$ represents both the local and the global maximum of the utility function. ■

To illustrate (3.9) graphically, we consider $f\left(\gamma_k\right) = \left(1-\mathrm{e}^{-\gamma_k/2}\right)^M$ as a useful example for the efficiency function. Expressing $f'(\gamma_k)$ in terms of $f\left(\gamma_k\right)$ and rearranging terms, we get

$$\gamma_k^*\left(1-\gamma_k^*/\gamma_{0,k}\right) = \frac{2}{M}\left(\mathrm{e}^{+\gamma_k^*/2}-1\right). \tag{3.10}$$

The graphical solution is shown in Fig. 3.3. The solid lines report left-hand and right-hand side of (3.10), respectively, while the dashed lines correspond to the tangent lines of the two curves in $\gamma_k = 0$. In this particular case, $\ell = M$, $\gamma_{0,k} = 8.5$ and $\gamma_k^* \approxeq 7.54$.

Lemma 1 *The solution γ_k^* of (3.6) satisfies the condition*

$$0 \leq \gamma_k^* < \gamma_{0,k}. \tag{3.11}$$

Proof As $f\left(\gamma_k^*\right)$ is an increasing function of γ_k^*, $f'(\gamma_k^*) \geq 0$ for every γ_k^*. Since the existence of the solution is ensured by Theorem 3 and γ_k^* and $f\left(\gamma_k^*\right)$ are both greater than zero, the condition $\left(1-\gamma_k^*/\gamma_{0,k}\right) > 0$ must hold. ■

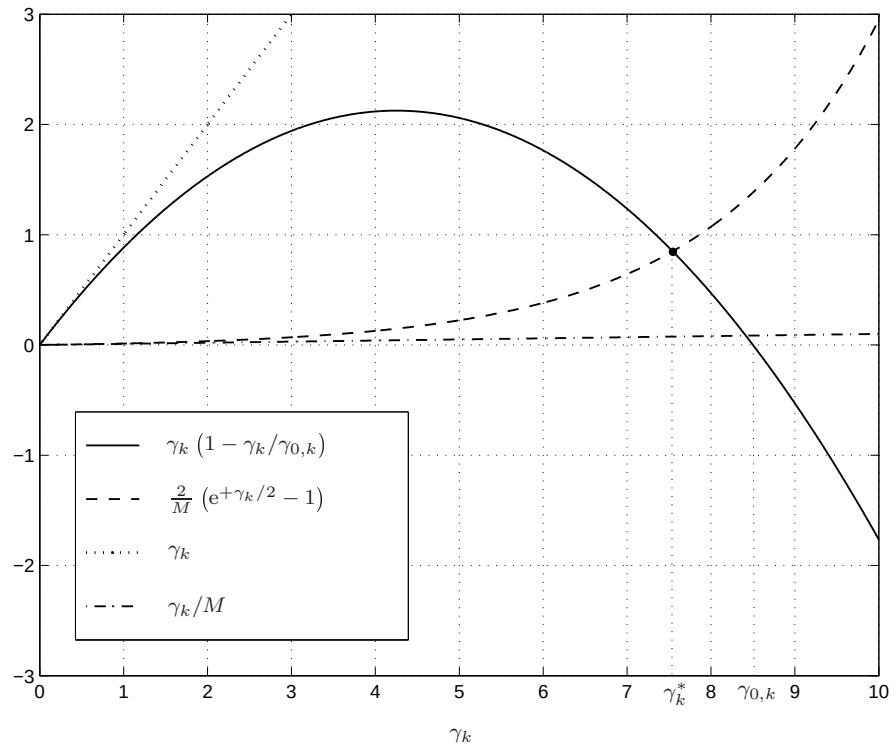

Figure 3.3: *Illustration of the equilibrium point ($\gamma_{0,k} = 8.5 = 9.3$ dB, $\ell = M = 100$).*

3.3.2 Uniqueness of the pure-strategy Nash equilibrium

The Nash equilibrium can be seen from another point of view. Using the concepts introduced in Sect. 1.2.2, the power level chosen by a *rational* self-optimizing user constitutes a *best response* to the powers chosen by other players. Formally, terminal k's best response $r_k : \mathcal{P}_{\setminus k} \to \mathcal{P}_k$ is the correspondence that assigns to each $\mathbf{p}_{\setminus k} \in \mathcal{P}_{\setminus k}$ the set

$$r_k\left(\mathbf{p}_{\setminus k}\right) = \left\{p_k \in \mathcal{P}_k : u_k\left(p_k, \mathbf{p}_{\setminus k}\right) \geq u_k\left(p_k', \mathbf{p}_{\setminus k}\right) \quad \text{for all } p_k' \in \mathcal{P}_k\right\}, \tag{3.12}$$

where $\mathcal{P}_{\setminus k}$ is the strategy space of all users excluding user k.

With the notion of a terminal's best response, the Nash equilibrium can be restated in a compact form: the power vector $\mathbf{p}^*$ is a Nash equilibrium of the NPCG $\mathcal{G} =$

$[\mathcal{K}, \{\mathcal{P}_k\}, \{u_k(\mathbf{p})\}]$ if and only if $p_k^* \in r_k\left(\mathbf{p}_{\setminus k}^*\right)$ for all $k \in \mathcal{K}$.

Prop. 1 *Using the above definition in the NPCG, with a slight abuse of notation, terminal k's best response to a given interference vector* $\mathbf{p}_{\setminus k}$ *is [110]*

$$r_k\left(\mathbf{p}_{\setminus k}\right) = \min(\overline{p}, p_k^*), \tag{3.13}$$

where

$$\begin{aligned} p_k^* &= \arg\max_{p_k \in \mathbb{R}^+} u_k\left(p_k, \mathbf{p}_{\setminus k}\right) \\ &= \frac{\gamma_k^*\left(\sum_{j \neq k} h_{kj}^{(MAI)} p_j + \sigma^2\right)}{h_k^{(SP)}\left(1 - \gamma_k^*/\gamma_{0,k}\right)} \end{aligned} \tag{3.14}$$

is the unconstrained maximizer of the utility in (3.3) (see Fig. 3.2). Furthermore, p_k^* *is unique.*

Proof Using Theorem 3, for a given interference, the SINR γ_k^* corresponds to the transmit power p_k^* as in (3.14). Since γ_k^* is the unique maximizer of the utility, the correspondence between the transmit power and the SINR must be studied. As can be verified, (3.14) represents the equation of a hyperbola passing through the origin, with the asymptotes parallel to the Cartesian axes. In particular, the vertical asymptote is $\gamma_k^* = \gamma_{0,k}$. Therefore, using Lemma 1, there exists a one-to-one correspondence between the transmit power, $p_k^* \in [0, +\infty)$, and the SINR, $\gamma_k^* \in [0, \gamma_{0,k})$. Thus, p_k^* is also unique. If $p_k^* \notin \mathcal{P}_k$ for some user k, since it is not a feasible point, then p_k^* cannot be the best response to a given $\mathbf{p}_{\setminus k}$. In this case, we observe that $\partial u_k(\mathbf{p}) / \partial p_k \leq 0$ for any $\gamma_k \leq \gamma_k^*$, and hence for any $p_k \leq p_k^*$. This implies that the utility function is increasing in that region. Since $\overline{p}$ is the largest power in the strategy space, it yields the highest utility among all $p_k \leq \overline{p}$ and thus is the best response to $\mathbf{p}_{\setminus k}$. ■

It is worth noting that, at any equilibrium of the NPCG, a terminal either attains the utility maximizing SINR γ_k^* or it fails to do so and transmits at maximum power $\overline{p}$.

Theorem 4 *The NPCG* $\mathcal{G} = [\mathcal{K}, \{\mathcal{P}_k\}, \{u_k(\mathbf{p})\}]$ *has a unique pure-strategy Nash equilibrium.*

Proof By Theorem 3, we know that there exists an equilibrium in the NPCG. Let $\mathbf{p}$ denote the Nash equilibrium in the NPCG. By definition, the Nash equilibrium must satisfy $\mathbf{p} = \mathbf{r}(\mathbf{p})$, where $\mathbf{r}(\mathbf{p}) = [r_1(\mathbf{p}), \ldots, r_K(\mathbf{p})]$.

Using Yates' framework [137], the fixed point $\mathbf{p} = \mathbf{r}(\mathbf{p})$ is unique if the correspondence $\mathbf{r}(\mathbf{p})$ is a *standard function*, i.e., if it satisfies the following properties:

1. positivity: $\mathbf{r}(\mathbf{p}) > 0$;
2. monotonicity: if $\mathbf{p} \geq \mathbf{p}'$, then $\mathbf{r}(\mathbf{p}) \geq \mathbf{r}(\mathbf{p}')$;
3. scalability: for all $\eta > 1$, $\eta\mathbf{r}(\mathbf{p}) > \mathbf{r}(\eta\mathbf{p})$.

It is apparent that $r_k(\mathbf{p}) = r_k(\mathbf{p}_{\setminus k})$. Taking into account (3.13) and (3.14), the first condition translates into $p_k^* > 0$ for all $k \in \mathcal{K}$. Using (2.6), (2.9) and (3.11), the proof is straightforward. Recalling (3.13) and (3.14), the second and the third condition are also apparent, since $\mathbf{p}_{\setminus k}$ modifies only the numerator of (3.14). Therefore, since $\mathbf{r}(\mathbf{p})$ is a standard function, the Nash equilibrium of the NPCG is unique. ■

3.4 The best-response iterative algorithm

3.4.1 Implementation

In the following, we present an iterative algorithm that applies to the UWB wireless network described in Chapter 2 to distributely achieve the Nash equilibrium of the NPCG proposed in Sect. 3.3. This algorithm is applicable to all types of Rake receivers, as well as to any kind of channel model. The description of the algorithm is as follows.

The best-response power-control (BRPC) algorithm

Consider a network with K users, a processing gain $N = N_f \cdot N_c$, a channel with L fading paths, and a maximum transmit power $\overline{p}$.

1. Simulate the channel fading coefficients $\boldsymbol{\alpha}_k$ for all users according to the chosen channel model.
2. Set the Rake receivers coefficients $\boldsymbol{\beta}_k$ for all users according to the chosen receiver (i.e., according to the processing matrix $\mathbf{G}$).

3. Compute the SP term, $h_k^{(\mathrm{SP})}$, the SI term, $h_k^{(\mathrm{SI})}$, the MAI term, $h_{kj}^{(\mathrm{MAI})}$, according to (2.7)-(2.9), and the optimum SINR, γ_k^*, solution of (3.6), for all users.
4. Initialize randomly the transmit powers of all users $\mathbf{p}^{(0)}$ within the range $[0, \overline{p}]$.
5. Set $m = 0$.
6. Compute the received SINR $\gamma_k^{(m)}$ at the AP for each user according to (2.6).
7. Set $k = 1$.
8. Adjust the kth transmit power according to (3.13) and to
$$p_k^{(m+1)} = p_k^{(m)} \cdot \frac{\gamma_k^*}{\gamma_k^{(m)}} \cdot \frac{1 - \gamma_k^{(m)}/\gamma_{0,k}}{1 - \gamma_k^*/\gamma_{0,k}}, \tag{3.15}$$
where $\gamma_{0,k}$ is defined as in (3.7).
9. $k = k + 1$.
10. If $k \leq K$, then go back to Step 8.
11. $m = m + 1$.
12. Stop if the powers have converged; otherwise, go to Step 6.

This is a best-response algorithm, since at each stage m a user decides to transmit at a power that maximizes its own utility (i.e., its best-response strategy), given the current conditions of the system. Note that, from (3.6), γ_k^* depends on the efficiency function $f(\gamma_k)$ and the SSIR $\gamma_{0,k}$ only. This means that γ_k^* can be assumed constant when the channel characteristics remain unchanged, irrespective of the transmit powers $\mathbf{p}^{(m)}$ and of the channel coefficients of the other users. As will be better shown in Chapter 4, this allows the users to compute their own γ_k^* at Step 3 independently of each other before the iterative updating mechanism starts.

Looking at Step 8, it may appear from (3.14) that the each user should know its own transmit power $p_k^{(m)}$ and SSIR $\gamma_{0,k}$, as well as some other quantities ($p_j^{(m)}$ and $h_{kj}^{(\mathrm{MAI})}$ for $j \neq k$) relevant to all of the other users in the network. On the contrary, it turns out that user k only needs to know its own received SINR at the AP $\gamma_k^{(m)}$. In fact, the term due to interference-plus-noise in (3.14) can be obtained from (2.6) as
$$\sum_{j \neq k} h_{kj}^{(\mathrm{MAI})} p_j^{(m)} + \sigma^2 = h_k^{(\mathrm{SP})} p_k^{(m)} \cdot \frac{1 - \gamma_k^{(m)}/\gamma_{0,k}}{\gamma_k^{(m)}}, \tag{3.16}$$

where $p_k^{(m)}$ is the transmit power of user k at the mth iteration. Therefore, after straightforward manipulation, (3.14) translates into the noncooperative update (3.15). The received SINR $\gamma_k^{(m)}$ can be fed back to the user terminal from the AP, along with SP and SI terms. This represents the only amount of feedback information required by the BRPC algorithm, which allows for a completely distributed scheme. Note that (3.15) reduces to the update mechanism in the algorithm by Foschini and Miljanic when $\gamma_{0,k} \to \infty$. This degenerated case will be further detailed in Chapter 4.

Finally, it is worth noting that the BRPC algorithm works for any initial transmit power vector $\mathbf{p}^{(0)}$, as stated in Step 4. However, the total amount of power consumed by each user k to reach the Nash equilibrium can be reduced by a proper choice of the initial allocation $\mathbf{p}^{(0)}$, which assumes that the networks is a single-user (SU) system.

Prop. 2 *If each user k chooses $p_k^{(0)}$ such that*

$$p_k^{(0)} = \min\left(\overline{p}, p_{k,SU}^{(0)}\right), \tag{3.17}$$

where

$$p_{k,SU}^{(0)} = \frac{\sigma^2}{h_k^{(SP)}} \cdot \frac{\gamma_k^*}{1 - \gamma_k^*/\gamma_{0,k}}, \tag{3.18}$$

the updated transmit powers $\left\{p_k^{(m)}\right\}$ represent a nondecreasing sequence converging to the Nash equilibrium.

Proof The sequence $\left\{p_k^{(m)}\right\}$ is nondecreasing if and only if $p_k^{(m+1)} \geq p_k^{(m)}$ for all m. In view of the update (3.15), this is verified if and only if $\gamma_k^{(m)} \leq \gamma_k^*$ for all m. In particular, this condition must hold for $m = 0$. Supposing $p_{k,SU}^{(0)} \leq \overline{p}$, combining (2.6) and (3.18) yields

$$\begin{aligned}
\gamma_k^{(0)} &= \frac{\sigma^2 \cdot \gamma_k^* / \left(1 - \gamma_k^*/\gamma_{0,k}\right)}{\frac{\sigma^2}{\gamma_{0,k}} \cdot \gamma_k^* / \left(1 - \gamma_k^*/\gamma_{0,k}\right) + \sum_{j \neq k} h_{kj}^{(\mathrm{MAI})} p_j^{(0)} + \sigma^2} \\
&\leq \frac{\sigma^2 \cdot \gamma_k^* / \left(1 - \gamma_k^*/\gamma_{0,k}\right)}{\frac{\sigma^2}{\gamma_{0,k}} \cdot \gamma_k^* / \left(1 - \gamma_k^*/\gamma_{0,k}\right) + \sigma^2} \\
&= \left(\frac{1}{\gamma_{0,k}} + \frac{1 - \gamma_k^*/\gamma_{0,k}}{\gamma_k^*}\right)^{-1} \\
&= \gamma_k^*,
\end{aligned} \tag{3.19}$$

Table 3.1: *List of parameters used in the simulations.*

K, number of users	4
L, number of channel paths	20
N_c, number of possible pulse positions in a frame	10
N_f, number of frames	8
M, total number of bits per packet	100 b
D, number of information bits per packet	100 b
R, bit rate	100 kb/s
σ^2, AWGN power at the receiver	5×10^{-16} W
$\overline{p}$, maximum power constraint	1 nW

where the inequality follows from $h_{kj}^{(\mathrm{MAI})} p_j^{(0)} \geq 0$ for all $j \neq k$. Hence, $p_k^{(1)} \geq p_k^{(0)}$ when $p_k^{(0)} = p_{k,SU}^{(0)}$.

If this mechanism is employed by all users in the network, $\mathbf{p}^{(1)} \geq \mathbf{p}^{(0)}$. In view of the monotonicity of standard function $\mathbf{r}(\mathbf{p})$, shown in the proof of Theorem 4, the sequence $\left\{\mathbf{p}^{(m)}\right\}$ is nondecreasing and bounded above by $\mathbf{p}^*$. Theorem 4 implies that $\left\{\mathbf{p}^{(m)}\right\}$ must converge to $\mathbf{p}^*$.

This conclusion holds even if $p_{k,SU}^{(0)} > \overline{p}$ for some users $k \in \mathcal{K}$. By means of Lemma 1, which states the monotonic one-to-one correspondence between $p_k^{(m)}$ and $\gamma_k^{(m)}$, $\gamma_k^{(0)} = \gamma_k\left(\overline{p}, \mathbf{p}_{\backslash k}\right) < \gamma_k\left(p_{k,SU}^{(0)}, \mathbf{p}_{\backslash k}\right)$. Therefore, (3.19) still holds, and the same conclusion applies. ■

Fig. 3.4 reports the transmit power $p_k^{(m)}$ for a generic user k as a function of the iteration index m for a particular network snapshot. Simulations are performed using the design parameters listed in Table 3.1. We use the efficiency function $f(\gamma_k) = (1 - \mathrm{e}^{-\gamma_k/2})^M$ as a reasonable approximation to the PSR [50, 110]. To model the UWB scenario, the channel gains are assumed to be Rayleigh-distributed. A detailed discussion on the channel model is provided in Chapter 4. The solid line shows the update sequence when all users choose their initial transmit powers according to (3.17) and (3.18). The dashed and dotted lines represent the update sequences for

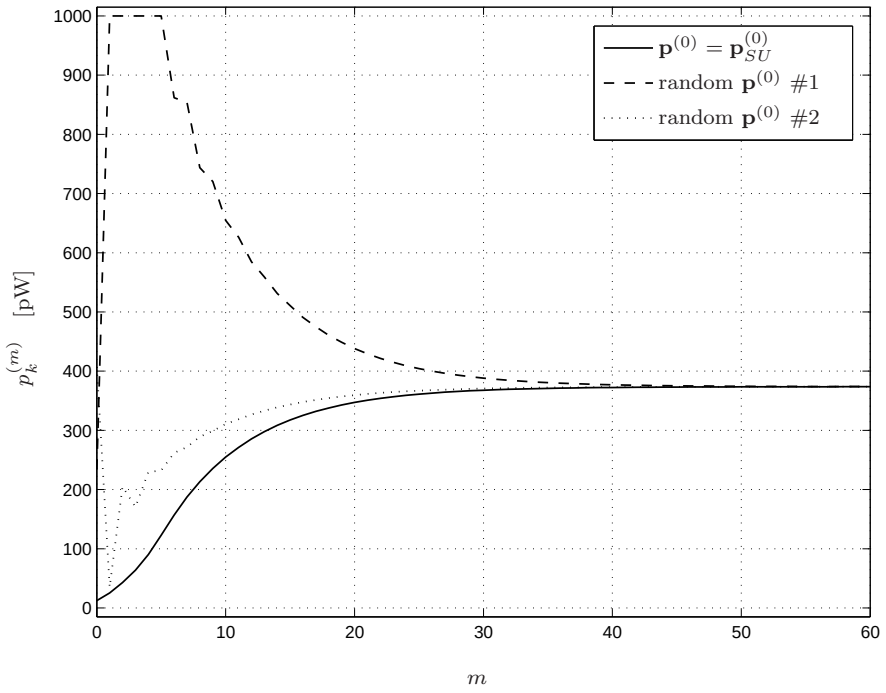

Figure 3.4: *Transmit power as a function of the iteration step for a generic user k.*

two random allocations $\mathbf{p}^{(0)}$. As can be seen, the initialization outlined in Prop. 2 produces a nondecreasing sequence that converges to the transmit power p_k^* faster than the others and saving as much power as possible. It is worth noting that a distributed implementation is possible even in this case, provided that the terminals are able to measure the output variance due to ambient AWGN σ^2.

Similarly, Fig. 3.5 depicts the achieved SINR $\gamma_k^{(m)}$ for the network realization used for the results of Fig. 3.4. Analogous considerations about the behavior of the algorithm can be drawn.

3.4.2 Convergence to the Nash equilibrium

The BRPC algorithm can be shown to converge to a unique fixed point using the properties of standard power control [137], following the same steps as in the proof of

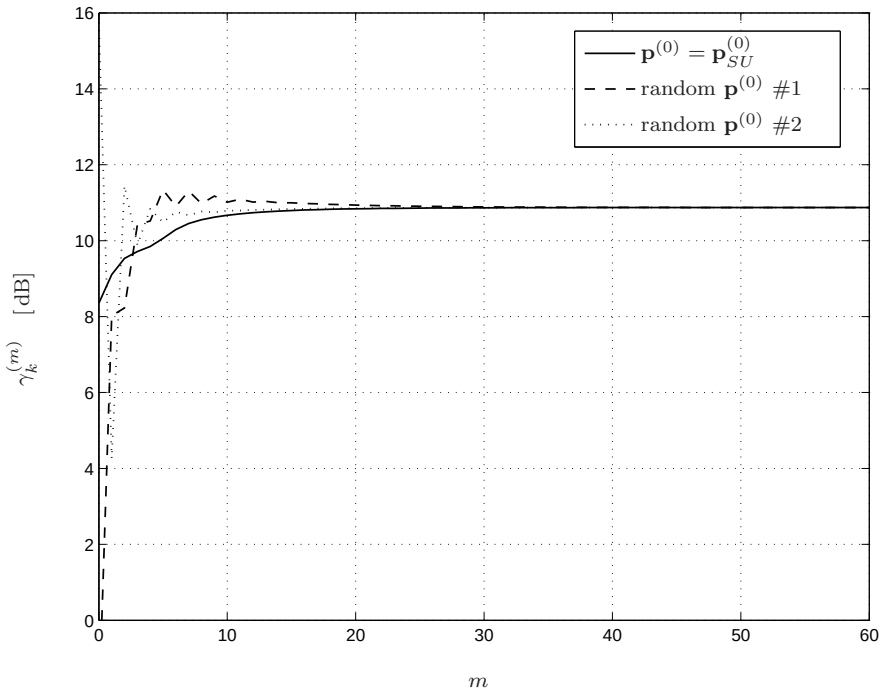

Figure 3.5: *Achieved SINR at the AP as a function of the iteration step for a generic user k.*

Theorem 4.

In fact, the existence of (at least) one pure-strategy Nash equilibrium in the NPCG $\mathcal{G} = [\mathcal{K}, \{\mathcal{P}_k\}, \{u_k(\mathbf{p})\}]$ is ensured by Theorem 3, whereas the uniqueness is shown in Theorem 4. Since the update (3.15) represents the best response p_k^* to a given set of interferers $\mathbf{p}_{\setminus k}$, it is apparent that the unique fixed point of the BRPC algorithm corresponds to the unique Nash equilibrium of the NPCG $\mathcal{G}$. Hence, the BRPC algorithm can be used to allow all the terminals in the considered network to achieve the Nash equilibrium of $\mathcal{G}$ in a distributed manner.

The convergence of the BRPC algorithm can also be verified using the analytical tools of game theory. As stated in Sect. 3.3, the NPCG $\mathcal{G}$ represents a static (strategic-form) game. Following the definitions introduced in Sect. 1.3, it is apparent that, by

iterating the game $\mathcal{G}$ through the BRPC algorithm, the users in the network play a repeated myopic game. The shortsight lies in that the users do not consider the convergence speed of the algorithm, i.e., the proposed formulation of the game does not assign a discount factor to each iteration of the BRPC algorithm.

To prove that the BRPC algorithm converges to the unique Nash equilibrium of the proposed game $\mathcal{G}$, we resort to the theory of *supermodular games*, introduced in 1979 by Topkis [123, 124] and used by Saraydar [110] and Altman and Altman [6] in the context of power control. In a supermodular power control game, each player's desire to increase its power increases with an increase in other players' power, i.e., the best response of a terminal is monotone nondecreasing in interferers' (opponents') strategy. Using a method similar to that described in [110], the repeated game $\mathcal{G}$ can be shown to belong to the class of supermodular games. This allows the convergence of the algorithm to be studied through the analytical tools derived in [124]. Such tools are expedient to prove that the distributed scheme proposed in Sect. 3.4.1 leads to a system of best-response correspondences that have a unique fixed point, i.e., that the BRPC algorithm converges to the unique Nash equilibrium of the NPCG $\mathcal{G}$ discussed in Sect. 3.3.

Chapter 4

Analysis of the Nash equilibrium

In Chapter 3, we have proven that a Nash equilibrium for the proposed noncooperative power control game exists and is unique. In this Chapter, we study the properties of this equilibrium.

In particular, Sect. 4.1 identifies the main properties of the Nash solution of the power control game, which is shown to depend on the interfering terms due to SI and MAI. To provide a theoretical description of the Nash equilibrium which is independent of the channel snapshot, Sect. 4.2 proposes a large-system analysis of the interference. To better understand the interplay between the network parameters and the performance of the distributed algorithm, a specific channel model is considered. Making use of the asymptotical values for SI and MAI terms derived in Sect. 4.2, Sect. 4.3 shows the analytical description of the relevant performance indexes of the network, namely transmit powers and achieved utilities. System design criteria, such as minimum spreading factor and loss of PRake-based networks with respect to ARake-based networks, are also derived. Simulation results are presented to validate the theoretical analysis.

4.1 Properties of the Nash equilibrium

Although the existence of a unique pure-strategy Nash equilibrium in the NPCG $\mathcal{G}$ described in Sect. 3.3 is ensured by Theorems 3 and 4, it is of interest to study the properties of this solution and thus to evaluate the performance of the system. Fur-

thermore, the knowledge of the main features of the Nash solution can also profitably serve as a network design criterion, as is better explained in the remainder of this chapter.

As is apparent from inspecting (3.6), unlike previous work in this area (e.g., [79, 85, 110, 114]), the SINR achieved at the Nash equilibrium γ_k^* is dependent on k. This is due to the SI term in (2.6), which arises when modeling the wireless channel as a frequency-selective one. As a consequence, at the Nash equilibrium each user attains a different level of SINR. More importantly, the only term dependent on k in (3.6) is the SSIR $\gamma_{0,k}$, which is affected only by the channel of user k. This means that γ_k^* can be assumed constant when the channel characteristics remain unchanged, irrespective of the transmit powers $\mathbf{p}$ and of the channel coefficients of the other users. For convenience of notation, we can express γ_k^* as a function of $\gamma_{0,k}$:

$$\gamma_k^* = \Gamma\left(\gamma_{0,k}\right). \tag{4.1}$$

Fig. 4.1 shows the shape of γ_k^* as a function of $\gamma_{0,k}$, where the efficiency function is taken as $f\left(\gamma_k\right) = \left(1 - \mathrm{e}^{-\gamma_k/2}\right)^M$, with $M = 100$. Even though γ_k^* is shown for values of $\gamma_{0,k}$ approaching 0 dB, it is worth emphasizing that $\gamma_{0,k} > 10$ dB in most practical situations.

As can be noticed, the NPCG proposed herein represents a generalization of the power control games discussed thoroughly in literature [40, 55, 79, 85, 109, 110], in which the power update mechanism follows the formulation by Foschini and Miljanic. If $L = 1$, i.e., in a flat-fading scenario, we obtain from (2.8) and (3.7) that $\gamma_{0,k} = \infty$ for all k. This implies that $\gamma_k^* = \Gamma\left(\infty\right) = \overline{\gamma}^*$ is the same for every $k \in \mathcal{K}$, and thus it is possible to apply the approach proposed, e.g., in [110].

Assumption 1 *To simplify the analysis, let us assume the typical case of multiuser UWB systems, where $N \gg K$. In addition, $\overline{p}$ is considered sufficiently large that $p_k < \overline{p}$ for those users who achieve γ_k^*. In particular, when $N \gg K$, at the Nash equilibrium the following property holds:*

$$h_k^{(SP)} p_k^* \simeq q > 0, \qquad \forall k \in \mathcal{K}. \tag{4.2}$$

The heuristic derivation of (4.2) can be justified by SI reduction due to the hypothesis $N \gg K > 1$. Using (2.8), $\gamma_{0,k} \gg 1$ for all k. Hence, the noncooperative solution will be similar to that studied, e.g., in [79].

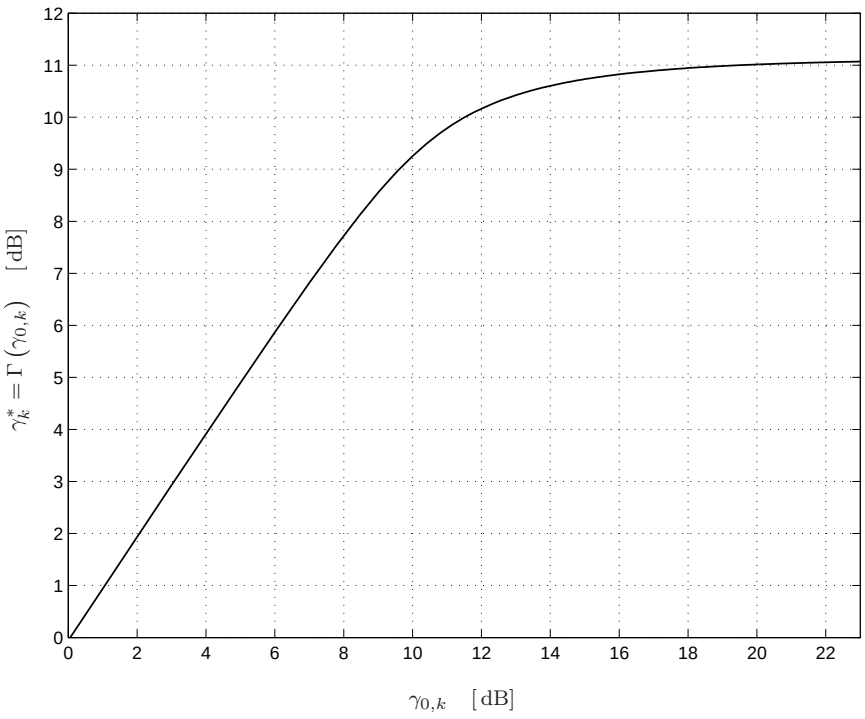

Figure 4.1: *Shape of γ_k^* as a function of $\gamma_{0,k}$ ($M = 100$).*

The validity of this assumption is verified through extensive simulations using the UWB channel model reported in [28]. Table 4.1 reports the ratio σ_q^2/η_q^2 of the variance σ_q^2 to the squared mean value η_q^2 of the values $q = h_k^{(\mathrm{SP})} p_k^*$, obtained averaging 10 000 realizations of channel coefficients for different network parameters using ARake receivers. We can see that, when the processing gain is much greater than the number of users, $\sigma_q^2/\eta_q^2 \ll 1$. Hence, (4.2) can be used to carry out the theoretical analysis of the Nash equilibrium. It is worth emphasizing that similar results are achieved using different channel models and/or PRake receivers.

The following proposition helps identify the Nash equilibrium for a given set of channel realizations.

Prop. 3 *A necessary and sufficient condition for a desired SINR γ_k^* to be achievable*

Table 4.1: *Ratio σ_q^2/η_q^2 for different network parameters.*

	(L,K)			
(N_c,N_f)	*(20,8)*	*(20,16)*	*(50,8)*	*(50,16)*
(30,10)	$9.4\text{E}-4$	$3.2\text{E}-3$	$4.8\text{E}-4$	$1.7\text{E}-3$
(30,50)	$2.9\text{E}-5$	$6.4\text{E}-5$	$1.6\text{E}-5$	$3.4\text{E}-5$
(50,10)	$2.9\text{E}-4$	$6.8\text{E}-4$	$1.5\text{E}-4$	$3.7\text{E}-4$
(50,50)	$1.0\text{E}-5$	$2.2\text{E}-5$	$0.6\text{E}-5$	$1.2\text{E}-5$
(100,10)	$6.7\text{E}-5$	$1.5\text{E}-4$	$3.7\text{E}-5$	$7.8\text{E}-5$
(100,50)	$0.3\text{E}-5$	$0.6\text{E}-5$	$0.1\text{E}-5$	$0.3\text{E}-5$

is

$$\gamma_k^* \cdot \left(\gamma_{0,k}^{-1} + \zeta_k^{-1}\right) < 1, \quad \forall k \in \mathcal{K}, \tag{4.3}$$

where $\gamma_{0,k}$ is defined as in (3.7), and

$$\zeta_k^{-1} = \sum_{\substack{j=1 \\ j\neq k}}^{K} \frac{h_{kj}^{(MAI)}}{h_j^{(SP)}}. \tag{4.4}$$

When (4.3) holds, each user can reach the optimum SINR, and the minimum power solution to do so is to assign each user k a transmit power

$$p_k^* = \frac{1}{h_k^{(SP)}} \cdot \frac{\sigma^2 \gamma_k^*}{1 - \gamma_k^* \cdot \left(\gamma_{0,k}^{-1} + \zeta_k^{-1}\right)}. \tag{4.5}$$

When (4.3) does not hold, the users cannot achieve γ_k^* simultaneously, and some of them would end up transmitting at the maximum power $\overline{p}$.

Proof Based on Prop. 1, when all users reach the Nash equilibrium, their transmit powers are

$$p_k^* = \frac{\gamma_k^* \left(\sum_{j\neq k} h_{kj}^{(\mathrm{MAI})} p_j^* + \sigma^2\right)}{h_k^{(\mathrm{SP})} \left(1 - \gamma_k^*/\gamma_{0,k}\right)}. \tag{4.6}$$

Using Assumption 1 in (4.6), it is straightforward to obtain:

$$q \cdot \left[1 - \gamma_k^* \cdot \left(\gamma_{0,k}^{-1} + \zeta_k^{-1}\right)\right] = \sigma^2 \gamma_k^* > 0, \tag{4.7}$$

which implies

$$\gamma_k^* \cdot \left(\gamma_{0,k}^{-1} + \zeta_k^{-1}\right) < 1, \tag{4.8}$$

proving necessity. It is also straightforward to show that, if each terminal k uses transmit power p_k^* as in (4.5), all terminals will achieve the SINR requirement, finishing the proof of sufficiency.

Finally, consider any other joint distribution of powers and channel realizations, and let $q' = \inf_{k\in\mathcal{K}} \left\{h_k^{(\mathrm{SP})} p_k^*\right\}$. Then, from (4.6), by definition of q', for some k

$$q' = \frac{\gamma_k^* \left(\sum_{j\neq k} h_{kj}^{(\mathrm{MAI})} p_j^* + \sigma^2\right)}{1 - \gamma_k^*/\gamma_{0,k}}. \tag{4.9}$$

Hence,

$$\begin{aligned} q'\left(1 - \gamma_k^*/\gamma_{0,k}\right) &= \gamma_k^* \left(\sum_{j\neq k} h_{kj}^{(\mathrm{MAI})} p_j^* + \sigma^2\right) \\ &= \gamma_k^* \left(\sum_{j\neq k} \frac{h_{kj}^{(\mathrm{MAI})}}{h_j^{(\mathrm{SP})}} \cdot h_j^{(\mathrm{SP})} p_j^* + \sigma^2\right) \\ &\geq \gamma_k^* \left(\sum_{j\neq k} \frac{h_{kj}^{(\mathrm{MAI})}}{h_j^{(\mathrm{SP})}} q' + \sigma^2\right) \\ &= \gamma_k^* \left(\zeta_k^{-1} q' + \sigma^2\right), \end{aligned} \tag{4.10}$$

where the inequality holds due to definition of q'. Therefore,

$$q'\left(1 - \gamma_k^*/\gamma_{0,k} - \gamma_k^*/\zeta_k\right) \geq \gamma_k^* \sigma^2, \tag{4.11}$$

and thus

$$q' \geq \frac{\sigma^2 \gamma_k^*}{1 - \gamma_k^* \left(\gamma_{0,k}^{-1} + \zeta_k^{-1}\right)} = q. \tag{4.12}$$

By definition, $q' = q$.

This means that assigning powers according to (4.5) does indeed give the minimal power solution. ■

4.2 Large-system analysis of the interference

Based on Prop. 3, the amount of transmit power p_k^* required to achieve the target SINR γ_k^* will depend not only on the gain $h_k^{(\mathrm{SP})}$, but also on the SI term $h_k^{(\mathrm{SI})}$ (through $\gamma_{0,k}$) and the interferers $h_{kj}^{(\mathrm{MAI})}$ (through ζ_k). In order to derive some quantitative results for the utility function and for the transmit powers independent of SI and MAI terms, it is possible to resort to a *large-system analysis* [14]. For convenience of notation, we introduce the following definitions, with $\mathbb{V}\mathrm{ar}[\cdot]$ denoting the variance of a random variable:

- let $\mathbf{D}_j^{\alpha}$ be a diagonal matrix whose elements are

$$\left\{\mathbf{D}_j^{\alpha}\right\}_l = \sqrt{\mathbb{V}\mathrm{ar}\left[\alpha_l^{(j)}\right]}; \tag{4.13}$$

- let $\mathbf{D}_k^{\beta}$ be a diagonal matrix whose elements are

$$\left\{\mathbf{D}_k^{\beta}\right\}_l = \sqrt{\mathbb{V}\mathrm{ar}\left[\beta_l^{(k)}\right]}; \tag{4.14}$$

- let $\mathbf{C}_j^{\alpha}$ be an $L \times (L-1)$ matrix whose elements are

$$\left\{\mathbf{C}_j^{\alpha}\right\}_{li} = \sqrt{\frac{\mathbb{V}\mathrm{ar}\left[\{\mathbf{A}_j\}_{li}\right]}{L}}; \tag{4.15}$$

- let $\mathbf{C}_j^{\beta}$ be an $L \times (L-1)$ matrix whose elements are

$$\left\{\mathbf{C}_k^{\beta}\right\}_{li} = \sqrt{\frac{\mathbb{V}\mathrm{ar}\left[\{\mathbf{B}_k\}_{li}\right]}{L}}; \tag{4.16}$$

- let $\varphi(\cdot)$ be the matrix operator

$$\varphi(\cdot) = \lim_{L\to\infty} \frac{1}{L}\,\mathrm{Tr}(\cdot), \tag{4.17}$$

  where $\mathrm{Tr}(\cdot)$ is the trace operator.

Theorem 5 *Assume that $\alpha_l^{(k)}$ are zero-mean random variables (RVs) independent across k and l, and $\mathbf{G}$ is a deterministic diagonal matrix (thus implying that $\alpha_l^{(k)}$ and $\beta_m^{(j)}$ are dependent only when $j = k$ and $m = l$). In the asymptotic case where K and*

N_f are finite,[1] *while $L, N_c \to \infty$, with the ratio N_c/L approaching a constant, the term ζ_K^{-1} converges almost surely (a.s.) to*

$$\zeta_k^{-1} \overset{a.s.}{\to} \frac{1}{N} \sum_{\substack{j=1 \\ j \neq k}}^{K} \frac{\varphi\left(\mathbf{D}_j^{\alpha} \mathbf{C}_k^{\beta} \mathbf{C}_k^{\beta^H} \mathbf{D}_j^{\alpha}\right) + \varphi\left(\mathbf{D}_k^{\beta} \mathbf{C}_j^{\alpha} \mathbf{C}_j^{\alpha^H} \mathbf{D}_k^{\beta}\right)}{\varphi\left(\mathbf{D}_j^{\alpha} \mathbf{D}_j^{\beta}\right) \cdot \varphi\left(\mathbf{D}_k^{\alpha} \mathbf{D}_k^{\beta}\right)}. \tag{4.18}$$

Proof To prove that $N\zeta_k^{-1}$ converges a.s. to non-random limits, we focus on the ratio

$$\begin{aligned} N \frac{h_{kj}^{(\mathrm{MAI})}}{h_j^{(\mathrm{SP})}} &= \frac{\left|\left|\mathbf{B}_k^H \cdot \boldsymbol{\alpha}_j\right|\right|^2 + \left|\left|\mathbf{A}_j^H \cdot \boldsymbol{\beta}_k\right|\right|^2 + \left|\boldsymbol{\beta}_k^H \cdot \boldsymbol{\alpha}_j\right|^2}{\left(\boldsymbol{\beta}_k^H \cdot \boldsymbol{\alpha}_k\right) \cdot \left(\boldsymbol{\beta}_j^H \cdot \boldsymbol{\alpha}_j\right)} \\ &= \frac{\frac{1}{L^2}\left[\left|\left|\mathbf{B}_k^H \cdot \boldsymbol{\alpha}_j\right|\right|^2 + \left|\left|\mathbf{A}_j^H \cdot \boldsymbol{\beta}_k\right|\right|^2 + \left|\boldsymbol{\beta}_k^H \cdot \boldsymbol{\alpha}_j\right|^2\right]}{\frac{1}{L}\left(\boldsymbol{\beta}_k^H \cdot \boldsymbol{\alpha}_k\right) \cdot \frac{1}{L}\left(\boldsymbol{\beta}_j^H \cdot \boldsymbol{\alpha}_j\right)}. \end{aligned} \tag{4.19}$$

It is sufficient to show that both numerator and denominator of (4.19) converge a.s. to a non-random limit. Let

$$\begin{aligned} \boldsymbol{\beta}_k &= \mathbf{G}\boldsymbol{\alpha}_k \\ &= \left(\mathbf{G} \circ \mathbf{D}_k^{\alpha}\right) \mathbf{w}^{(k)} \\ &= \mathbf{D}_k^{\beta} \mathbf{w}^{(k)}, \end{aligned} \tag{4.20}$$

where

$$\mathbf{w}^{(k)} = \left(\mathbf{D}_k^{\alpha}\right)^{-1} \boldsymbol{\alpha}_k; \tag{4.21}$$

$\mathbf{D}_k^{\alpha}$ and $\mathbf{D}_k^{\beta}$ are defined as in (4.13) and (4.14), respectively; the operator $\circ$ denotes the Hadamard (element-wise) product; and the matrix $\mathbf{G}$ is dependent on the type of Rake receiver employed. Using (4.20) and (4.21), by Theorem 7, presented in the

[1] In order for the analysis to be consistent, and also considering regulations by the FCC [31], it is worth noting that N_f could not be smaller than a certain threshold ($N_f \geq 5$).

Appendix A, we obtain

$$\begin{aligned}\frac{1}{L^2}\left|\left|\mathbf{B}_k^H\cdot\boldsymbol{\alpha}_j\right|\right|^2 &\overset{a.s.}{\to} \varphi\left(\frac{1}{L}\mathbf{D}_j^{\alpha}\mathbf{B}_k\mathbf{B}_k^H\mathbf{D}_j^{\alpha}\right)\\ &= \lim_{L\to\infty}\frac{1}{L^2}\sum_{i=1}^{L}\{\mathbf{D}_j^{\alpha}\}_i^2\sum_{l=i+1}^{L}\left(\beta_l^{(k)}\right)^2\\ &= \lim_{L\to\infty}\frac{1}{L^2}\sum_{l=1}^{L-1}\left(\beta_{l+1}^{(k)}\right)^2\sum_{m=1}^{l}\{\mathbf{D}_j^{\alpha}\}_m^2\\ &= \lim_{L\to\infty}\frac{1}{L}\sum_{l=1}^{L-1}\chi_l, \end{aligned}\tag{4.22}$$

where $\varphi(\cdot)$ is defined as in (4.17), and

$$\chi_l = \frac{1}{L}\left(\beta_{l+1}^{(k)}\right)^2\sum_{m=1}^{l}\left\{\mathbf{D}_j^{\alpha}\right\}_m^2 \tag{4.23}$$

are independent random variables, with

$$\mathbb{E}\left[\chi_l\right] = \frac{1}{L}\left\{\mathbf{D}_k^{\beta}\right\}_{l+1}^2\sum_{m=1}^{l}\left\{\mathbf{D}_j^{\alpha}\right\}_m^2 \tag{4.24}$$

and

$$\begin{aligned}\mathbb{V}\mathrm{ar}\left[\chi_l\right] &= \frac{1}{L^2}\mathbb{V}\mathrm{ar}\left[\left(\beta_{l+1}^{(k)}\right)^2\right]\left(\sum_{m=1}^{l}\left\{\mathbf{D}_j^{\alpha}\right\}_m^2\right)^2\\ &\le \mathbb{V}\mathrm{ar}\left[\left(\beta_{l+1}^{(k)}\right)^2\right]\cdot\left(\frac{\mathrm{Tr}\left(\left(\mathbf{D}_j^{\alpha}\right)^2\right)}{L}\right)^2\\ &< \infty. \end{aligned}\tag{4.25}$$

Using the weak version of the law of large numbers for non-i.i.d. random variables,

$$\begin{aligned}\lim_{L\to\infty}\frac{1}{L}\sum_{l=1}^{L-1}\chi_l &\overset{a.s.}{\to} \lim_{L\to\infty}\frac{1}{L}\sum_{l=1}^{L-1}\mathbb{E}\left[\chi_l\right]\\ &= \lim_{L\to\infty}\frac{1}{L^2}\sum_{l=1}^{L-1}\left\{\mathbf{D}_k^{\beta}\right\}_{l+1}^2\sum_{m=1}^{l}\{\mathbf{D}_j^{\alpha}\}_m^2\\ &= \varphi\left(\mathbf{D}_j^{\alpha}\mathbf{C}_k^{\beta}\mathbf{C}_k^{\beta H}\mathbf{D}_j^{\alpha}\right), \end{aligned}\tag{4.26}$$

where $\mathbf{C}_k^{\alpha}$ and $\mathbf{C}_k^{\beta}$ are defined as in (4.15) and (4.16), respectively.

Similar arguments yield

$$\frac{1}{L^2}\left|\left|\mathbf{A}_j^H \cdot \boldsymbol{\beta}_k\right|\right|^2 \overset{a.s.}{\to} \varphi\left(\mathbf{D}_k^{\beta}\mathbf{C}_j^{\alpha}\mathbf{C}_j^{\alpha\,H}\mathbf{D}_k^{\beta}\right). \tag{4.27}$$

Then applying Theorem 8, reported in the Appendix A, from (4.20) we obtain

$$\frac{1}{L}\boldsymbol{\beta}_k^H \cdot \boldsymbol{\alpha}_j \overset{a.s.}{\to} 0, \tag{4.28}$$

since $\boldsymbol{\beta}_k$ is independent of $\boldsymbol{\alpha}_j$. Analogously, using Theorem 7, from (4.21) we obtain

$$\frac{1}{L}\boldsymbol{\beta}_k^H \cdot \boldsymbol{\alpha}_k \overset{a.s.}{\to} \varphi\left(\mathbf{D}_k^{\alpha}\mathbf{D}_k^{\beta}\right). \tag{4.29}$$

Using (4.26)-(4.29), the result (4.18) is straightforward. ■

Theorem 6 *Assume $\alpha_l^{(k)}$ and $\mathbf{G}$ as in Theorem 5. In the asymptotic case where K and N_f are finite, while $L, N_c \to \infty$, with the ratio N_c/L approaching a constant,*

$$\gamma_{0,k}^{-1} \overset{a.s.}{\to} \frac{1}{N}\frac{\lim\limits_{L\to\infty}\dfrac{1}{L^2}\displaystyle\sum_{i=1}^{L-1}\phi_i^2 \cdot \sum_{l=1}^{i}\theta_k^2\left(l, L+l-i\right)}{\left(\varphi\left(\mathbf{D}_k^{\alpha}\mathbf{D}_k^{\beta}\right)\right)^2}, \tag{4.30}$$

where ϕ_i is defined as in (2.12) and

$$\theta_k\left(l, L+l-i\right) = \left\{\mathbf{D}_k^{\alpha}\right\}_l \left\{\mathbf{D}_k^{\beta}\right\}_{L+l-i} + \left\{\mathbf{D}_k^{\beta}\right\}_l \left\{\mathbf{D}_k^{\alpha}\right\}_{L+l-i}. \tag{4.31}$$

Proof In order to prove that $N/\gamma_{0,k}$ converges a.s. to a non-random limit, it is sufficient to show that both the numerator and the denominator converge to non-random limits. Note that

$$\begin{aligned}\left|\left|\boldsymbol{\Phi}\cdot\left(\mathbf{B}_k^H\cdot\boldsymbol{\alpha}_k + \mathbf{A}_k^H\cdot\boldsymbol{\beta}_k\right)\right|\right|^2 &= \sum_{i=1}^{L-1}\phi_i^2\cdot\left(\sum_{l=1}^{i}\alpha_l^{(k)}\beta_{L+l-i}^{(k)} + \sum_{l=1}^{i}\beta_l^{(k)}\alpha_{L+l-i}^{(k)}\right)^2 \\ &= \sum_{i=1}^{L-1}\phi_i^2\cdot\left(\sum_{l=1}^{i}\theta_k\left(l, L+l-i\right)\cdot\mathbf{w}_l^{(k)}\cdot\mathbf{w}_{L+l-i}^{(k)}\right)^2,\end{aligned} \tag{4.32}$$

where $\theta_k\left(l, L+l-i\right)$ is defined as in (4.31).

Following the same steps as in the proof of Theorem 5, after some algebraic manipulation, it can be proven that

$$\frac{1}{L^2}\left|\left|\boldsymbol{\Phi}\cdot\left(\mathbf{B}_k^H\cdot\boldsymbol{\alpha}_k+\mathbf{A}_k^H\cdot\boldsymbol{\beta}_k\right)\right|\right|^2 \overset{a.s.}{\to} \lim_{L\to\infty}\sum_{i=1}^{L-1}\phi_i^2\cdot\sum_{l=1}^{i}\frac{\theta_k^2\left(l,L+l-i\right)}{L^2}. \tag{4.33}$$

Using (4.29) and (4.33), the result (4.30) is straightforward. ■

It is worth emphasize that the results above can be applied to any kind of fading models, since only the second-order statistics are required. Furthermore, due to the symmetry of (4.18) and (4.30), it is easy to verify that the results are independent of large-scale fading models. Hence, Theorems 5 and 6 apply to any kind of channel, which may include both large- and small-scale statistics.

4.2.1 Hypotheses on the channel model

To better understand the performance of power control, in the following we derive the asymptotic values of the transmit powers p_k^* and the utilities u_k^* achieved at the Nash equilibrium by using the results (4.18) and (4.30) in a realistic UWB network scenario.

Channel modeling for UWB systems is still an open issue. In fact, while there exists a commonly agreed-on set of basic models for narrowband and wideband wireless channels [125], a similarly well accepted UWB channel model does not seem to exist. Recently, two models, namely IEEE 802.15.3a [45] and IEEE 802.15.4a [87], have been standardized to properly characterize the UWB environment. However, for ease of calculation, the expressions derived in the remainder of the paper consider the following simplifying assumptions:

- The channel gains are zero-mean independent complex Gaussian RVs with variances $\sigma_{k_l}^2$, i.e., $\alpha_l^{(k)}\sim\mathcal{CN}(0,\sigma_{k_l}^2)$. This assumption leads $\left|\alpha_l^{(k)}\right|$ to be Rayleigh-distributed with parameter $\sigma_{k_l}^2/2$. Although both IEEE 802.15.3a and 802.15.4a models include some forms of Nakagami-m distribution for the channel gains, the Rayleigh distribution, appealing for its analytical tractability, has recently been shown [112] to provide a good approximation for multipath propagation in UWB systems.

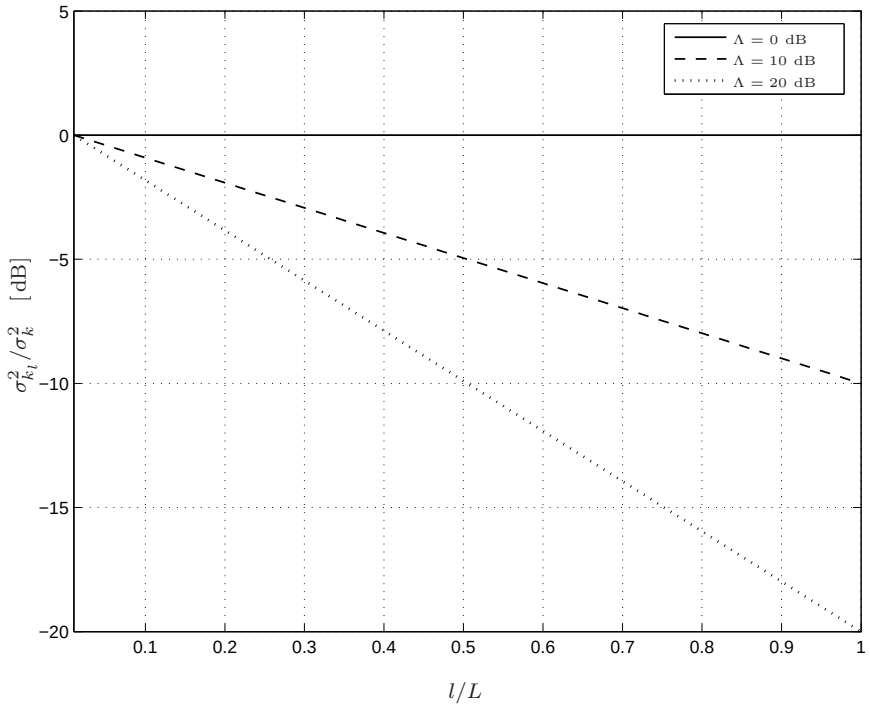

Figure 4.2: *Average power delay profile versus normalized excess delay.*

- Lately, a clustering phenomenon for the averaged power delay profile (aPDP) [62] in IR-UWB multipath channels has emerged from a large number of UWB measurement campaigns [30, 115]. However, owing to the analytical difficulties arising when considering such aspect, this work focuses on an exponentially decaying aPDP, as is customarily used in several UWB channel models [52,104]. This translates into the hypothesis

$$\sigma^2_{k_l} = \sigma^2_k \cdot \Lambda^{-\frac{l-1}{L-1}}, \tag{4.34}$$

where $\Lambda = \sigma^2_{k_1}/\sigma^2_{k_L}$ is the aPDP decay constant; and σ^2_k depends on the distance between user k and the AP. Fig. 4.2 shows the aPDP for some values of Λ versus the normalized excess delay, i.e., the ratio between the excess delay, lT_c, and the maximum excess delay considered, LT_c. It is easy to verify that $\Lambda = 0$ dB

represents the case of flat aPDP.

Using these hypotheses, the matrices $\mathbf{D}_k^{\alpha}$ and $\mathbf{D}_k^{\beta}$ can be expressed in terms of

$$\{\mathbf{D}_k^{\alpha}\}_l = \sigma_k \cdot \Lambda^{-\frac{l-1}{2(L-1)}} \cdot u\left[L-l\right], \tag{4.35}$$

$$\left\{\mathbf{D}_k^{\beta}\right\}_l = \sigma_k \cdot \Lambda^{-\frac{l-1}{2(L-1)}} \cdot u\left[r \cdot L-l\right], \tag{4.36}$$

respectively, where

$$u\left[n\right] = \begin{cases} 1, & n \geq 0, \\ 0, & n < 0. \end{cases} \tag{4.37}$$

In the following subsections, the model described above is employed to obtain closed-form expressions for the interference when PRake receivers are implemented at the AP.

4.2.2 PRake with exponentially decaying aPDP

Prop. 4 *In the asymptotic case where the hypotheses of Theorem 5 hold, when adopting a PRake with L_P coefficients according to the MRC scheme,*

$$\zeta_k^{-1} \overset{a.s.}{\rightarrow} \frac{K-1}{N} \cdot \mu\left(\Lambda, r\right), \tag{4.38}$$

where

$$\mu\left(\Lambda, r\right) = \frac{\left(\Lambda-1\right) \cdot \Lambda^{r-1}}{\Lambda^r - 1}, \tag{4.39}$$

and $r \triangleq L_P/L$, $0 < r \leq 1$.

For the sake of presentation, the proof is provided in Appendix B.1.

Prop. 5 *In the asymptotic case where the hypotheses of Theorem 6 hold, when adopting a PRake with L_P coefficients according to the MRC scheme,*

$$\gamma_{0,k}^{-1} \overset{a.s.}{\rightarrow} \frac{1}{N} \cdot \nu\left(\Lambda, r, \rho\right), \tag{4.40}$$

where $\rho \triangleq N_c/L$, $0 < \rho < \infty$, $r \triangleq L_P/L$, $0 < r \leq 1$, and

$$\nu(\Lambda, r, \rho) = \begin{cases} \dfrac{\Lambda\left(\Lambda^{\rho}-1\right)\left(4\Lambda^{2r}+3\Lambda^{\rho}-1\right)-2\Lambda^{r+\rho}\left(\Lambda^{r}+3\Lambda-1\right)\rho\log\Lambda}{2\left(\Lambda^{r}-1\right)^{2}\rho\Lambda^{1+\rho}\log\Lambda}, \\ \qquad \text{if } 0 \le \rho \le \min(r, 1-r); & (4.41a) \\ \dfrac{\Lambda\left(4\Lambda^{\rho}-1\right)\left(\Lambda^{2r}-1\right)-2\Lambda^{r+\rho}\left(3\Lambda r-\rho+\Lambda^{r}\rho\right)\log\Lambda}{2\left(\Lambda^{r}-1\right)^{2}\rho\Lambda^{1+\rho}\log\Lambda}, \\ \qquad \text{if } \min(r, 1-r) \le \rho \le \max(r, 1-r) \\ \qquad \text{and } r \le 1/2; & (4.41b) \\ \dfrac{-4\Lambda^{2+2r}-4\Lambda^{2+\rho}+\Lambda^{2(r+\rho)}+4\Lambda^{2+2r+\rho}+3\Lambda^{2+2\rho}}{2\left(\Lambda^{r}-1\right)^{2}\rho\Lambda^{2+\rho}\log\Lambda}, \\ \quad + \dfrac{-2\Lambda^{1+r+\rho}\left(r+3\Lambda\rho+\Lambda^{r}\rho-1\right)\log\Lambda}{2\left(\Lambda^{r}-1\right)^{2}\rho\Lambda^{2+\rho}\log\Lambda}, \\ \qquad \text{if } \min(r, 1-r) \le \rho \le \max(r, 1-r) \\ \qquad \text{and } r \ge 1/2; & (4.41c) \\ \dfrac{-\Lambda^{2+2r}-4\Lambda^{2+\rho}+\Lambda^{2(r+\rho)}+4\Lambda^{2+2r+\rho}}{2\left(\Lambda^{r}-1\right)^{2}\rho\Lambda^{2+\rho}\log\Lambda}, \\ \quad + \dfrac{-2\Lambda^{1+r+\rho}\left(r+3\Lambda r+\Lambda^{r}\rho-1\right)\log\Lambda}{2\left(\Lambda^{r}-1\right)^{2}\rho\Lambda^{2+\rho}\log\Lambda}, \\ \qquad \text{if } \max(r, 1-r) \le \rho \le 1; & (4.41d) \\ \dfrac{2\Lambda\left(\Lambda^{2r}-1\right)-\left(\Lambda^{r}+r+3\Lambda r-1\right)\Lambda^{r}\log\Lambda}{\left(\Lambda^{r}-1\right)^{2}\rho\Lambda\log\Lambda}, \\ \qquad \text{if } \rho \ge 1. & (4.41e) \end{cases}$$

The proof can be found in Appendix B.2.

Propositions 4 and 5 give accurate approximations for the MAI and SI terms in the general case of PRake receivers at the AP and of an exponentially decaying aPDP. Furthermore, these results confirm that the approximations are independent of large-scale fading models, as claimed in [15], since they do not depend on the variance of the users.

It is also possible to obtain results for more specific scenarios using (4.38) and (4.40)

with particular values of Λ and r, as shown in the following.

4.2.3 PRake with flat aPDP

The results presented above can be used to study the case of a channel model assuming flat aPDP. As already mentioned, the flat aPDP model is captured when $\Lambda = 1$. In order to obtain expressions suitable for this case, it is sufficient to let Λ go to 1 in both (4.38) and (4.40). The former yields

$$\lim_{\Lambda \to 1} \mu(\Lambda, r) = \frac{1}{r}, \tag{4.42}$$

whereas the result given by the latter is

$$\lim_{\Lambda \to 1} \nu(\Lambda, r, \rho) = \begin{cases} \dfrac{2r^2 + 2r - 4\rho r + \rho^2}{2r^2}, & \\ \qquad \text{if } 0 \le \rho \le \min(r, 1-r); & \text{(4.43a)} \\ \dfrac{1}{2}\left(\dfrac{2-\rho}{r} + \dfrac{r}{\rho} - 1\right), & \\ \qquad \text{if } \min(r, 1-r) \le \rho \le \max(r, 1-r) & \\ \qquad \text{and } r \le 1/2; & \text{(4.43b)} \\ \dfrac{r^3 + r^2(9\rho - 3) + r(3 - 9\rho^2) + 4\rho^3 - 3\rho^2 + 3\rho - 1}{6\rho r^2}, & \\ \qquad \text{if } \min(r, 1-r) \le \rho \le \max(r, 1-r) & \\ \qquad \text{and } r \ge 1/2; & \text{(4.43c)} \\ \dfrac{4r^3 - 3r^2 + 3r + (\rho - 1)^3}{6\rho r^2}, & \\ \qquad \text{if } \max(r, 1-r) \le \rho \le 1; & \text{(4.43d)} \\ \dfrac{4r^2 - 3r + 3}{6\rho r}, & \\ \qquad \text{if } \rho \ge 1. & \text{(4.43e)} \end{cases}$$

4.2.4 ARake with exponentially decaying aPDP

The results of Props. 4-5 can also describe the model of a wireless network using ARake receivers at the AP. As noticed in Sect. 2.2.2, an ARake receiver is a PRake receiver with $r = 1$. Letting r go to 1 in (4.38) and (4.40), it is possible to obtain approximations for the MAI and SI terms in a multipath channel with exponentially

decaying aPDP as follows:

$$\mu_A(\Lambda) = \lim_{r\to 1} \mu(\Lambda, r) = 1, \tag{4.44}$$

$$\nu_A(\Lambda, \rho) = \lim_{r\to 1} \nu(\Lambda, r, \rho) = \\ = \begin{cases} \dfrac{2\left(\Lambda^2 - 1 + \Lambda^{\rho} - \Lambda^{2-\rho} - 2\Lambda\rho\log\Lambda\right)}{(\Lambda-1)^2\,\rho\log\Lambda}, & \text{if } \rho \le 1, \\ \dfrac{2\left(\Lambda^2 - 1 - 2\Lambda\log\Lambda\right)}{(\Lambda-1)^2\,\rho\log\Lambda}, & \text{if } \rho \ge 1. \end{cases} \tag{4.45}$$

It is worth noting that the result for $\rho \le 1$ in (4.45) has been obtained by letting $r \to 1$ in (4.41c).

4.2.5 ARake with flat aPDP

The simplest case is represented by a wireless network using the ARake receivers at the AP, where the channel is assumed to have a flat aPDP. This situation can be captured by simultaneously letting both Λ and r go to 1 in (4.38) and (4.40). This approach gives

$$\lim_{\substack{\Lambda\to 1,\\ r\to 1}} \mu(\Lambda, r) = 1, \tag{4.46}$$

$$\lim_{\substack{\Lambda\to 1,\\ r\to 1}} \nu(\Lambda, r, \rho) = \begin{cases} \dfrac{2}{3}\left(\rho^2 - 3\rho + 3\right), & \text{if } \rho \le 1, \\ \dfrac{2}{3\rho}, & \text{if } \rho \ge 1. \end{cases} \tag{4.47}$$

As in (4.45), the result for $\rho \le 1$ in (4.47) has been obtained by letting $r \to 1, \Lambda \to 1$ in (4.41c).

4.2.6 Comments on the results

This subsection contains some comments on the results provided by Props. 4-5, applied both to the general case of the PRake receivers with an exponentially decaying aPDP and to its subcases.

Fig. 4.3 shows the shape of the term $\mu(\Lambda, r)$, proportional to the MAI as in (4.38), versus the ratio r for some values of Λ. The solid line represents $\Lambda = 0$ dB, while

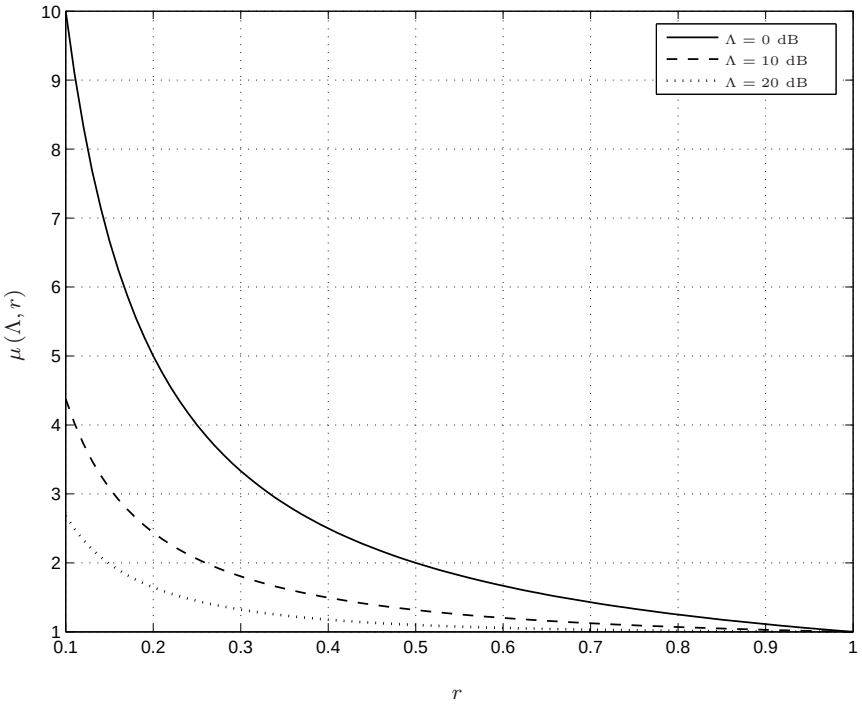

Figure 4.3: *Shape of* $\mu(\Lambda, r)$ *versus* r *for some values of* Λ.

the dashed and the dotted line depict $\Lambda = 10$ dB and $\Lambda = 20$ dB, respectively. As can be seen, $\mu(\Lambda, r)$ decreases as either Λ or r increases. Keeping r fixed, it makes sense that $\mu(\Lambda, r)$ is a decreasing function of Λ, since the received power of the other users is lower as Λ increases. Keeping Λ fixed, it makes sense that $\mu(\Lambda, r)$ is a decreasing function of r, since the receiver uses a higher number of coefficients, thus better mitigating the effect of MAI. Furthermore, it can be seen that, for an ARake, $\lim_{r \to 1} \mu(\Lambda, r) = \mu_A(\Lambda) = 1$ irrespectively of Λ.

Fig. 4.4 shows the shape of the term $\nu(\Lambda, r, \rho)$, proportional to the SI as in (4.40), versus the ratio r for some values of Λ and ρ. The solid line represents $\Lambda = 0$ dB, while the dashed and the dotted line depict $\Lambda = 10$ dB and $\Lambda = 20$ dB, respectively. The circles represent $\rho = 0.25$, while the square markers and the rhombi report the shape of $\nu(\Lambda, r, \rho)$ for $\rho = 1.0$ and $\rho = 4.0$, respectively. As can be verified, $\nu(\Lambda, r, \rho)$ decreases

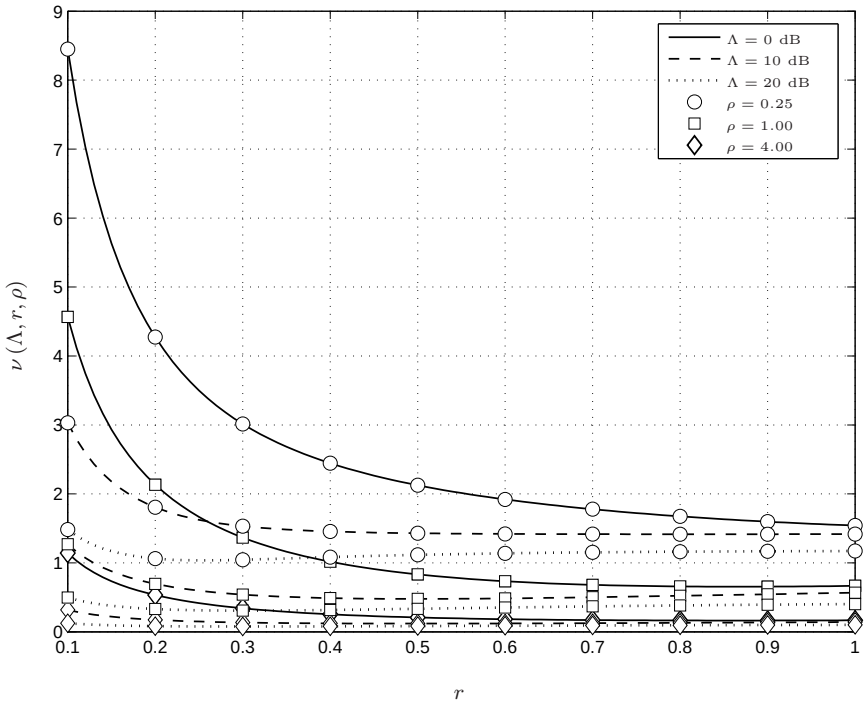

Figure 4.4: *Shape of $\nu(\Lambda, r, \rho)$ versus r for some values of Λ and ρ.*

as either ρ or Λ increases. This behavior of $\nu(\Lambda, r, \rho)$ with respect to ρ is justified by the higher resistance to multipath due to increasing the number of possible positions and thus the length of a single frame. This also agrees with the results of [50], where it has been shown that, for a fixed total processing gain N, systems with higher N_c outperform those with smaller N_c, due to higher mitigation of SI. Similarly to $\mu(\Lambda, r)$, it makes sense that $\nu(\Lambda, r, \rho)$ is a decreasing function of Λ when r and ρ are fixed, since the neglected paths are weaker as Λ increases. Taking into account the behavior of $\nu(\Lambda, r, \rho)$ as a function of r, it can be verified, either analytically or graphically, that $\nu(\Lambda, r, \rho)$ is not monotonically decreasing as r increases. In other words, an ARake receiver using MRC does not offer the optimum performance in mitigating the effect of SI, but it is outperformed by the PRake receivers whose r decreases as Λ increases. This behavior is due to the fact that the receiver uses MRC, which attempts to gather

all the signal energy to maximize the signal-to-noise ratio (SNR) and substantially ignores the effects of SI [70]. In this scenario, a minimum mean square error (MMSE) combining criterion [49], while more complex, might give a different comparison.

4.3 Performance of the Nash equilibrium

4.3.1 Analytical results

Making use of the previous analysis, it is possible to study the performance of the PRake receivers when the power control techniques described in Chapter 3 are adopted. Using Props. 4 and 5 in (3.1) and (4.5), it is straightforward to obtain the expressions for transmit powers p_k^* and utilities u_k^* achieved at the Nash equilibrium, which are independent of the channel realizations of the other users, and of SI:

$$p_k^* \overset{a.s.}{\to} \frac{1}{h_k^{(\mathrm{SP})}} \cdot \frac{N\sigma^2\Gamma\left(\frac{N}{\nu(\Lambda,r,\rho)}\right)}{N-\Gamma\left(\frac{N}{\nu(\Lambda,r,\rho)}\right)\cdot\left[(K-1)\mu\left(\Lambda,r\right)+\nu\left(\Lambda,r,\rho\right)\right]}, \tag{4.48}$$

$$u_k^* \overset{a.s.}{\to} h_k^{(\mathrm{SP})} \cdot \frac{D}{M} R_k \cdot f\left(\Gamma\left(\frac{N}{\nu\left(\Lambda,r,\rho\right)}\right)\right) \times \frac{N-\Gamma\left(\frac{N}{\nu(\Lambda,r,\rho)}\right)\cdot\left[(K-1)\mu\left(\Lambda,r\right)+\nu\left(\Lambda,r,\rho\right)\right]}{N\sigma^2\Gamma\left(\frac{N}{\nu(\Lambda,r,\rho)}\right)}. \tag{4.49}$$

Note that (4.48)-(4.49) require knowledge of the channel realization for user k (through $h_k^{(\mathrm{SP})}$).

Analogously, (4.3) translates into the system design parameter

$$N_f \geq \left\lceil \Gamma\left(\frac{N}{\nu\left(\Lambda,r,\rho\right)}\right)\cdot\frac{(K-1)\mu\left(\Lambda,r\right)+\nu\left(\Lambda,r,\rho\right)}{N_c}\right\rceil, \tag{4.50}$$

where $\lceil\cdot\rceil$ is the ceiling operator. Since the inequality (4.50) is independent of the channel realizations, it can serves as a design parameter, in that it specifies the minimum number of frames N_f that allows all users in the network to achieve the optimum SINR level γ_k^* without transmitting at the maximum power $\overline{p}$. As a consequence, (4.50) is expedient to evaluate the minimum spreading factor N required by the network to provide optimal performance (in the noncooperative sense).

Prop. 6 *In the asymptotic case where the hypotheses of Theorems 5-6 hold, the loss* Ψ *of a PRake receiver with respect to an ARake receiver in terms of achieved utilities converges a.s. to*

$$\Psi = \frac{u_{k_A}^*}{u_k^*} \overset{a.s.}{\to} \mu(\Lambda, r) \cdot \frac{f\left(\Gamma\left(\frac{N}{\nu_A(\Lambda,\rho)}\right)\right)}{f\left(\Gamma\left(\frac{N}{\nu(\Lambda,r,\rho)}\right)\right)} \cdot \frac{\Gamma\left(\frac{N}{\nu(\Lambda,r,\rho)}\right)}{\Gamma\left(\frac{N}{\nu_A(\Lambda,\rho)}\right)} \times \frac{N - \Gamma\left(\frac{N}{\nu_A(\Lambda,\rho)}\right)\left[(K-1)\mu_A(\Lambda) + \nu_A(\Lambda,\rho)\right]}{N - \Gamma\left(\frac{N}{\nu(\Lambda,r,\rho)}\right)\left[(K-1)\mu(\Lambda,r) + \nu(\Lambda,r,\rho)\right]}, \tag{4.51}$$

where $u_{k_A}^*$ *is the utility achieved by an ARake receiver.*

Proof At the Nash equilibrium, the transmit power for user k when using an ARake receiver at the AP, $p_{k_A}^*$, can be obtained from (4.5):

$$p_{k_A}^* = \frac{1}{h_k} \cdot \frac{\sigma^2 \Gamma(\gamma_{0,k_A})}{1 - \Gamma(\gamma_{0,k_A}) \cdot \left(\gamma_{0,k_A}^{-1} + \zeta_{k_A}^{-1}\right)}, \tag{4.52}$$

where the subscript A serves to emphasize that we are considering the case of an ARake, and where we have used the fact that $h_k^{(\mathrm{SP})}$ is equal to the channel gain $h_k = \boldsymbol{\alpha}_k^H \cdot \boldsymbol{\alpha}_k = ||\boldsymbol{\alpha}_k||^2$. Hence, (4.51) becomes

$$\Psi = \frac{h_k}{h_k^{(\mathrm{SP})}} \cdot \frac{f(\Gamma(\gamma_{0,k_A}))}{f(\Gamma(\gamma_{0,k}))} \cdot \frac{\Gamma(\gamma_{0,k})}{\Gamma(\gamma_{0,k_A})} \cdot \frac{1 - \Gamma(\gamma_{0,k_A}) \cdot \left(\gamma_{0,k_A}^{-1} + \zeta_{k_A}^{-1}\right)}{1 - \Gamma(\gamma_{0,k}) \cdot \left(\gamma_{0,k}^{-1} + \zeta_k^{-1}\right)}. \tag{4.53}$$

To show that Ψ converges a.s. to the non-random limit of (4.51), it is convenient to rewrite the ratio $h_k/h_k^{(\mathrm{SP})}$ as

$$\frac{h_k}{h_k^{(\mathrm{SP})}} = \frac{\frac{1}{L}\boldsymbol{\alpha}_k^H \cdot \boldsymbol{\alpha}_k}{\frac{1}{L}\boldsymbol{\beta}_k^H \cdot \boldsymbol{\alpha}_k}. \tag{4.54}$$

Following the same steps as in the proof of Theorem 5, it is possible to prove that

$$\frac{1}{L}\boldsymbol{\alpha}_k^H \cdot \boldsymbol{\alpha}_k \overset{a.s.}{\to} \varphi\left((\mathbf{D}_k^{\alpha})^2\right) \tag{4.55}$$

and, analogously,

$$\frac{1}{L}\boldsymbol{\beta}_k^H \cdot \boldsymbol{\alpha}_k \overset{a.s.}{\to} \varphi\left(\mathbf{D}_k^{\alpha}\mathbf{D}_k^{\beta}\right). \tag{4.56}$$

Table 4.2: *List of parameters used in the simulations.*

M, total number of bits per packet	100 b
D, number of information bits per packet	100 b
R, bit rate	100 kb/s
σ^2, AWGN power at the receiver	5×10^{-16} W
$\overline{p}$, maximum power constraint	1 μW

Taking into account (4.35),

$$\begin{aligned}\varphi\left((\mathbf{D}_k^{\alpha})^2\right) &= \lim_{L\to\infty} \frac{\sigma_k^2}{L} \sum_{l=1}^{L} \Lambda^{-\frac{l-1}{L-1}} \\ &= \sigma_k^2 \cdot \frac{\Lambda - 1}{\Lambda \log \Lambda}. \end{aligned} \tag{4.57}$$

Using (4.54) and (4.57), and considering the proof of Prop. 4, reported in Appendix B.1, particularly (B.1),

$$\frac{h_k}{h_k^{(\mathrm{SP})}} \overset{a.s.}{\to} \mu\left(\Lambda, r\right), \tag{4.58}$$

where $\mu\left(\Lambda, r\right)$ is defined as in (4.39).

Making use of (4.38), (4.40), (4.44), (4.45) and (4.58), when the hypotheses of Theorems 5-6 hold, (4.53) converges a.s. to (4.51). ■

Equation (4.51) also provides a system design criterion. Given L, N_c, N_f, K and Λ, a desired loss Ψ can in fact be achieved using the ratio r obtained by numerically inverting (4.51). Unlike (4.48)-(4.49), this result is independent of all channel realizations.

4.3.2 Simulation Results

In this subsection, we show numerical results for the analysis presented in the previous subsection. Simulations are performed using the iterative algorithm described in detail in Sect. 3.4. The systems we examine have the design parameters listed in Table 4.2. We use the efficiency function $f\left(\gamma_k\right) = \left(1 - \mathrm{e}^{-\gamma_k/2}\right)^M$ as a reasonable approximation

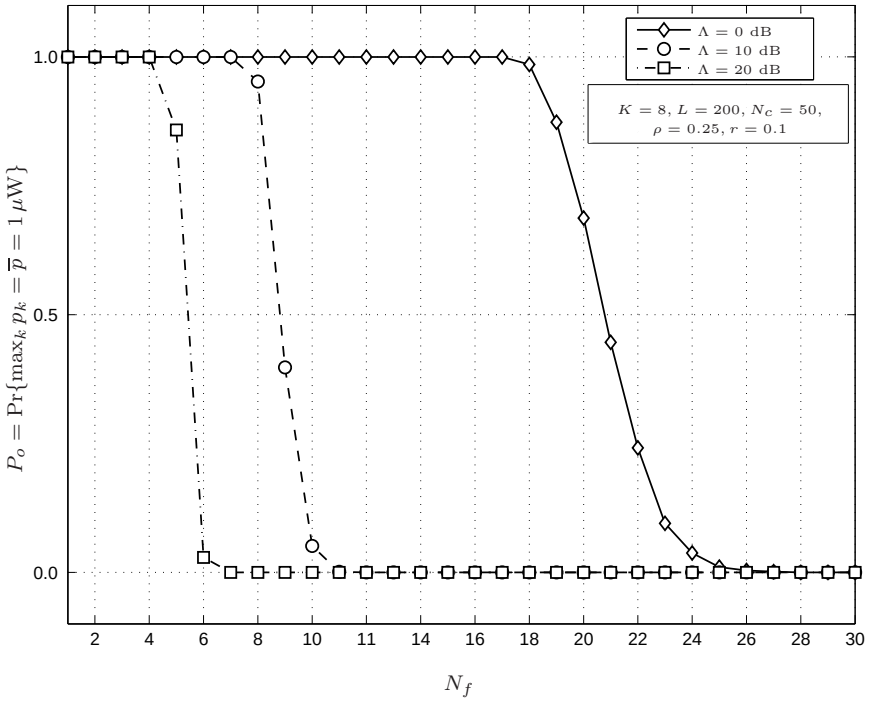

Figure 4.5: *Probability of having at least one user transmitting at maximum power versus number of frames.*

to the PSR [50, 110]. To model the UWB scenario, the channel gains are assumed as in Sect. 4.2.1, with $\sigma_k^2 = 0.3 d_k^{-2}$, where d_k is the distance between the kth user and the AP. Distances are assumed to be uniformly distributed between 3 and 20 m.

Fig. 4.5 shows the probability P_o of having at least one user transmitting at the maximum power, i.e., $P_o = \Pr\{\max_k p_k = \overline{p} = 1\,\mu\text{W}\}$, as a function of the number of frames N_f. We consider 10 000 realizations of the channel gains, using a network with $K = 8$ users, $N_c = 50$, $L = 200$ (thus $\rho = 0.25$), and PRake receivers with $L_P = 20$ coefficients (and thus $r = 0.1$). The solid line represents the case $\Lambda = 0$ dB, while the dashed and the dash-dotted lines depict the cases $\Lambda = 10$ dB and $\Lambda = 20$ dB, respectively. Note that the slope of P_o increases as Λ increases. This phenomenon is due to reducing the effects of neglected path gains as Λ becomes higher, which, given N_f, results in having more homogeneous effects of neglected

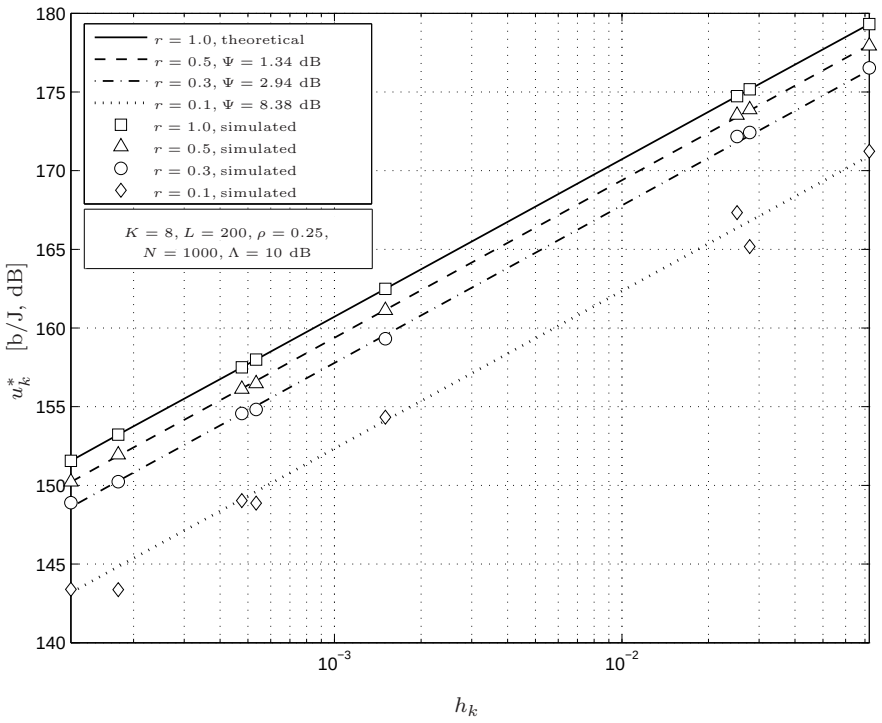

Figure 4.6: *Achieved utility versus channel gain at the Nash equilibrium for different Rake receiver complexities r.*

gains. Using the parameters above in (4.50), the minimum value of N_f that allows all K users to simultaneously achieve the optimum SINRs is $N_f = \{21, 9, 6\}$ for $\Lambda = \{0 \text{ dB}, 10 \text{ dB}, 20 \text{ dB}\}$, respectively. As can be seen, the analytical results closely match those from simulations, and thus (4.50) can be used to evaluate the minimum spreading factor N of the network, as already stated in Sect. 4.3.1. It is worth emphasizing that (4.50) is valid for both L and L_P going to ∞, as stated in Props. 4-5. In this example, $L_P = 20$, which does not fulfill this hypothesis. This explains the slight mismatch between theoretical and simulation results, especially for small Λ's. However, showing numerical results for a feasible system is more interesting than simulating a network with a very high number of PRake coefficients.

Fig. 4.6 shows a comparison between analytical and numerical achieved utilities as a

function of the channel gains $h_k = ||\boldsymbol{\alpha}_k||^2$. The network has the following parameters: $K = 8$, $L = 200$, $N_c = 50$, $N_f = 20$, $\Lambda = 10$ dB, $\rho = 0.25$. The markers correspond to the simulation results given by a single realization of the path gains. Some values of the number of coefficients of the PRake receiver are considered. In particular, the square markers report the results for the ARake ($r = 1$), while triangles, circles and rhombi show the cases $r = \{0.5, 0.3, 0.1\}$, respectively. The solid line represents the theoretical achieved utility, computed using (4.49). The dashed, the dash-dotted and the dotted lines have been obtained by subtracting from (4.49) the loss Ψ, computed as in (4.51). Using the parameters above, $\Psi = \{1.34 \text{ dB}, 2.94 \text{ dB}, 8.38 \text{ dB}\}$ for $r = \{0.5, 0.3, 0.1\}$, respectively. As before, the larger the number of L_P coefficients is, the smaller the difference between theoretical analysis and simulations is. It is worth noting that the theoretical results do not consider the actual values of $h_k^{(\text{SP})}$, as required in (4.49),[2] since they make use of the asymptotic approximation (4.51). As can be verified, the analytical results closely match the actual performance of the PRake receivers, especially recalling that the results are not averaged. Only a single random channel realization is in fact considered, because we want to emphasize that not only this approximation is accurate on average, but also that the normalized mean square error (nmse) $\text{nmse}\,(u_k^*) = \mathbb{E}\left\{\left[\left(u_{k_A}^*/\Psi - u_k^*\right)/u_k^*\right]^2\right\}$ is considerably low, where $\mathbb{E}\{\cdot\}$ denotes expectation; $u_{k_A}^*$ and Ψ are *computed* following (4.49) and (4.51), respectively; and u_k^* represents the *experimental* utility at the Nash equilibrium. In fact, by averaging over 10 000 channel realizations using the same network parameters, $\text{nmse}\,(u_k^*) = \{1.4 \times 10^{-3}, 5.9 \times 10^{-3}, 6.3 \times 10^{-2}\}$ for $r = \{0.5, 0.3, 0.1\}$, respectively, As a conclusion, this allows every network fulfilling the above described hypotheses to be studied with the proposed tools.

Fig. 4.7 shows the loss Ψ versus the ratio r for some values of Λ and ρ. The network parameters are set as follows: $K = 8$, $N_f = 20$, and $L = 200$. The solid lines represent $\Lambda = 0\,\text{dB}$, while the dashed lines depict $\Lambda = 10\,\text{dB}$. The circles represent $N_c = 50$ (and thus $\rho = 0.25$), while the square markers report $N_c = 200$ (and thus $\rho = 1.0$). As is obvious, Ψ is a decreasing function of r. Furthermore, Ψ is a decreasing function of Λ, since the received power associated to the paths neglected by the PRake receiver is lower as Λ increases. Similarly, keeping the number of multiple paths L fixed, Ψ decreases as ρ increases. This complies with theory [50], since increasing the

[2] This is also valid for the case ARake, since $h_k^{(\text{SP})} = h_k$.

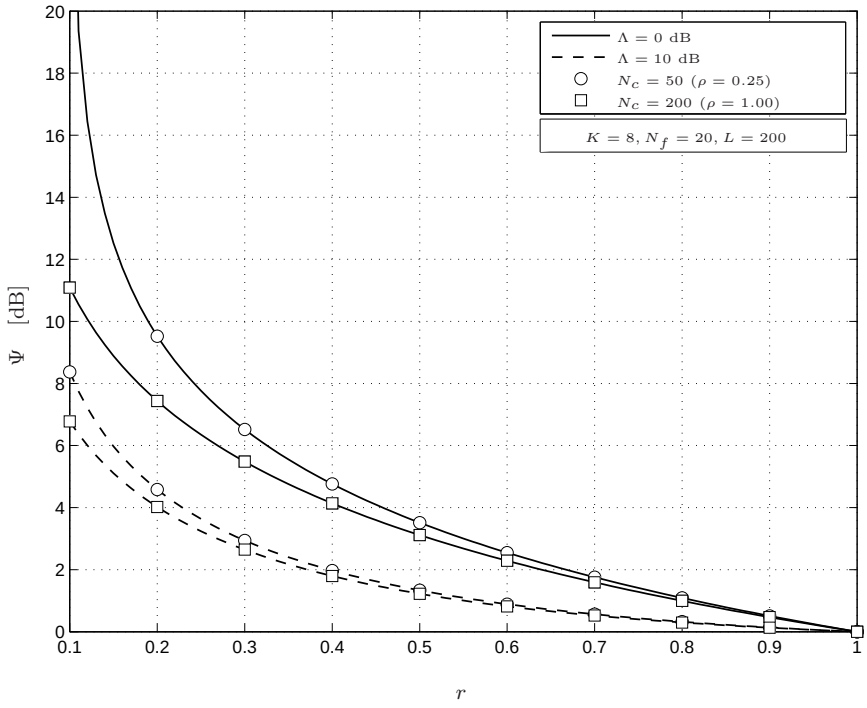

Figure 4.7: *Shape of the loss Ψ versus r for some values of Λ and ρ.*

processing gain provides higher robustness against multipath. As a consequence, a system with a lower ρ benefits more from a higher number of fingers at the receiver than a system with a higher ρ does. Hence, when ρ is lower, a PRake receiver performs worse, i.e., Ψ is higher.

It is worth stating that the proposed analysis is mainly focused on energy efficiency. Hence, the main performance index here is represented by the achieved utility at the Nash equilibrium. However, more traditional measures of performance such as SINR or BER can be obtained using the parameters derived here. In fact, typical target SINRs at the AP can be computed using $\gamma_k^* = \Gamma\left(N/\nu\left(\Lambda, r, \rho\right)\right)$, as derived in the previous sections. Similarly, the BER can be approximated by $Q\left(\sqrt{\gamma_k^*}\right)$ [50], where $Q(\cdot)$ denotes the complementary cumulative distribution function of a standard normal random variable.

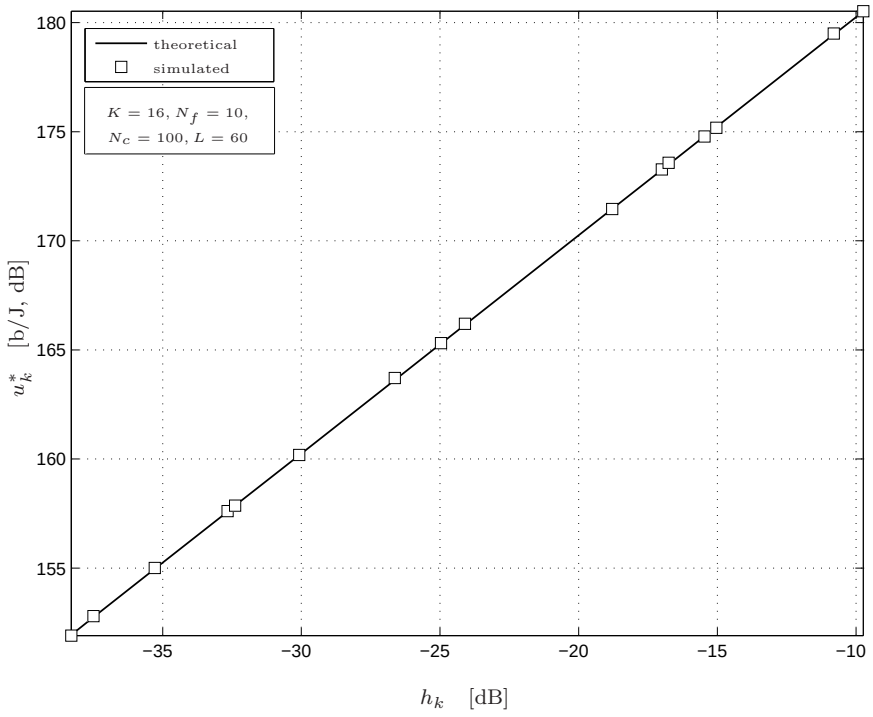

Figure 4.8: *Achieved utility versus channel gain at the Nash equilibrium for the ARake receiver using the channel model [28].*

It is interesting to observe that, in the case of ARake receivers in a flat-fading environment ($\Lambda = 0$ dB), the results derived in Sect. 4.2.5 can also capture a more realistic UWB scenario, simulated according to the model described in [28]. As an example, Fig. 4.8 shows the utilities achieved at the Nash equilibrium as functions of the channel gains h_k. These results have been obtained using random channel realizations for $K = 16$ users. The number of possible pulse positions is $N_c = 100$, while the number of paths is $L = 60$, in order to satisfy the large system assumption with $\nu_A\,(\Lambda = 0 \text{ dB}, \rho = 1.67) = 0.4$. The number of frame is $N_f = 10$, thus leading to a processing gain $N = 1000 \gg K$. The line represents the theoretical values of (4.49) when using an ARake, whereas the square markers report the simulations results. We can see that the simulations match closely with the theoretical results.

Chapter 5

Social optimality of the Nash solution

The outcome of the distributed power control algorithm (the Nash equilibrium) for the UWB-based wireless network modeled in Chapter 2 has been thoroughly discussed in Chapter 3 and Chapter 4. To evaluate how effective the Nash equilibrium is, i.e., to compare its performance to that of other power allocation schemes, it is important to measure the loss of the distributed solution with respect to the centralized optimization. As already outlined in Sect. 1.2.3, this comparison is motivated by the need to assess the tradeoff between pros and cons of a decentralized scheme.

In particular, Sect. 5.1 provides an analytical comparison between the two approaches using the large-system analysis proposed in the previous chapter. Sect. 5.2 presents some numerical results to support the theoretical conclusions.

5.1 Analytical results

Using the definitions introduced in Sect. 1.2.3, the solution to the power control game is said to be Pareto-optimal if there exists no other power allocation $\mathbf{p}$ for which one or more users can improve their utilities without reducing the utility of any of the other users. It can be shown that the Nash equilibrium presented in Chapter 4 is not Pareto-optimal [110]. This means that it is possible to improve the utility of one or more users without harming other users. On the other hand, it can be shown that

the solution to the following social problem gives the Pareto-optimal frontier [85]

$$\tilde{\mathbf{p}} = \arg\max_{\mathbf{p}} \sum_{k=1}^{K} \lambda_k u_k(\mathbf{p}), \tag{5.1}$$

for $\lambda_k \in \mathbb{R}^+$ (the set of positive real numbers). Pareto-optimal solutions are, in general, difficult to obtain. Here, we *conjecture* that the Pareto-optimal solution occurs when all users achieve the same SINRs, $\tilde{\gamma}$. This approach is chosen not only because SINR balancing ensures fairness among users in terms of throughput and delay [85], but also because, for large systems, the Nash equilibrium is achieved when all SINRs are similar. We also consider the hypothesis $\lambda_1 = \cdots = \lambda_K = 1$, suitable for a scenario without priority classes. Hence, the summation presented in (5.1) reduces to

$$u_{\text{network}}(\mathbf{p}) = \sum_{k=1}^{K} u_k(\mathbf{p}), \tag{5.2}$$

which is analogous to the performance parameter introduced in Sect. 1.4.1 as a measure of the efficiency of the distributed solution. As a consequence, the maximization (5.1) can be written as

$$\tilde{\mathbf{p}} = \arg\max_{\mathbf{p}} \frac{f(\gamma(\mathbf{p}))}{\left(\sum_{k=1}^{K} p_k^{-1}\right)^{-1}}. \tag{5.3}$$

In a network where the hypotheses of Assumption 1, Theorem 5 and Theorem 6 are fulfilled, and the channel is modeled as stated in Sect. 4.2.1, at the Nash equilibrium all users achieve a certain output SINR γ_k with $h_k^{(\text{SP})} p_k^* \simeq q(\gamma_k)$, where

$$q(\gamma) = \frac{N\sigma^2\gamma}{N - \gamma \cdot [(K-1)\mu(\Lambda, r) + \nu(\Lambda, r, \rho)]}, \tag{5.4}$$

with $\rho = N_c/L$. Therefore, (5.3) can be expressed as

$$\gamma_k = \arg\max_{\gamma} \frac{f(\gamma)}{q(\gamma)} \sum_{k=1}^{K} h_k^{(\text{SP})} \simeq \tilde{\gamma}, \tag{5.5}$$

since there exists a one-to-one correspondence between γ and $\mathbf{p}$. It should be noted that, while the maximizations in (3.5) consider no cooperation among users, (5.3) assumes that users cooperate in choosing their transmit powers. That means that the relationship between the user's SINR and transmit power will be different from that in the noncooperative case.

Prop. 7 *In a network where $L, N_c \to \infty$ and $N \gg K$, the Nash equilibrium approaches the socially optimal solution in terms of total network utility $u_{network}(\mathbf{p})$.*

Proof The solution $\tilde{\gamma}$ to (5.5) must satisfy the first-order necessary optimizing condition $d\left(f\left(\gamma\right)/q\left(\gamma\right)\right)/d\gamma|_{\gamma=\tilde{\gamma}} = 0$. Using this fact, combined with (5.4), gives us the equation that must be satisfied by the solution of the maximization problem in (5.5):

$$f'(\tilde{\gamma}) \cdot \tilde{\gamma} \left[1 - \tilde{\gamma} \cdot \frac{(K-1)\mu\left(\Lambda, r\right) + \nu\left(\Lambda, r, \rho\right)}{N}\right] = f\left(\tilde{\gamma}\right). \tag{5.6}$$

We see from (5.6) that the socially optimal solution differs from the solution (3.6) of the noncooperative utility-maximizing method, since (5.6) also takes into account the contribution of the interferers. In particular,

$$\tilde{\gamma} = \Gamma\left(\frac{N}{(K-1)\mu\left(\Lambda, r\right) + \nu\left(\Lambda, r, \rho\right)}\right). \tag{5.7}$$

Since the function $\Gamma\left(\cdot\right)$ is increasing with its argument for any S-shaped $f\left(\gamma\right)$ (as can also be seen in Fig. 4.1), and since $N/\left[(K-1)\mu\left(\Lambda, r\right) + \nu\left(\Lambda, r, \rho\right)\right] \leq N/\nu\left(\Lambda, r, \rho\right) \cong \gamma_{0,k}$ for all k [from (4.38) and (4.40)],

$$\tilde{\gamma} \leq \gamma_k^* \leq \overline{\gamma}^*, \tag{5.8}$$

due to (4.1) and (5.7), where $\overline{\gamma}^* = \Gamma\left(\infty\right)$ is the SINR at the Nash equilibrium for the flat-fading scenario. On the other hand, assuming $N \gg K$ and $0 < \rho < \infty$ implies $\tilde{\gamma} \to \overline{\gamma}^*$. From (5.8), it is apparent that $\gamma_k^* \to \overline{\gamma}^*$ as well. This means that, in almost all typical scenarios, the target SINR for the noncooperative game, γ_k^*, is close to the target SINR for the socially optimal solution, $\tilde{\gamma}$. Consequently, the average utility provided by the Nash equilibrium is close to the one achieved according to the socially optimal solution. ■

The validity of this theoretical analysis is confirmed by numerical results presented in the remainder of this chapter.

5.2 Simulation results

Fig. 5.1 shows the normalized utility u_k/h_k as a function of the ratio ρ. We consider 10 000 random realization of a network with $K = 16$ users, $N_f = 20$ frames, $L = 100$

Table 5.1: *List of parameters used in the simulations.*

M, total number of bits per packet	100 b
D, number of information bits per packet	100 b
R, bit rate	100 kb/s
σ^2, AWGN power at the receiver	5×10^{-16} W
$\overline{p}$, maximum power constraint	1 μW

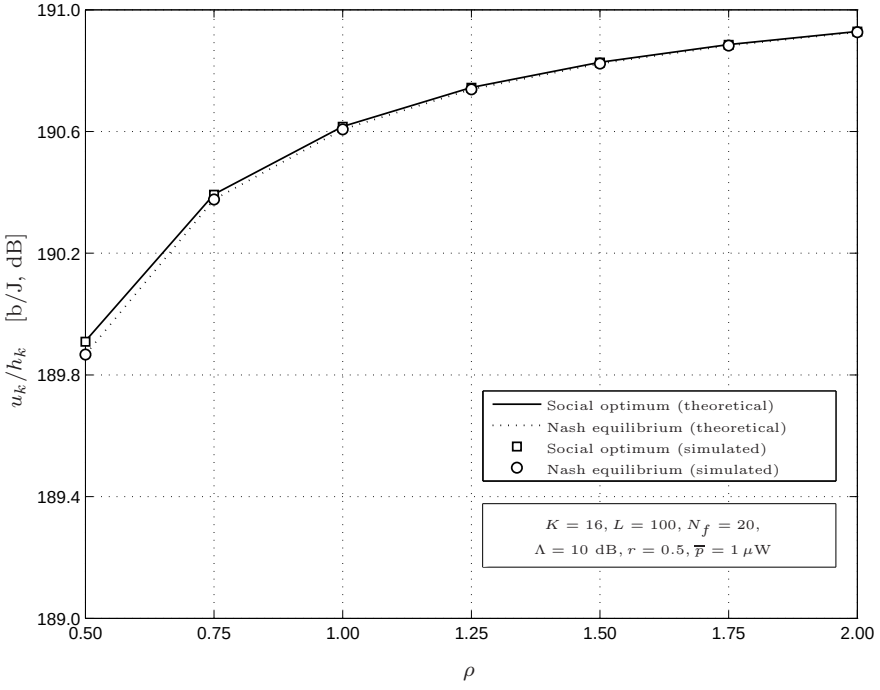

Figure 5.1: *Comparison of the normalized utility versus the load factor for the noncooperative and socially optimal solutions.*

and PRake receivers with $L_P = 50$ fingers at the AP (and thus $r = 0.5$). The other parameters can be found in Table 5.1. The lines represent theoretical values of Nash equilibrium (NE) (dotted line), using (4.49), and of the social optimum

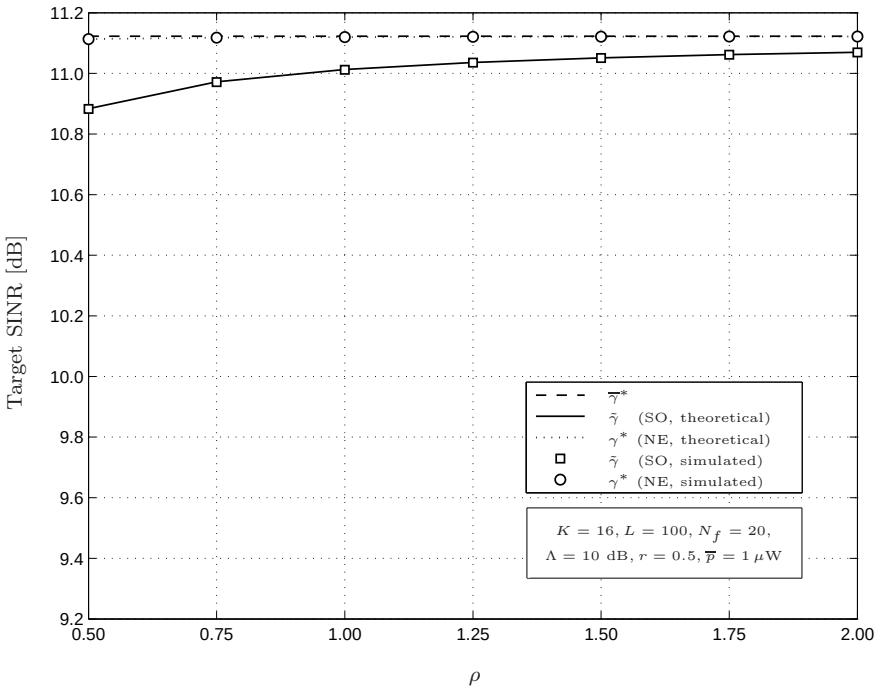

Figure 5.2: *Comparison of the target SINR versus load factor for the noncooperative and socially optimal solutions.*

(SO) solution (solid line), using (3.3) with $\gamma_k = \tilde{\gamma}$ that follows from the numerical solution of (5.3). The markers correspond to the simulation results, which use the efficiency function $f(\gamma_k) = (1 - \mathrm{e}^{-\gamma_k/2})^M$ presented for the previous results. The channel is modeled following the considerations presented in Sect. 4.2.1. The circles represent the averaged solution of the iterative algorithm (3.15), while the square markers show averaged numerical results (through a complete numerical search) of the maximization (5.1), with $\lambda_k = 1$. As can be seen, the difference between the noncooperative approach and the socially optimal solution is vanishingly small.

Similar conclusions can be drawn by inspecting Fig. 5.2, which compares the target SINRs of the noncooperative solutions with the target SINRs of the socially optimal solutions. As before, the lines correspond to the theoretical values, while the markers represent the simulation results. It is seen that, in both cases, the average target

Table 5.2: *Average loss of the Nash solution with respect to the social optimum.*

ρ	$u_{\text{network}}(\tilde{\mathbf{p}})/u_{\text{network}}(\mathbf{p}^*)$ [dB]
0.50	0.67
0.75	0.35
1.00	0.21
1.25	0.14
1.50	0.10
1.75	0.08
2.00	0.06

SINRs for the Nash equilibrium, γ^*, and the average target SINRs for the social optimum solution, $\tilde{\gamma}$, are very close to $\overline{\gamma}^*$, as shown in Prop. 7.

Table 5.2 shows the average loss of the Nash equilibrium with respect to the social optimum solution as a function of the load factor ρ when the total utility of the network $u_{\text{network}}(\mathbf{p})$ is considered. In particular, we report the average loss of the distributed solution (Nash equilibrium) with respect to the centralized solution (social optimum) over 10 000 realization of the network, with the following parameters: $K = 16$ users, $N_f = 20$ frames, $L = 100$ and PRake receivers with $L_P = 50$ fingers at the AP (and thus $r = 0.5$). It is interesting to note that, although the Nash solution performs similarly to the centralized solution in terms of *normalized* utility (see Figs. 5.1 and 5.2), the difference in terms of the *effective* $u_{\text{network}}(\mathbf{p})$ is not negligible. However, such loss, far below 1 dB for any ρ, can be considered acceptable if compared to the notable advantages of a distributed algorithm discussed in Sect. 3.1.

Furthermore, another prominent feature of the Nash solution can be identified by inspecting the two approaches much in detail. Fig. 5.3 reports the transmit power as a function of the channel gain for an example network using the same parameters employed for the results of Table 5.2. In the considered network, the channel conditions are rather unbalanced among the users, i.e., the near-far effect is stronger and an effective power control scheme is particularly desirable. The square markers represent the transmit power $\tilde{p}_k$ of the (numerical) socially optimal solution, whereas

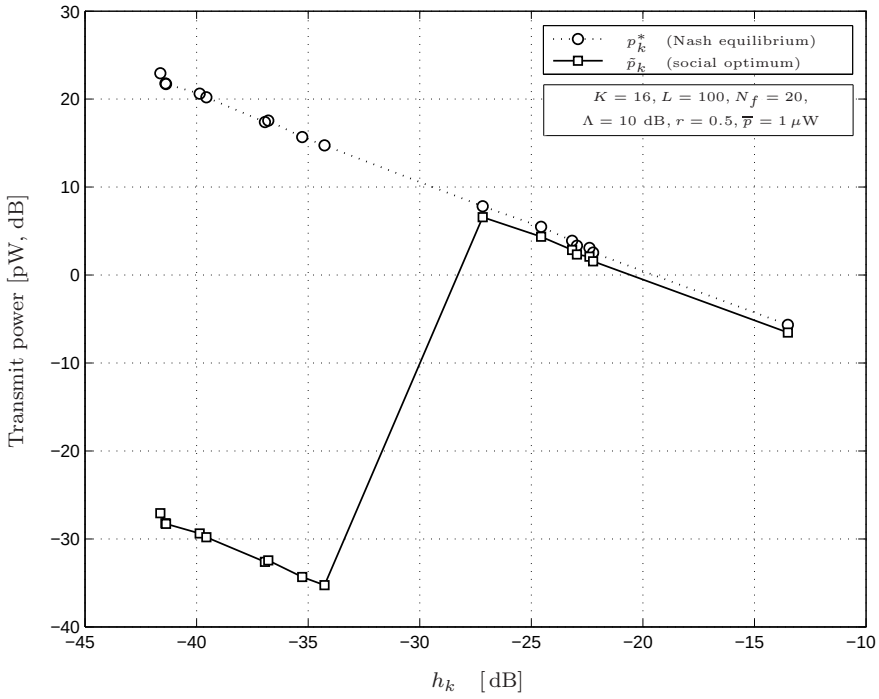

Figure 5.3: *Transmit power versus channel gain for noncooperative and socially optimal solutions for an example network realization.*

the circles report the power p_k^* at the Nash equilibrium, obtained through the BRPC algorithm. As can be seen, the optimal solution from the point of view of the network is that power allocation that allows users with good channel conditions to transmit at considerable powers (and thus to achieve a relevant throughput) while preventing users with bad channel conditions from transmitting. This outcome resembles the waterfilling solution used for digital subscriber line (DSL) [118]. In fact, if the network is considered as a unique entity aiming at maximizing the energy efficiency, the aggregate ratio throughput to transmit power can be maximized when the channel gains of the transmitting terminals are above a certain threshold. As a consequence, although $\tilde{\mathbf{p}}$ provides the maximum total energy efficiency of the network, such allocation is highly unfair.

This can be verified in Fig. 5.4, where the achieved utilities are plotted as functions

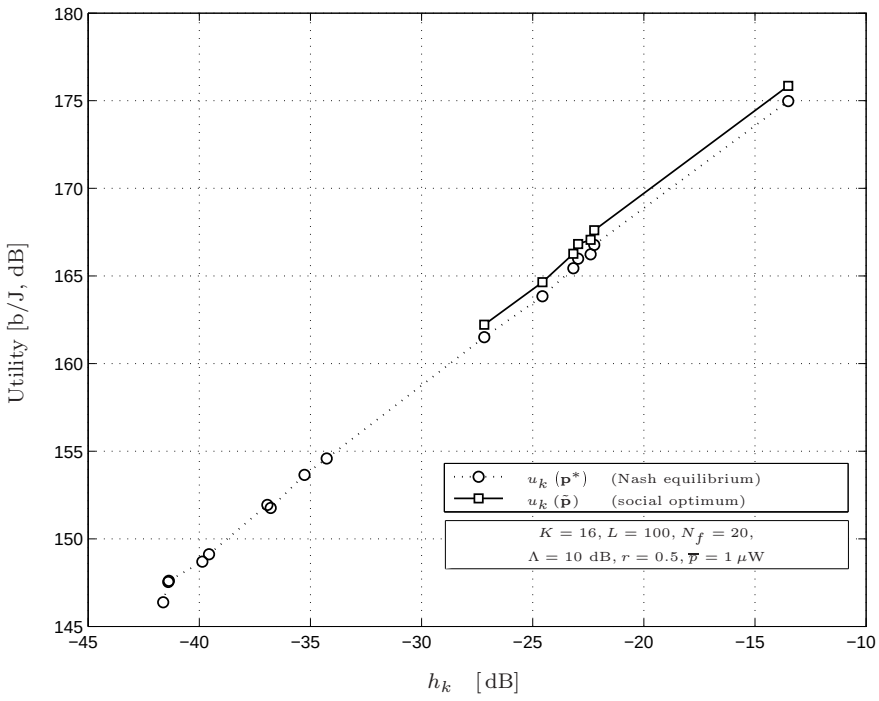

Figure 5.4: *Achieved utility versus channel gain for noncooperative and socially optimal solutions for an example network realization.*

of the channel gains for the distributed solution (circles) and the socially optimal solution (square markers), respectively. Due to the choice of a logarithmic scale for the utilities, Fig. 5.4 does not report the utilities achieved at the socially optimal solution for users with lower channel gains. For these users, $u_k(\tilde{\mathbf{p}}) = 0$. Alternatively, the Nash equilibrium guarantees *fairness* to the network, since every user is allowed to communicate with the AP. In this situation, the claims used in the proof of Prop. 7 do not hold anymore, since the SINR at the social optimum $\tilde{\gamma}_k$ is different for each user (more precisely, $\tilde{\gamma}_k \cong \gamma_k^*$ for users with good channel conditions, and $\tilde{\gamma}_k \cong 0$ for users with bad channel conditions). However, it is interesting to note that the contributions of users with bad channel conditions in terms of the aggregate utility are marginal. Therefore, the final conclusions about the performance of noncooperative (distributed) and centralized solutions still hold. This is in fact confirmed by the

results of Table 5.2, which provides the evidence that fairness can be achieved at the expense of a reduced overall network utility on the order of fractions of decibel.

Chapter 6

Comparison between UWB and CDMA networks

The analysis of noncooperative power control schemes conducted so far has been primarily focused on high-speed infrastructure data networks using UWB technology as the multiple access technique. As motivated in Sect. 2.1, UWB technology can represent a breakthrough solution to design state-of-the-art data networks thanks to the numerous appealing features outlined in Sect. 2.1. In addition to UWB, another effective option to perform multiple access in wideband wireless networks is provided by DS-CDMA (here abbreviated CDMA). CDMA is in fact a mature access technique for wireless networking, due to its well-known robustness and ease of implementation [102].

It is thus interesting to compare the performance of the two access schemes in terms of achieved utility at the Nash equilibrium. As already stated in Sect. 2.2.2, the large bandwidth occupancy of the transmitted signals implies the frequency selectivity of the channel. To perform a fair comparison, systems with *equal* spreading factor operating in a dense multipath environment are considered.

Both the frequency-selective and the flat-fading scenarios are considered. In particular, Sect. 6.1 contains the analytical tools to evaluate the performance of the two access schemes in the frequency-selective environment, whereas Sect. 6.2 analyzes the performance in flat-fading channels. Simulations are provided to validate the theoretical results.

6.1 Frequency-selective fading

A wideband wireless network employing UWB technology as the multiple access technique can be modeled as described in Sect. 2.2. Applying the power control algorithm proposed in Chapter 3, and using the large-system analysis developed in Chapter 4, the utility achieved at the Nash equilibrium can be evaluated using (4.49), which is reported here for the reader's convenience:

$$u_{k_U}^* \overset{a.s.}{\to} h_k^{(\mathrm{SP})} \cdot \frac{D}{M} R_k \cdot f\left(\Gamma\left(\frac{N}{\nu\left(\Lambda, r, \rho\right)}\right)\right) \times \frac{N - \Gamma\left(\frac{N}{\nu(\Lambda,r,\rho)}\right) \cdot \left[(K-1)\mu\left(\Lambda, r\right) + \nu\left(\Lambda, r, \rho\right)\right]}{N\sigma^2\Gamma\left(\frac{N}{\nu(\Lambda,r,\rho)}\right)}, \tag{6.1}$$

where the subscript U is used to emphasize that this approximation applies to the UWB-based network [11].

To derive an analogous result for the case of a CDMA-based network, it is worth resorting to the UWB signal model developed in detail in Sect. 2.2.1. In this model, it is straightforward to note that (2.1) can describe the uplink signal of a random CDMA system with spreading factor N and K users in the special when $T_f = T_c$ (and thus $N_c = 1$). In fact, when $N_c = 1$, the ternary sequence $\mathbf{s}^{(k)}$ introduced in (2.2) reduces to a binary sequence with independent chips $s_n^{(k)} = \pm 1$. As a consequence, the sufficient statistic for detecting information symbols can be written similarly to that of classical CDMA systems [50].

This remark allows us to apply the framework developed in the previous chapters to CDMA-based networks as well, provided that $N_c = 1$.

Prop. 8 *Assume that $\alpha_l^{(k)}$ are zero-mean RVs independent across k and l, and $\mathbf{G}$ is a deterministic diagonal matrix (thus implying that $\alpha_l^{(k)}$ and $\beta_m^{(j)}$ are dependent only when $j = k$ and $m = l$). In the asymptotic case where the number of users K and the number of frames N_f are finite, while the number of paths is $L \to \infty$, the term utility achieved at the Nash equilibrium $u_{k_C}^*$ converges a.s. to*

$$u_{k_C}^* \overset{a.s.}{\to} h_k^{(SP)} \cdot \frac{D}{M} R_k \cdot f\left(\Gamma\left(\frac{N}{\nu_0\left(\Lambda, r\right)}\right)\right) \times \frac{N - \Gamma\left(\frac{N}{\nu_0(\Lambda,r)}\right) \cdot \left[(K-1)\mu\left(\Lambda, r\right) + \nu_0\left(\Lambda, r\right)\right]}{N\sigma^2\Gamma\left(\frac{N}{\nu_0(\Lambda,r)}\right)}, \tag{6.2}$$

where the subscript C denotes a CMDA-based network, and

$$\nu_0(\Lambda, r) = \frac{\Lambda + \Lambda^r - 2\Lambda^{1+r}}{\Lambda - \Lambda^{1+r}}. \tag{6.3}$$

Proof The achieved utility $u^*_{k_C}$ can be derived making use of the results presented in Chapter 4. In particular, Prop. 5 can be adapted to the case of a CDMA network by letting the ratio $\rho = N_c/L$ go to 0, as follows from the condition $N_c = 1$. Hence, the term proportional to SI becomes

$$\nu_0(\Lambda, r) = \lim_{\rho \to 0} \nu(\Lambda, r, \rho) = \frac{\Lambda + \Lambda^r - 2\Lambda^{1+r}}{\Lambda - \Lambda^{1+r}}, \tag{6.4}$$

as stated in (6.3). Using (6.3) in (6.1), the result (6.2) is straightforward. ■

Fig. 6.1 shows the shape of $\nu(\Lambda, r, \rho)$ as a function of r for some values of Λ and ρ. With a slight abuse of notation, $\nu_0(\Lambda, r)$ is reported as $\nu(\Lambda, r, 0)$ (triangular markers), while circles and square markers depict $\rho = 0.25$ and $\rho = 1.0$, respectively. As can be noted, $\nu_0(\Lambda, r) > \nu(\Lambda, r, \rho_1) > \nu(\Lambda, r, \rho_2)$ for any $\rho_2 > \rho_1 > 0$. This result is justified by the higher resistance to multipath due to increasing the length of a single frame [50]. Furthermore, keeping ρ fixed, $\nu(\Lambda, r, \rho)$ decreases both as Λ and as r increases. The first behavior makes sense, since the effect of multipath (and thus of SI) is higher in channels with lower Λ. The second behavior reflects the fact that exploiting the diversity by adding a higher number of fingers (and thus increasing r) results in better mitigating the frequency-selective fading.

As already stated in the introduction, the performance of the two access schemes can compared fairly when the respective networks show the same spreading factor. Since a CDMA-based network can be treated as a UWB-based network with $N_c = 1$, the assignment $N_f = N$ most hold.

Prop. 9 *When $L \to \infty$, the loss Ω of a CDMA system with respect to a UWB scheme with N_c possible pulse positions converges a.s. to*

$$\Omega \triangleq 10\log_{10}(u^*_{k_U}/u^*_{k_C}) \overset{a.s.}{\to} (10\log_{10} e)\cdot\omega \qquad \text{[dB]} \tag{6.5}$$

where

$$\omega \triangleq \frac{\Gamma\left(\frac{N}{\nu(\Lambda,r,\rho)}\right)\cdot\Delta\nu(\Lambda, r, \rho)}{N - \Gamma\left(\frac{N}{\nu(\Lambda,r,\rho)}\right)\cdot[(K-1)\mu(\Lambda, r) + \nu(\Lambda, r, \rho)]}, \tag{6.6}$$

with $\Delta\nu(\Lambda, r, \rho) = \nu_0(\Lambda, r) - \nu(\Lambda, r, \rho)$.

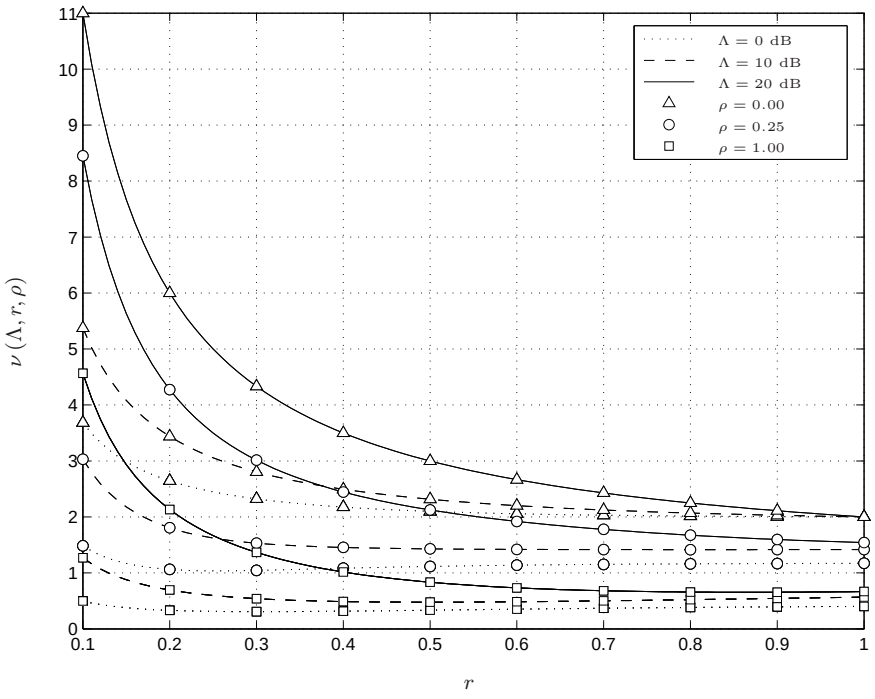

Figure 6.1: *Shape of $\nu(\Lambda, r, \rho)$ versus r for some values of Λ and ρ.*

Proof Recalling (3.6), it can be noted that the slope of $\Gamma(\gamma_{0,k})$ is very small for large values of $\gamma_{0,k}$. Using the hypothesis $N \gg K > 1$, a good approximation for $\Gamma(N/\nu_0(\Lambda, r))$ is $\Gamma(N/\nu(\Lambda, r, \rho))$. Therefore, using (6.1),

$$\frac{u^*_{k_U}}{u^*_{k_C}} \approxeq \frac{N - \Gamma\left(\frac{N}{\nu(\Lambda,r,\rho)}\right) \cdot [(K-1)\mu(\Lambda, r) + \nu(\Lambda, r, \rho)]}{N - \Gamma\left(\frac{N}{\nu(\Lambda,r,\rho)}\right) \cdot [(K-1)\mu(\Lambda, r) + \nu_0(\Lambda, r)]} \tag{6.7}$$

$$= \frac{1}{1-\omega}, \tag{6.8}$$

with ω defined as in (6.6). Recalling that $N \gg 1$, it is easy to verify that $\omega \ll 1$. Hence, using a first-order Taylor series approximation, the result (6.5) is straightforward. ■

As already specified (see also Fig. 6.1), $\Delta\nu(\Lambda, r, \rho) > 0$ for any $\rho > 0$. Hence, Prop. 9

Table 6.1: *List of parameters used in the simulations.*

M, total number of bits per packet	100 b
D, number of information bits per packet	100 b
R, bit rate	100 kb/s
σ^2, AWGN power at the receiver	5×10^{-16} W
$\overline{p}$, maximum power constraint	1 μW

states that, using an equal spreading factor in the same multipath scenario, any UWB system outperforms the corresponding CDMA schemes. The gap $\Delta\nu\,(\Lambda, r, \rho)$ can thus interpreted as a measure of how effective increasing the length of a single frame (i.e., increasing N_c) is in terms of multipath resistance.

Nevertheless, typical values of the network parameters yield very small values of Ω, especially as N increases.[1] Hence, using game-theoretic power control techniques, performance of the two multiple access schemes is practically equivalent.

Numerical results confirm this analysis. Simulations are performed using the iterative algorithm described in detail in Sect. 3.4. The systems we examine have the design parameters listed in Table 6.1. We use the efficiency function $f\,(\gamma_k) = (1 - \mathrm{e}^{-\gamma_k/2})^M$ as a reasonable approximation to the PSR [50, 110]. To model the UWB scenario, the channel gains are assumed as in Sect. 4.2.1, with $\sigma_k^2 = 0.3 d_k^{-2}$, where d_k is the distance between user k and the access point. Distances are assumed to be uniformly distributed between 3 and 30 m.

Fig. 6.2 shows a comparison between analytical and simulated normalized utilities $u_k^*/h_k^{(\mathrm{SP})}$ at the Nash equilibrium as a function of the spreading factor N. A network with $K = 10$ users is considered, while the aPDP is assumed to be exponentially decaying with $\Lambda = 20$ dB. The number of paths is $L = 200$, thus satisfying the large-system assumption. Light and dark lines depict the cases ARake ($r = 1$) and PRake ($r = 0.2$), respectively. Lines represent theoretical results provided by (6.1). In particular, solid lines show analytical values for CDMA ($N_c = 1$), while dashed and dotted lines report the UWB scenario, with $N_c = 10$ and $N_c = 50$, respectively. The markers show the simulation results averaged over 10 000 network realizations.

[1] As expected, larger spreading factors better mitigate multipath effects.

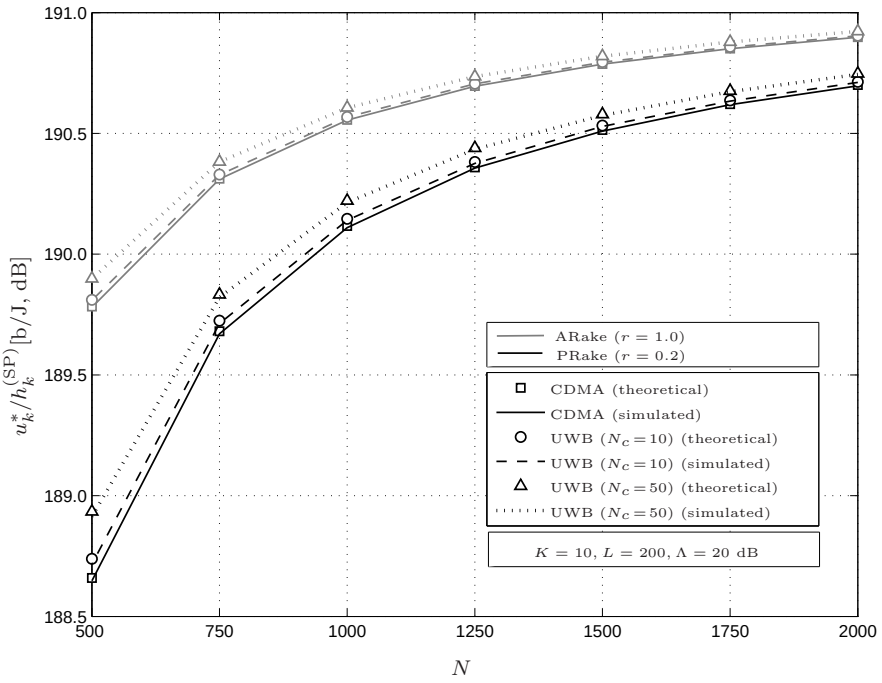

Figure 6.2: *Comparison of normalized utilities versus the spreading factor for RCDMA and IR-UWB schemes.*

As expected, the performance loss of CDMA with respect to UWB is negligible (less than 1 dB) when compared with the normalized achieved utilities. A first conclusion is that, based on game-theoretic power control analysis, the performance of these two multiple access schemes is practically equivalent. Numerical results also show that, with N fixed, a higher r provides smaller difference in performance between the two multiple access schemes. This is reasonable, since exploiting the diversity by adding a higher number of fingers (and thus increasing r) results in better mitigation of frequency-selective fading.

Similar considerations can be made by examining the results shown in Fig. 6.3, where we report the loss of CDMA with respect to UWB with $N_c = 50$. The decay constant of the channel is assumed to be $\Lambda = 20$ dB. Light and dark lines represent $K = 10$ and $K = 20$, respectively. The solid lines depict the case ARake, while the dashed

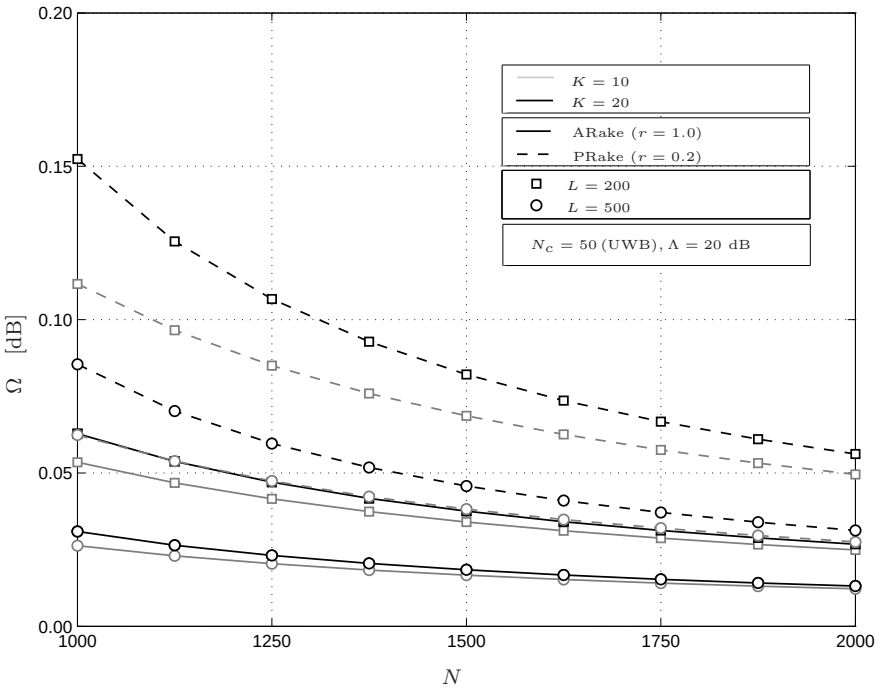

Figure 6.3: *Performance loss of CDMA with respect to UWB for different values of the system parameters.*

lines show the case PRake ($r = 0.2$). The square markers and the circles report the theoretical results with $L = 200$ and $L = 500$ multiple paths, respectively. It can be seen that the loss Ω is always very small. In addition, it is seen that Ω decreases as L increases. This can be justified since UWB cannot further mitigate the effect of denser and denser multipath in an N_c-fixed scenario, and thus its behavior is more similar to that of CDMA systems. Note that this statement is not in contrast with the comments about Fig. 6.2, since the comparison would be completely different if we considered IR-UWB with fixed N and variable N_c. In fact, if we choose N_c such that ρ is constant accordingly to the increasing L, Ω remains unchanged, as is apparent from (6.5)-(6.6).

6.2 Flat fading

The framework developed in Chapter 4 is also valid to study the performance of energy-efficient power control in a flat-fading scenario [12]. Even though the asymptotic behavior of the achieved utilities at the Nash equilibrium is obtained for a large number of multiple paths L, the flat-fading scenario can still be captured by letting the decaying constant Λ go to infinity: $\Lambda \to \infty$.

This mathematical artifice is in fact expedient to describe the case of a single component by simply reducing the power of the other channel paths to 0. In this scenario, the Rake receiver at the access point reduces to a simple matched filter. Hence, for ease of calculation, it is convenient to elaborate on (4.44)-(4.45), derived in Sect. 4.2.4, for an all-Rake receiver, rather than on (4.38)-(4.41), derived in Sect. 4.2.2 and valid for the general case of PRake.

In particular, (4.44) reports the asymptotic value of the term due to MAI ζ_k^{-1}, which is equal to $\zeta_k^{-1} = (K-1)/N$ irrespective of all the network parameters (including Λ). Analogously, (4.45) derives the behavior for the term due to SI $\gamma_{0,k}^{-1}$. In this case, it is straightforward to verify that

$$\lim_{\Lambda \to \infty} \nu_A(\Lambda, \rho) = 0, \tag{6.9}$$

and thus $\gamma_{0,k}^{-1} \overset{a.s.}{\to} \nu_A(\Lambda, \rho)/N = 0$. This implies that, under the assumption of flat-fading,

i) the MAI is independent of the multiple access scheme; and

ii) the SI is null, irrespective of the multiple access scheme.

As a consequence, the utilities achieved at the Nash equilibrium by CDMA-based schemes is identical to that of UWB-based networks.

This result matches with intuitive considerations. In fact, the absence of multiple paths (and hence of SI) makes the protection induced by TH vanish. A further support to this proof can be provided in terms of the TH-UWB spreading sequence $\mathbf{s}^{(k)}$. The dependence of the terms in the sequence is in fact limited to those belonging to the same frame only. Since each frame contains only one monocycle, the contribution given by the other time slots can be neglected in terms of power-related issues. It turns out that the only valuable terms $s_n^{(k)}$ in the sequence are binary, independent and identically distributed, which corresponds to the case of the CDMA scheme.

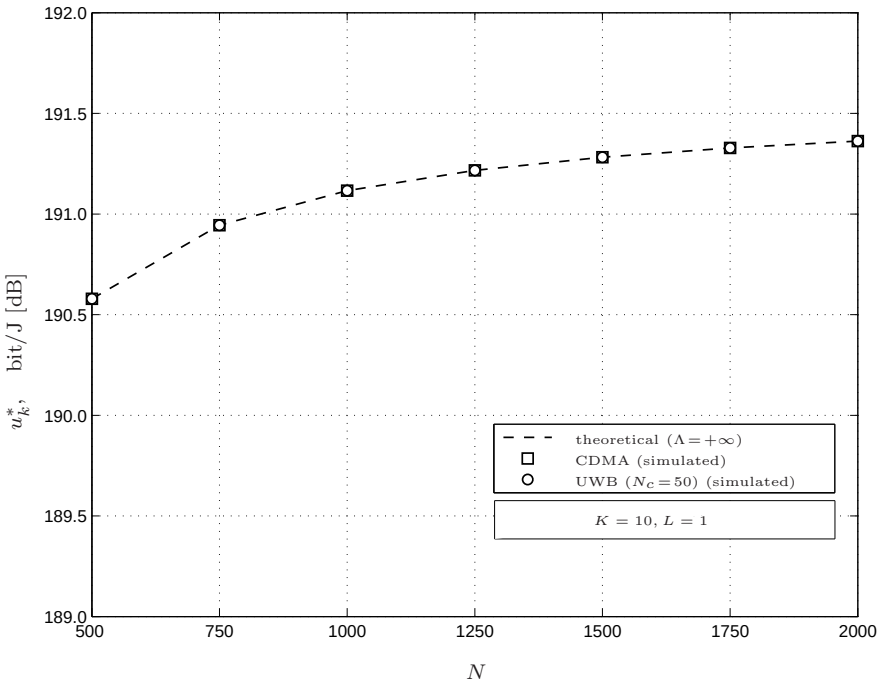

Figure 6.4: *Comparison of normalized utilities versus the spreading factor for CDMA and UWB schemes.*

Fig. 6.4 offers a comparison of theoretical and simulation results for the normalized utilities for both multiple access schemes. As can be seen, irrespective of the network parameters, the performance achieved by TH-UWB and CDMA schemes is the same. To further confirm this finding, the results are also in accordance with the analysis conducted by Meshkati *et al.* [85] for the joint maximization of power control and receiver selection for CDMA wireless networks in the case of flat-fading channels and matched filters.

Chapter 7

Conclusions and perspectives

In this thesis, we used a game-theoretic approach to study distributed power control techniques in the uplink of wideband wireless communication networks. In particular, we focused our research on wireless networks using ultrawideband (UWB) as the physical-layer multiple access technique. UWB technology is considered to be a potential candidate for multiuser high-speed data networks. However, the scope of this thesis is not limited to UWB-based systems, since the proposed framework is general enough to encompass code division multiple access (CDMA) networks as a subcase.

The main concern in the identification of the game has been power efficiency. This has led us to the use of a utility function that maximizes the life of a battery-operated terminal: the ratio between the correctly delivered bits in a packet versus the energy spent to deliver those bits.

When each user adopts a best-response strategy, which consists of updating its transmit power according to the throughput obtained at the access point, all users achieve a unique stable equilibrium from which no terminal wishes to unilaterally deviate (the Nash equilibrium). Our large-system analysis suggests that this happens irrespective of the statistics of the channel taps (assuming a tapped-delay line model), and of the kind of Rake receiver that is adopted at the access point to cope with multipath propagation. Such analysis is fairly general and captures a few different scenarios: the wireless channel can be either frequency-selective with exponential decay, or frequency-flat, or frequency-selective with flat power delay profile; the receiver can be either partial- or all-Rake with maximal ratio combining.

Our (closed-form) result for the distributed power control can be compared with the optimal power allocation in a social sense, which corresponds to a centralized

solution under the control of the access point. The typical degradation in terms of energy efficiency of distributed control with respect to such an optimum turns out to be negligible. This paves the way for the use of game-theoretic power control techniques in wireless networks when energy efficiency is the main concern.

We also have shown that our framework and the relevant conclusions are further applicable to classical random CDMA, which pays only a small degradation in terms of achieved utility with respect to UWB.

The resource allocation schemes presented in this thesis could be further refined by considering mixed strategies, where the user terminals choose their transmit powers according to an optimal probability distribution. This introduces additional signal processing at the mobile terminal, which however does not represent a technological limit. On the other hand, enlarging the set of allowable powers might increase the potentiality of the power control algorithm.

Further improvements in the achieved performance could be obtained by modeling the power control scheme as a repeated game, in which the convergence speed of the algorithm is considered in the utility function. This solution might mitigate the additional computational power required by the mixed-strategy scenario.

An alternative approach to pure energy-efficiency-driven control would be replacing the goodput of the link with its Shannon capacity [43], assuming that the terminal uses adaptive coding and modulation (ACM) to stay as close as possible to capacity for each channel condition.

Further benefits can be provided by devising more elaborate cross-layer optimizations, which consider other aspects of the network. As an example, medium access control (MAC) schemes can also be considered as part of a more general resource allocation strategy due to the competitive (and hence game-theoretic) nature of the medium contention. Some results along these lines can be found in [84]. If power allocation is designed jointly with the MAC strategy according to the utility-maximizing criteria described above, more effective resource allocation is guaranteed to all the terminals in the network.

Appendix A

Properties of random vectors

The results presented in this appendix are introduced to perform the large-system analysis of the NPCG presented in Chapter 4.

Lemma 2 ([16]) *Consider an n-dimensional vector $\mathbf{r}_n = [R_1, \ldots, R_n]$ with independent and identically distributed (i.i.d.) standardized (complex) entries (i.e. $\mathbb{E}[R_i] = 0$ and $\mathbb{E}[|R_i|^2] = 1$, with $\mathbb{E}[\cdot]$ denoting expectation), and let $\mathbf{C}_n$ be an $n \times n$ (complex) matrix independent of $\mathbf{r}_n$. For any $p \in \mathbb{N}$,*

$$\mathbb{E}\left[\left|\mathbf{r}_n^H \mathbf{C}_n \mathbf{r}_n - \mathrm{Tr}(\mathbf{C}_n)\right|^p\right] = K_p \left(\left(\mathbb{E}\left[|R_1|^4\right] \mathrm{Tr}\left(\mathbf{C}_n \mathbf{C}_n^H\right)\right)^{p/2} + \mathbb{E}\left[|R_1|^{2p}\right] \mathrm{Tr}\left(\mathbf{C}_n \mathbf{C}_n^H\right)^{p/2}\right), \tag{A.1}$$

where the constant K_p does not depend either on n or on $\mathbf{C}_n$.

Theorem 7 *Consider an n-dimensional vector $\mathbf{x}_n = \frac{1}{\sqrt{n}}[X_1, \ldots, X_n]$ with i.i.d. standardized (complex) entries with finite eighth moment, and let $\mathbf{C}_n$ be an $n \times n$ (complex) matrix independent of $\mathbf{x}_n$ with uniformly bounded spectral radius for all n. Under these hypotheses,*

$$\mathbf{x}_n^H \mathbf{C}_n \mathbf{x}_n \overset{a.s.}{\to} \frac{1}{n} \mathrm{Tr}(\mathbf{C}_n). \tag{A.2}$$

Proof Using Lemma 2 and Markov's inequality,

$$\begin{aligned} \Pr\left[\left|\mathbf{x}_n^H \mathbf{C}_n \mathbf{x}_n - \frac{1}{n}\mathrm{Tr}(\mathbf{C}_n)\right| > \epsilon\right] &\leq \frac{\mathbb{E}\left[\left|\mathbf{x}_n^H \mathbf{C}_n \mathbf{x}_n - \frac{1}{n}\mathrm{Tr}(\mathbf{C}_n)\right|^4\right]}{\epsilon^4} \\ &\leq \kappa \cdot \frac{1}{n^2 \cdot \epsilon^4}, \end{aligned} \tag{A.3}$$

where $\kappa < \infty$ is a constant value independent of n. Thus,

$$\sum_{n=1}^{\infty} \Pr\left[\left|\mathbf{x}_n^H \mathbf{C}_n \mathbf{x}_n - \frac{1}{n}\operatorname{Tr}(\mathbf{C}_n)\right| > \epsilon\right] < \infty. \tag{A.4}$$

Using the Borel-Cantelli lemma [21], the result (A.2) is straightforward.

Theorem 8 *Suppose* $\mathbf{x}_n = [X_1, \ldots, X_n]$ *and* $\mathbf{y}_n = [Y_1, \ldots, Y_n]$ *are* n*-dimensional independent vectors with i.i.d. standardized (complex) entries with finite eighth moment, and* $\mathbf{C}_n$ *is an* $n \times n$ *matrix (complex) independent on* $\mathbf{x}_n$ *and* $\mathbf{y}_n$ *with uniformly bounded spectral radius for all* n*. Then,*

$$\mathbf{x}_n^H \mathbf{C}_n \mathbf{y}_n \overset{a.s.}{\rightarrow} 0. \tag{A.5}$$

Proof The proof can be obtained using the same steps as that of Theorem 7.

Appendix B

Proofs of Props. 4 and 5

This appendix contains the proofs of Props. 4 and 5, reported in Sect. 4.2.2.

B.1 Proof of Prop. 4

To derive (4.38), we make use of the result (4.18) of Theorem 5. Using the hypotheses shown in Sect. 4.2, $\mathbf{D}_k^{\alpha}$ and $\mathbf{D}_k^{\beta}$ are represented by (4.35) and (4.36), respectively.

Hence, focusing on the denominator of (4.18),

$$\begin{aligned}\varphi\left(\mathbf{D}_k^{\alpha}\mathbf{D}_k^{\beta}\right) &= \lim_{L\to\infty}\frac{1}{L}\sum_{l=1}^{L}\left\{\mathbf{D}_k^{\alpha}\mathbf{D}_k^{\beta}\right\}_l \\ &= \lim_{L\to\infty}\frac{\sigma_k^2}{L}\sum_{l=1}^{rL}\Lambda^{-\frac{l-1}{L-1}} \\ &= \sigma_k^2\cdot\frac{\Lambda^r-1}{\Lambda^r\log\Lambda}. \end{aligned} \tag{B.1}$$

Analogously,

$$\varphi\left(\mathbf{D}_j^{\alpha}\mathbf{D}_j^{\beta}\right) = \sigma_j^2\cdot\frac{\Lambda^r-1}{\Lambda^r\log\Lambda}. \tag{B.2}$$

Using (2.10), (2.11) and (4.34), after some algebraic manipulation, we obtain

$$\left\{\mathbf{C}_j^{\alpha}\mathbf{C}_j^{\alpha H}\right\}_{ll} = \frac{\sigma_j^2}{L}\left(\sum_{m=l+1}^{L}\Lambda^{-\frac{m-1}{L-1}}\right)u\left[L-1-l\right], \tag{B.3}$$

$$\left\{\mathbf{C}_k^{\beta}\mathbf{C}_k^{\beta H}\right\}_{ll} = \frac{\sigma_k^2}{L}\left(\sum_{m=l+1}^{rL}\Lambda^{-\frac{m-1}{L-1}}\right)u\left[rL-1-l\right], \tag{B.4}$$

where $u[\cdot]$ is defined as in (4.37). The terms in the numerator of (4.18) thus translate into

$$\begin{aligned}\varphi\left(\mathbf{D}_j^{\alpha}\mathbf{C}_k^{\beta}\mathbf{C}_k^{\beta\,H}\mathbf{D}_j^{\alpha}\right) &= \lim_{L\to\infty}\frac{1}{L}\sum_{l=1}^{L}\left\{\mathbf{D}_j^{\alpha}\right\}_l^2\left\{\mathbf{C}_k^{\beta}\mathbf{C}_k^{\beta\,H}\right\}_{ll}\\ &= \lim_{L\to\infty}\frac{\sigma_k^2\sigma_j^2}{L^2}\sum_{l=1}^{rL-1}\Lambda^{-\frac{l-1}{L-1}}\sum_{m=l+1}^{rL}\Lambda^{-\frac{m-1}{L-1}}\\ &= \sigma_k^2\sigma_j^2\cdot\frac{\Lambda^{-2r}\left(\Lambda^r-1\right)^2}{2\left(\log\Lambda\right)^2}\end{aligned} \tag{B.5}$$

and

$$\begin{aligned}\varphi\left(\mathbf{D}_k^{\beta}\mathbf{C}_j^{\alpha}\mathbf{C}_j^{\alpha\,H}\mathbf{D}_k^{\beta}\right) &= \lim_{L\to\infty}\frac{1}{L}\sum_{l=1}^{L}\left\{\mathbf{D}_k^{\beta}\right\}_l^2\left\{\mathbf{C}_j^{\alpha}\mathbf{C}_j^{\alpha\,H}\right\}_{ll}\\ &= \lim_{L\to\infty}\frac{\sigma_k^2\sigma_j^2}{L^2}\sum_{l=1}^{rL}\Lambda^{-\frac{l-1}{L-1}}\sum_{m=l+1}^{L}\Lambda^{-\frac{m-1}{L-1}}\\ &= \sigma_k^2\sigma_j^2\cdot\frac{\Lambda^{-1-2r}\left(\Lambda^r-1\right)\left(\Lambda-2\Lambda^r+\Lambda^{r+1}\right)}{2\left(\log\Lambda\right)^2}.\end{aligned} \tag{B.6}$$

Using (B.1)-(B.2) and (B.5)-(B.6),

$$\begin{aligned}\frac{h_{kj}^{(\mathrm{MAI})}}{h_j^{(\mathrm{SP})}} &\overset{a.s.}{\to} \frac{1}{N}\cdot\frac{\varphi\left(\mathbf{D}_j^{\alpha}\mathbf{C}_k^{\beta}\mathbf{C}_k^{\beta\,H}\mathbf{D}_j^{\alpha}\right)+\varphi\left(\mathbf{D}_k^{\beta}\mathbf{C}_j^{\alpha}\mathbf{C}_j^{\alpha\,H}\mathbf{D}_k^{\beta}\right)}{\varphi\left(\mathbf{D}_j^{\alpha}\mathbf{D}_j^{\beta}\right)\cdot\varphi\left(\mathbf{D}_k^{\alpha}\mathbf{D}_k^{\beta}\right)}\\ &= \frac{1}{N}\cdot\frac{(\Lambda-1)\,\Lambda^{r-1}}{\Lambda^r-1}.\end{aligned} \tag{B.7}$$

Using (B.7), the result (4.38) is straightforward. ■

B.2 Proof of Prop. 5

To derive (4.40), we make use of the result (4.30) of Theorem 5. Using the hypotheses shown in Sect. 4.2, $\mathbf{D}_k^{\alpha}$ and $\mathbf{D}_k^{\beta}$ are represented by (4.35) and (4.36), respectively. The denominator can be obtained following the same steps as for the proof of Prop. 4:

$$\left(\varphi\left(\mathbf{D}_k^{\alpha}\mathbf{D}_k^{\beta}\right)\right)^2 = \sigma_k^4\cdot\frac{\left(\Lambda^r-1\right)^2}{\Lambda^{2r}\left(\log\Lambda\right)^2}. \tag{B.8}$$

Following (4.31),

$$\theta_k^2\left(l, L+l-i\right) = \sigma_k^4 \cdot \Lambda^{-\frac{L+2l-i-2}{L-1}} \cdot w\left[l,i\right], \tag{B.9}$$

where

$$\begin{aligned} w\left[l,i\right] &= u\left[rL-l\right] + u\left[rL-L+i-l\right] \\ &\quad + 2u\left[rL-l\right] \cdot u\left[rL-L+i-l\right] \end{aligned} \tag{B.10}$$

has been introduced for convenience of notation.

In order to obtain explicit expressions for $w\left[l,i\right]$, it is convenient to split the range of r into the two following cases.

- $r \leq 1/2$: taking into account all the possible values of l and i,

$$w\left[l,i\right] = \begin{cases} 4, & \text{if } L-rL+1 \leq i \leq L-1 \text{ and} \\ & \quad 1 \leq l \leq rL-L+i; \\ 1, & \text{either if } 1 \leq i \leq rL \text{ and } 1 \leq l \leq 1, \\ & \text{or if } rL \leq i \leq L-rL \text{ and } 1 \leq l \leq rL, \\ & \text{or if } L-rL+1 \leq i \leq L-1 \text{ and} \\ & \quad rL-L+i+1 \leq l \leq rL; \\ 0, & \text{elsewhere.} \end{cases} \tag{B.11}$$

Substituting (4.31) and (B.11) in the numerator of (4.30) yields

$$\begin{aligned} &\frac{1}{\sigma_k^4}\sum_{i=1}^{L-1}\phi_i^2 \cdot \sum_{l=1}^{i}\theta_k^2\left(l, L+l-i\right) = \\ &\quad = \sum_{i=1}^{rL}\phi_i^2 \cdot \sum_{l=1}^{i}\Lambda^{-\frac{L+2l-i-2}{L-1}} \\ &\quad + \sum_{i=rL+1}^{L-rL}\phi_i^2 \cdot \sum_{l=1}^{rL}\Lambda^{-\frac{L+2l-i-2}{L-1}} \\ &\quad + \sum_{i=L-rL+1}^{L-1}\phi_i^2 \cdot \sum_{l=1}^{rL-L+i}4\Lambda^{-\frac{L+2l-i-2}{L-1}} \\ &\quad + \sum_{i=L-rL+1}^{L-1}\phi_i^2 \cdot \sum_{l=rL-L+i+1}^{rL}\Lambda^{-\frac{L+2l-i-2}{L-1}}; \end{aligned} \tag{B.12}$$

- $r \geq 1/2$: taking into account all the possible values of l and i,

$$w\left[l,i\right]=\begin{cases}4, & \text{either if } L-rL+1\leq i\leq rL \text{ and}\\ & \qquad 1\leq l\leq rL-L+i,\\ & \text{or if } rL+1\leq i\leq L-1 \text{ and}\\ & \qquad 1\leq l\leq rL-L+i;\\ 1, & \text{either if } 1\leq i\leq L-rL \text{ and } 1\leq l\leq 1,\\ & \text{or if } L-rL+1\leq i\leq rL \text{ and}\\ & \qquad rL-L+i+1\leq l\leq i,\\ & \text{or if } rL+1\leq i\leq L-1 \text{ and}\\ & \qquad rL-L+i+1\leq l\leq rL;\\ 0, & \text{elsewhere.}\end{cases} \tag{B.13}$$

Substituting (4.31) and (B.13) in the numerator of (4.30) yields

$$\begin{aligned}\frac{1}{\sigma_k^4}\sum_{i=1}^{L-1}\phi_i^2\cdot\sum_{l=1}^{i}\theta_k^2\left(l,L+l-i\right)=\\ =\sum_{i=1}^{L-rL}\phi_i^2\cdot\sum_{l=1}^{i}\Lambda^{-\frac{L+2l-i-2}{L-1}}\\ +\sum_{i=L-rL+1}^{rL}\phi_i^2\cdot\sum_{l=1}^{rL-L+i}4\Lambda^{-\frac{L+2l-i-2}{L-1}}\\ +\sum_{i=L-rL+1}^{rL}\phi_i^2\cdot\sum_{l=rL-L+i+1}^{i}\Lambda^{-\frac{L+2l-i-2}{L-1}}\\ +\sum_{i=rL+1}^{L-1}\phi_i^2\cdot\sum_{l=1}^{rL-L+i}4\Lambda^{-\frac{L+2l-i-2}{L-1}}\\ +\sum_{i=rL+1}^{L-1}\phi_i^2\cdot\sum_{l=rL-L+i+1}^{rL}\Lambda^{-\frac{L+2l-i-2}{L-1}}.\end{aligned} \tag{B.14}$$

In order to obtain (4.41a)-(4.41e), the explicit values of ϕ_i^2 must be used. From

(2.12)-(2.13) follows

$$\phi_i^2 = \begin{cases} (L-i)/N_c, & \text{either if } N_c \leq L \text{ and} \\ & \qquad L - N_c + 1 \leq i \leq L-1, \\ & \text{or if } N_c \geq L \text{ and } 1 \leq i \leq L-1; \\ 1, & \text{if } N_c \leq L \text{ and } 1 \leq i \leq L - N_c. \end{cases} \tag{B.15}$$

As in the case of r, it is convenient to separate the range of $\rho = N_c/L$ in the following cases.

- $0 \leq \rho \leq \min(r, 1-r)$: substituting (B.15) in (B.12) and (B.14), they both yield

$$\begin{aligned} \frac{1}{\sigma_k^4} \lim_{L\to\infty} \frac{1}{L^2} \sum_{i=1}^{L-1} \phi_i^2 \cdot \sum_{l=1}^{i} \theta_k^2 \left(l, L+l-i\right) = \\ = \frac{\Lambda\left(\Lambda^r - 1\right)\left(4\Lambda^{2r} + 3\Lambda^\rho - 1\right)}{2\Lambda^{\rho+2r+1}\rho\left(\log\Lambda\right)^3} \\ - \frac{2\Lambda^{r+\rho}\left(\Lambda^r + 3\Lambda - 1\right)\rho\log\Lambda}{2\Lambda^{\rho+2r+1}\rho\left(\log\Lambda\right)^3}. \end{aligned} \tag{B.16}$$

  Making use of (4.30), (B.8) and (B.16), the results (4.40) and (4.41a) are straightforward.

- $\min(r, 1-r) \leq \rho \leq \max(r, 1-r)$ and $r \leq 1/2$: substituting (B.15) in (B.12) yields

$$\begin{aligned} \frac{1}{\sigma_k^4} \lim_{L\to\infty} \frac{1}{L^2} \sum_{i=1}^{L-1} \phi_i^2 \cdot \sum_{l=1}^{i} \theta_k^2 \left(l, L+l-i\right) = \\ = \frac{\Lambda\left(\Lambda^{2r} - 1\right)\left(4\Lambda^\rho - 1\right)}{2\Lambda^{\rho+2r+1}\rho\left(\log\Lambda\right)^3} \\ - \frac{2\Lambda^{r+\rho}\left(3\Lambda r - \rho + \Lambda^r\rho\right)\log\Lambda}{2\Lambda^{\rho+2r+1}\rho\left(\log\Lambda\right)^3}. \end{aligned} \tag{B.17}$$

  Making use of (4.30), (B.8) and (B.17), the results (4.40) and (4.41b) are straightforward.

- $\min(r, 1-r) \leq \rho \leq \max(r, 1-r)$ and $r \geq 1/2$: substituting (B.15) in (B.14)

yields

$$\begin{aligned}\frac{1}{\sigma_k^4}\lim_{L\to\infty}\frac{1}{L^2}\sum_{i=1}^{L-1}\phi_i^2\cdot\sum_{l=1}^{i}\theta_k^2\left(l,L+l-i\right)=\\ =\frac{-4\Lambda^{2+2r}-4\Lambda^{2+\rho}+\Lambda^{2(r+\rho)}+4\Lambda^{2+2r+\rho}}{2\Lambda^{2+2r+\rho}\rho\left(\log\Lambda\right)^3}\\ +\frac{3\Lambda^{2+2\rho}-2\rho^{\rho+r+1}\left(\Lambda^r\rho+3\Lambda\rho+r-1\right)\log\Lambda}{2\Lambda^{2+2r+\rho}\rho\left(\log\Lambda\right)^3}.\end{aligned}\tag{B.18}$$

Making use of (4.30), (B.8) and (B.18), the results (4.40) and (4.41c) are straightforward.

- $\max(r,1-r)\leq\rho\leq 1$: substituting (B.15) into (B.12) and (B.14), they both yield

$$\begin{aligned}\frac{1}{\sigma_k^4}\lim_{L\to\infty}\frac{1}{L^2}\sum_{i=1}^{L-1}\phi_i^2\cdot\sum_{l=1}^{i}\theta_k^2\left(l,L+l-i\right)=\\ =\frac{-\Lambda^{2+2r}-4\Lambda^{2+\rho}+\Lambda^{2(r+\rho)}+4\Lambda^{2+2r+\rho}}{2\Lambda^{2+2r+\rho}\rho\left(\log\Lambda\right)^3}\\ -\frac{2\rho^{\rho+r+1}\left(\Lambda^r\rho+3\Lambda r+r-1\right)\log\Lambda}{2\Lambda^{2+2r+\rho}\rho\left(\log\Lambda\right)^3}.\end{aligned}\tag{B.19}$$

Making use of (4.30), (B.8) and (B.19), the results (4.40) and (4.41d) are straightforward.

- $\rho=N_c/L\geq 1$: substituting (B.15) into (B.12) and (B.14), they both yield

$$\begin{aligned}\frac{1}{\sigma_k^4}\lim_{L\to\infty}\frac{1}{L^2}\sum_{i=1}^{L-1}\phi_i^2\cdot\sum_{l=1}^{i}\theta_k^2\left(l,L+l-i\right)=\\ =\frac{2\Lambda\left(\Lambda^{2r}-1\right)-\left(\Lambda^r+r+3\Lambda r-1\right)\Lambda^r\log\Lambda}{\Lambda^{2r+1}\rho\left(\log\Lambda\right)^3}.\end{aligned}\tag{B.20}$$

Making use of (4.30), (B.8) and (B.20), the results (4.40) and (4.41e) are straightforward.

■

Bibliography

[1] J. M. Aein, "Power balancing in systems employing frequency reuse," *COMSAT Technical Review*, vol. 3, no. 2, pp. 277–300, Fall 1973.

[2] H. Alavi and R. W. Nettleton, "Downstream power control for a spread-spectrum cellular mobile radio system," in *Proc. IEEE Global Telecommunications Conf.*, Miami, FL, Nov. 1982, pp. 84–88.

[3] T. Alpcan and T. Başar, "A hybrid systems model for power control in multicell wireless data networks," *Performance Evaluation*, vol. 57, no. 4, pp. 477–495, Aug. 2004.

[4] T. Alpcan, T. Başar, and S. Dey, "A power control game based on outage probabilities for multicell wireless data networks," vol. 5, no. 4, pp. 890–899, Apr. 2006.

[5] T. Alpcan, T. Başar, R. Srikant, and E. Altman, "CDMA uplink power control as a noncooperative game," *Wireless Networks*, vol. 8, no. 6, pp. 659–670, Nov. 2002.

[6] E. Altman and Z. Altman, "S-modular games and power control in wireless networks," *IEEE Trans. Automat. Contr.*, vol. 48, no. 5, pp. 839–842, May 2003.

[7] E. Altman, K. Avrachenkov, G. Miller, and B. Prabhu, "Discrete power control: Cooperative and non-cooperative optimization," in *Proc. IEEE Int. Conf. Computer Communications*, Anchorage, AK, May 2007, pp. 37–45.

[8] E. Altman, T. Boulogne, R. E. Azouzi, T. Jimenez, and L.Wynter, "A survey on networking games in telecommunications," *Computers and Operations Research*, vol. 33, no. 2, pp. 286–311, Feb. 2006.

[9] R. J. Aumann and M. Maschler, "Game theoretic analysis of a bankruptcy problem from the Talmud," *Journal of Economic Theory*, vol. 36, pp. 195–213, 1985.

[10] E. Baccarelli, M. Biagi, and C. Pelizzoni, "A distributed power-allocation and signal-shaping game for the competitively optimal throughput-maximization of multiple-antenna ad hoc networks," *IEEE Trans. Veh. Technol.*, vol. 55, no. 6, pp. 1862–1876, Nov. 2006.

[11] G. Bacci, M. Luise, and H. V. Poor, "Performance comparison of energy-efficient power control for CDMA and multiuser UWB networks," in *Proc. IST Mobile & Wireless Summit*, Budapest, Hungary, July 2007.

[12] ——, "Energy-efficient power control is (almost) equivalent for DS-CDMA and TH-UWB," *IEE Electronics Letters*, vol. 44, no. 8, pp. 555–557, Apr. 2008.

[13] ——, "Game theory and power control in ultrawideband networks," *Physical Communication*, vol. 1, no. 1, pp. 21–39, 1st Quarter 2008.

[14] ——, "Performance of rake receivers in IR-UWB networks using energy-efficient power control," *IEEE Trans. Wireless Commun.*, 2008, to appear.

[15] G. Bacci, M. Luise, H. V. Poor, and A. M. Tulino, "Energy-efficient power control in impulse radio UWB wireless networks," *IEEE J. Select. Topics Signal Processing*, vol. 1, no. 3, pp. 508–520, Oct. 2007.

[16] Z. D. Bai and J. W. Silverstein, "No eigenvalues outside the support of the limiting spectral distribution of large dimensional sample covariance matrices," *Annals of Probability*, vol. 26, no. 1, pp. 316–345, 1998.

[17] T. W. Barrett, "History of ultra wideband (UWB) radar and communications: Pioneers and innovators," in *Proc. Progress in Electromagnetics Research Symposium*, Cambridge, MA, July 2000.

[18] W. J. Baumol and S. M. Goldfield, *Precursors in Mathematical Economics: An Anthology.* London, England: London School of Economics and Political Science, 1968.

[19] J. Bertrand, "Théorie mathématique de la richesse social," *Journal des Savants*, vol. 67, pp. 499–508, 1883.

[20] S. M. Betz and H. V. Poor, "Energy efficiency in multi-hop CDMA networks: A game theoretic analysis," in *Proc. Int. Conf. Parallel and Distributed Systems*, Minneapolis, MN, July 2006.

[21] P. Billingsley, *Probability and Measure*. New York, NY: Wiley, 1995.

[22] S. Buzzi, V. Massaro, and H. V. Poor, "Power control and receiver design for energy-efficiency in multipath CDMA channels with bandlimited waveforms," in *Proc. Annual Conf. on Information Sciences and Systems*, Baltimore, MD, Mar. 2007.

[23] S. Buzzi and H. V. Poor, "Non-cooperative games for spreading code optimization, power control and receiver design in wireless data networks," in *Proc. European Wireless Conf.*, Paris, France, Apr. 2007.

[24] ——, "Power control algorithms in CDMA channels based on large system analysis," in *Proc. IEEE Int. Symp. Information Theory*, Nice, France, June 2007.

[25] ——, "Joint receiver and transmitter optimization for energy-efficient CDMA communications," *IEEE J. Select. Areas Commun.*, 2008, to appear.

[26] S. Buzzi, D. Saturnino, and H. V. Poor, "Stochastic non-cooperative games for energy efficiency in wireless data networks," in *Proc. Tyrrhenian Int. Workshop on Digital Communication*, Naples, Italy, Sept. 2007.

[27] D. Cassioli and F. Mazzenga, "Spectral analysis of UWB multiple access schemes using random scrambling," *IEEE Trans. Wireless Commun.*, vol. 3, no. 5, pp. 1637–1647, Sept. 2004.

[28] D. Cassioli, M. Z. Win, and A. F. Molisch, "The ultra-wide bandwidth indoor channel: From statistical model to simulations," *IEEE J. Select. Areas Commun.*, vol. 20, no. 6, pp. 1247–1257, Aug. 2002.

[29] R. Chen, J. G. Andrews, R. W. Heath, and A. Ghosh, "Uplink power control in multi-cell spatial multiplexing wireless systems," vol. 6, no. 7, pp. 2700–2711, July 2007.

[30] C.-C. Chong, Y. Kim, and S.-S. Lee, "A modified S-V clustering channel model for the UWB indoor residential environment," in *Proc. IEEE Veh. Technol. Conf.*, Stockholm, Sweden, May-Jun. 2005, pp. 58–62.

[31] F. C. Commission, "02-48: First report and order," U. S. Federal Communications Commission, Tech. Rep. FCC 02-48, 2002.

[32] A. A. Cournot, "Recherches sur les principes mathématiques de la théorie des richesses," 1838.

[33] D. Debreu, "A social equilibrium existence theorem," *Proc. Nat. Acad. Sciences*, vol. 38, pp. 886–893, 1952.

[34] M. Decina and V. Trecordi, "Convergence of telecommunications and computing to networking models for integrated services and applications," *Proc. IEEE*, vol. 85, no. 12, pp. 1887–1914, Dec. 1997.

[35] F. Edgeworth, "La teoria pura del monopolio," *Giornale degli Economisti*, vol. 15, pp. 13–31, 1897.

[36] D. Famolari, N. B. Mandayam, D. J. Goodman, and V. Shah, "A new framework for power control in wireless data networks: Games, utility and pricing," in *Wireless Multimedia Network Technologies*, R. Ganesh, K. Pahlavan, and Z. Zvonar, Eds. Boston, MA: Kluwer Academic Publishers, 1999, pp. 289–310.

[37] K. Fan, "Fixed point and minimax theorems in locally convex topological linear spaces," *Proc. Nat. Acad. Sciences*, vol. 38, pp. 121–126, 1952.

[38] M. Félegyházi, "Non-cooperative behavior in wireless networks," Ph.D. dissertation, École Polytechnique Fédérale de Lausanne (EFPL), Lausanne, Switzerland, 2007.

[39] M. Félegyházi and J.-P. Hubaux, "Game theory in wireless networks: A tutorial," École Polytechnique Fédérale de Lausanne (EFPL), Tech. Rep. EPFL LCA-REPORT-2006-002, June 2007.

[40] N. Feng, S.-C. Mau, and N. B. Mandayam, "Pricing and power control for joint network-centric and user-centric radio resource management," *IEEE Trans. Commun.*, vol. 52, no. 9, pp. 1547–1557, Sept. 2004.

[41] ——, "Joint network-centric and user-centric radio resource management in a multicell system," *IEEE Trans. Commun.*, vol. 53, no. 7, pp. 1114–1118, July 2005.

[42] E. Fishler and H. V. Poor, "Low-complexity multiuser detectors for time-hopping impulse-radio systems," *IEEE Trans. Signal Processing*, vol. 50, no. 9, pp. 1440–1450, Sept. 2002.

[43] D. A. Fittipaldi and M. Luise, "Power-saving and capacity-maximizing power control criteria in CDMA wireless ad hoc networks," in *Proc. IST Mobile & Wireless Summit*, Mykonos, Greece, June 2006.

[44] J. R. Foerster, "The performance of a direct-sequence spread ultra wideband system in the presence of multipath, narrowband interference, and multiuser interference," in *Proc. IEEE Conf. Ultra-Wideband Systems and Technologies*, Baltimore, MD, May 2002, pp. 87–92.

[45] ——, "Channel modeling sub-committee report (final)," IEEE P802.15 Working Group for Wireless Personal Area Networks, Tech. Rep. IEEE P802.15-02/490r1-SG3a, Feb. 2007.

[46] G. J. Foschini and Z. Miljanic, "A simple distributed autonomous power control algorithm and its convergence," *IEEE Trans. Veh. Technol.*, vol. 42, no. 4, pp. 641–646, Nov. 1993.

[47] J. Friedman, "A non-cooperative equilibrium for supergames," *Review of Economic Studies*, vol. 38, pp. 1–12, 1971.

[48] D. Fudenberg and J. Tirole, *Game Theory*. Cambridge, MA: MIT Press, 1991.

[49] S. Gezici, H. Kobayashi, H. V. Poor, and A. F. Molisch, "Optimal and sub-optimal linear receivers for time-hopping impulse radio systems," in *Proc. Int. Workshop on Ultra Wideband Systems*, Kyoto, Japan, May 2004, pp. 11–15.

[50] ——, "Performance evaluation of impulse radio UWB systems with pulse-based polarity randomization," *IEEE Trans. Signal Processing*, vol. 53, no. 7, pp. 2537–2549, July 2005.

[51] S. Gezici, Z. Tian, G. B. Biannakis, H. Kobayashi, A. F. Molisch, H. V. Poor, and Z. Sahinoglu, "Localization via ultra-wideband radios: A look at positioning aspects for future sensor networks," *IEEE Signal Processing Mag.*, vol. 22, no. 4, pp. 70–84, July 2005.

[52] S. S. Ghassemzadeh, L. J. Greenstein, T. Sveinsson, A. Kavcic, and V. Tarokh, "UWB delay profile models for residential and commercial indoor environments," *IEEE Trans. Veh. Technol.*, vol. 54, no. 4, pp. 1235–1244, July 2005.

[53] R. Gibbons, *A Primer in Game Theory.* Harlow, England: FT Prentice Hall, 1992.

[54] I. L. Glicksberg, "A further generalization of the Kakutani fixed point theorem with application to Nash equilibrium points," *Proc. Nat. Acad. Sciences*, vol. 38, pp. 170–174, 1952.

[55] D. J. Goodman and N. B. Mandayam, "Power control for wireless data," *IEEE Personal Commun.*, vol. 7, no. 2, pp. 48–54, Apr. 2000.

[56] ——, "Network assisted power control for wireless data," in *Proc. IEEE Veh. Technol. Conf.*, Rhodes, Greece, May 2001, pp. 1022–1026.

[57] ——, "Network assisted power control for wireless data," *Mobile Networks and Applications*, vol. 6, no. 5, pp. 409–415, Sept. 2001.

[58] S. A. Grandhi, R. Vijayan, D. J. Goodman, and J. Zander, "Centralized power control in cellular radio systems," *IEEE Trans. Veh. Technol.*, vol. 42, no. 4, pp. 466–468, Nov. 1993.

[59] S. Gunturi and F. Paganini, "Game theoretic approach to power control in cellular CDMA," in *Proc. IEEE Veh. Technol. Conf.*, Orlando, FL, Oct. 2003, pp. 2362–2366.

[60] Z. Han and K. J. R. Liu, "Noncooperative power-control game and throughput game over wireless networks," vol. 53, no. 10, pp. 1625–1629, Oct. 2005.

[61] J. Harsanyi, "Games with incomplete information played by Bayesian players," *Management Science*, vol. 14, pp. 159–182, 320–334, 486–502, 1967-68.

[62] H. Hashemi, "The indoor radio propagation channel," *Proc. IEEE*, vol. 81, no. 7, pp. 943–968, July 1993.

[63] M. Hayajneh and C. T. Abdallah, "Statistical learning theory to evaluate the performance of game theoretic power control algorithms for wireless data in arbitrary channels," in *Proc. IEEE Wireless Commun. and Networking Conf.*, New Orleans, LA, Mar. 2003, pp. 723–728.

[64] ——, "Distributed joint rate and power control game-theoretic algorithms for wireless data," *IEEE Commun. Lett.*, vol. 8, no. 8, pp. 511–513, Aug. 2004.

[65] J. Huang, "Wireless resource allocation: Auctions, games and optimization," Ph.D. dissertation, Northwestern University, Chicago, IL, Dec. 2005.

[66] W. L. Huang and K. B. Letaief, "Cross-layer scheduling and power control combined with adaptive modulation for wireless ad hoc networks," vol. 55, no. 4, pp. 728–739, Apr. 2007.

[67] O. Ileri, S.-C. Mau, and N. B. Mandayam, "Pricing for enabling forwarding in self-configuring ad hoc networks," *IEEE J. Select. Areas Commun.*, vol. 23, no. 1, pp. 151–162, Jan. 2005.

[68] *Information Technology - Open Systems Interconnection - Basic Reference Model: The Basic Model*, ITU-T Std. Recommendation X.200, July 1994.

[69] H. Ji and C.-Y. Huang, "Non-cooperative uplink power control in cellular radio systems," *Wireless Networks*, vol. 41, no. 3, pp. 233–240, Mar. 1998.

[70] A. G. Klein, D. R. Brown III, D. L. Goeckel, and C. R. Johnson, Jr., "RAKE reception for UWB communication systems with intersymbol interference," in *Proc. IEEE Int. Workshop on Signal Processing Advances for Wireless Communications*, Rome, Italy, June 2003, pp. 244–248.

[71] S. Koskie and Z. Gajic, "A Nash game algorithm for SIR-based power control in 3G wireless CDMA networks," *IEEE/ACM Trans. Networking*, vol. 13, no. 5, pp. 1017–1026, Oct. 2005.

[72] H. Kuhn, "Extensive games and the problem of information," *Annals of Mathematics Studies*, vol. 28, pp. 193–216, 1953.

[73] C. J. Le-Martret and G. B. Giannakis, "All-digital PAM impulse radio for multiple-access through frequency-selective multipath," in *Proc. IEEE Global Telecommunications Conference (GLOBECOM)*, San Francisco, CA,, Nov.-Dec. 2000, pp. 77–81.

[74] K.-K. Leung and C. W. Sung, "An opportunistic power control algorithm for cellular network," *IEEE/ACM Trans. Networking*, vol. 14, no. 3, pp. 470–478, June 2006.

[75] C. Liang and K. R. Dandekar, "Power management in MIMO ad hoc networks: A game-theoretic approach," vol. 6, no. 4, pp. 1164–1170, Apr. 2007.

[76] A. B. MacKenzie and L. A. DaSilva, *Game Theory for Wireless Engineers.* San Rafael, CA: Morgan & Claypool, 2006.

[77] A. B. MacKenzie and S. B. Wicker, "Game theory in communications: Motivation, explanation, and application to power control," in *Proc. IEEE Global Telecommunications Conference (GLOBECOM)*, San Antonio, TX, Nov. 2001, pp. 821–826.

[78] P. Maillé, "Auctioning for downlink transmission power in CDMA cellular systems," in *Proc. ACM Int. Symp. Modeling, Analysis and Simulation of Wireless and Mobile Systems*, Venice, Italy, Oct. 2004, pp. 293–296.

[79] F. Meshkati, M. Chiang, H. V. Poor, and S. C. Schwartz, "A game-theoretic approach to energy-efficient power control in multicarrier CDMA systems," *IEEE J. Select. Areas Commun.*, vol. 24, no. 6, pp. 1115–1129, June 2006.

[80] F. Meshkati, A. J. Goldsmith, H. V. Poor, and S. C. Schwartz, "A game-theoretic approach to energy-efficient modulation in CDMA networks with delay QoS constraints," *IEEE J. Select. Areas Commun.*, vol. 25, no. 6, pp. 1069–1078, Aug. 2007.

[81] F. Meshkati, D. Guo, H. V. Poor, and S. C. Schwartz, "A unified approach to energy-efficient power control in large CDMA systems," *IEEE Trans. Wireless Commun.*, 2008, to appear.

[82] F. Meshkati, H. V. Poor, and S. C. Schwartz, "Energy-efficient resource allocation in wireless networks," *IEEE Signal Processing Mag.*, vol. 24, no. 3, pp. 58–68, May 2007.

[83] ——, "Energy efficiency-delay tradeoffs in multiple-access networks," *IEEE Trans. Inform. Theory*, 2008, to appear.

[84] F. Meshkati, H. V. Poor, S. C. Schwartz, and R. Balan, "Energy-efficient resource allocation in wireless networks with quality-of-service constraints," *IEEE Trans. Commun.*, 2008, to appear.

[85] F. Meshkati, H. V. Poor, S. C. Schwartz, and N. B. Mandayam, "An energy-efficient approach to power control and receiver design in wireless data networks," *IEEE Trans. Commun.*, vol. 53, no. 11, pp. 1885–1894, Nov. 2005.

[86] H. J. Meyerhoff, "Method for computing the optimum power balance in multibeam satellites," *COMSAT Technical Review*, vol. 4, no. 1, pp. 139–146, Spring 1974.

[87] A. F. Molisch, "IEEE 802.15.4a channel model - final report," IEEE 802.15 Wireless Personal Area Network Low Rate Alternative PHY Task Group 4a (TG4a), Tech. Rep., Nov. 2004.

[88] ——, "Ultrawideband propagation channels-theory, measurement, and modeling," *IEEE Trans. Veh. Technol.*, vol. 54, no. 5, pp. 1528–1545, Sept. 2005.

[89] Y.-P. Nakache and A. F. Molisch, "Spectral shape of UWB signals influence of modulation format, multiple access scheme, and pulse shape," in *Proc. IEEE Veh. Technol. Conf.*, Jeju, Korea, Apr. 2003, pp. 2510–2514.

[90] J. F. Nash, "The bargaining problem," *Econometrica*, vol. 18, pp. 155–162, 1950.

[91] ——, "Equilibrium points in N-person games," *Proc. National Academy of Sciences of the United States of America*, vol. 36, no. 1, pp. 48–49, Jan. 1950.

[92] ——, "Non-cooperative games," *Annals of Mathematics*, vol. 54, no. 2, pp. 286–295, Sept. 1951.

[93] ——, "Two-person cooperative games," *Econometrica*, vol. 21, pp. 128–140, 1953.

[94] R. W. Nettleton, "Traffic theory and interference management for a spread spectrum cellular mobile radio system," in *Proc. IEEE Int. Conf. Commun.*, Seattle, WA, June 1980, pp. 24.5.1–24.5.5.

[95] R. W. Nettleton and H. Alavi, "Power control for a spread spectrum cellular mobile radio system," in *Proc. IEEE Veh. Technol. Conf.*, Toronto, Canada, May 1983, pp. 242–246.

[96] D. Niyato and E. Hossain, "Radio resource management games in wireless networks: An approach to bandwidth allocation and admission control for polling service in IEEE 802.16," *IEEE Wireless Commun.*, vol. 14, no. 1, pp. 27–35, Feb. 2007.

[97] Official Journal of the European Union, issue 23/02/2007, "Commission decision of 21 February 2007 on allowing the use of the radio spectrum for equipment using ultra-wideband technology in a harmonised manner in the Community," Electronic Communications Committee, Tech. Rep. 2007/131/EC (notified under document number C(2007) 522), 2007.

[98] M. J. Osborne and A. Rubinstein, *A Course in Game Theory*. Cambridge, MA: MIT Press, 1994.

[99] D. P. Palomar, J. M. Cioffi, and M. A. Lagunas, "Uniform power allocation in MIMO channels: A game-theoretic approach," *IEEE Trans. Inform. Theory*, vol. 49, no. 7, pp. 1707–1727, July 2003.

[100] C. Park and T. S. Rappaport, "Short-range wireless communications for next-generation networks: UWB, 60 GHz millimeter-wave WPAN, and ZigBee," *IEEE Wireless Commun.*, vol. 14, no. 4, pp. 70–78, Aug. 2007.

[101] J. Ponstein, "Seven kinds of convexity," *SIAM Rev.*, vol. 9, no. i, pp. 115–119, Jan. 1967.

[102] J. G. Proakis, *Digital Communications*, 4th ed. New York, NY: McGraw-Hill, 2001.

[103] R. C. Qiu, H. Liu, and X. Shen, "Ultra-wideband for multiple access communications," *IEEE Commun. Mag.*, vol. 43, no. 2, pp. 80–87, Feb. 2005.

[104] T. Q. S. Quek and M. Z. Win, "Analysis of UWB transmitted-reference communication systems in dense multipath channels," *IEEE J. Select. Areas Commun.*, vol. 23, no. 9, pp. 1863–1874, Sept. 2005.

[105] A. W. Roberts and D. E. Varberg, *Convex Functions.* New York, NY: Academic Press, 1973.

[106] V. Rodriguez, "An analytical foundation for resource management in wireless communications," in *Proc. IEEE Global Telecommunications Conference (GLOBECOM)*, San Francisco, CA, Dec. 2003, pp. 898–902.

[107] T. Roughgarden, *Selfish Routing and the Price of Anarchy.* Cambridge, MA: MIT Press, 2005.

[108] S. Roy, J. R. Foerster, V. S. Somayazulu, and D. G. Leeper, "Ultrawideband radio design: The promise of high-speed, short-range wireless connectivity," *Proc. IEEE*, vol. 92, no. 2, pp. 295–311, Feb. 2004.

[109] C. U. Saraydar, N. B. Mandayam, and D. J. Goodman, "Pricing and power control in a multicell wireless data network," *IEEE J. Select. Areas Commun.*, vol. 19, no. 10, pp. 1883–1892, Oct. 2001.

[110] ——, "Efficient power control via pricing in wireless data networks," *IEEE Trans. Commun.*, vol. 50, no. 2, pp. 291–303, Feb. 2002.

[111] R. A. Scholtz, "Multiple access with time-hopping impulse modulation," in *Proc. IEEE Military Communications Conf. (MILCOM)*, Boston, MA, Oct. 1993, pp. 447–450.

[112] U. G. Schuster and H. Bölcskei, "Ultrawideband channel modeling on the basis of information-theoretic criteria," *IEEE Trans. Wireless Commun.*, vol. 6, no. 7, pp. 2464–2475, July 2007.

[113] R. Selten, "Spieltheoretische Behandlung eines Oligopolmodells mit Nachfrageträgheit," *Zeitschrift für die gesamte Staatswissenschaft*, vol. 12, pp. 301–324, 1965.

[114] V. Shah, N. B. Mandayam, and D. J. Goodman, "Power control for wireless data based on utility and pricing," in *Proc. IEEE Int. Symp. Personal, Indoor, and Mobile Radio Commun.*, Boston, MA, Sept. 1998, pp. 1427–1432.

[115] W. P. Siriwongpairat, W. Su, and K. J. R. Liu, "Performance characterization of multiband UWB communication systems using Poisson cluster arriving fading paths," *IEEE J. Select. Areas Commun.*, vol. 24, no. 4, pp. 745–751, Apr. 2006.

[116] V. Srivastava, J. Neel, A. B. MacKenzie, R. Menon, L. A. DaSilva, J. E. Hicks, J. H. Reed, and R. P. Gilles, "Using game theory to analyze wireless ad hoc networks," *IEEE Commun. Surveys & Tutorials*, vol. 7, no. 4, pp. 46–56, 4th Quarter 2005.

[117] C. A. St. Jean and B. Jabbari, "Game-theoretic power control in DS-CDMA wireless networks with successive interference cancellation," *IEE Electronics Letters*, vol. 42, no. 3, pp. 162–163, Feb. 2006.

[118] T. Starr, J. M. Cioffi, and P. J. Silverman, *Understanding Digital Subscriber Line Technology.* Upper Saddle River, NJ: Prentice-Hall, 1998.

[119] J. Sun and E. Modiano, "Opportunistic power allocation for fading channels with non-cooperative users and random access," in *Proc. Int. Conf. Broadband Networks*, Boston, MA, Oct. 2005, pp. 366–374.

[120] C. W. Sung and K.-K. Leung, "A generalized framework for distributed power control in wireless networks," *IEEE Trans. Inform. Theory*, vol. 51, no. 7, pp. 2625–2635, July 2005.

[121] C. W. Sung, K. W. Shum, and K.-K. Leung, "Stability of distributed power and signature sequence control for CDMA systems—A game-theoretic framework," *IEEE Trans. Inform. Theory*, vol. 52, no. 4, pp. 1775–1780, Apr. 2006.

[122] C. W. Sung and W. S. Wong, "A noncooperative power control game for multirate CDMA data networks," vol. 2, no. 1, pp. 186–194, Jan. 2003.

[123] D. M. Topkis, "Equilibrium points in nonzero sum n-person submodular games," *SIAM J. Control and Optimization*, vol. 17, no. 6, pp. 773–787, 1979.

[124] ——, *Supermodularity and Complementarity.* Princeton, NJ: Princeton University Press, 1998.

[125] D. N. C. Tse and P. Viswanath, *Fundamentals of Wireless Communications.* Cambridge, UK: Cambridge Univ. Press, 2005.

[126] A. W. Tucker, "A two-person dilemma," 1950, unpublished.

[127] S. Verdú, *Multiuser Detection.* Cambridge, U.K.: Cambridge University Press, 1998.

[128] J. von Neumann, "Zur Theorie der Gesellschaftsspiele," *Mathematische Annalen*, vol. 100, pp. 295–320, 1928.

[129] J. von Neumann and O. Morgenstern, *Theory of Games and Economic Behavior.* Princeton, NJ: Princeton University Press, 1944.

[130] Z. Wang, "Multi-carrier ultra-wideband multiple-access with good resilience against multiuser interference," in *Proc. Conf. Info. Sciences and Systems*, Baltimore, MD, Mar. 2003, pp. 87–92.

[131] M. Z. Win and R. A. Scholtz, "Impulse radio: How it works," *IEEE Commun. Lett.*, vol. 2, no. 2, pp. 36–38, Feb. 1998.

[132] ——, "Ultra-wide bandwidth time-hopping spread-spectrum impulse radio for wireless multiple-access communications," *IEEE Trans. Commun.*, vol. 48, no. 4, pp. 679–691, Apr. 2000.

[133] M. Xiao, N. B. Shroff, and E. K. P. Chong, "Resource management in power-controlled cellular wireless systems," *Wireless Communications and Mobile Computing*, vol. 1, no. 2, pp. 185–199, Apr.-June 2001.

[134] ——, "A utility-based power-control scheme in wireless cellular systems," *IEEE/ACM Trans. Networking*, vol. 11, no. 2, pp. 210–221, Apr. 2003.

[135] L. Yang and G. B. Giannakis, "Digital-carrier multi-band user codes for baseband UWB multiple access," *J. Commun. Networks*, vol. 5, no. 4, pp. 374–385, Dec. 2003.

[136] ——, "Ultra-wideband communications: An idea whose time has come," *IEEE Signal Processing Mag.*, vol. 21, no. 6, pp. 26–54, Nov. 2004.

[137] R. D. Yates, "A framework for uplink power control in cellular radio systems," *IEEE J. Select. Areas Commun.*, vol. 13, no. 9, pp. 1341–1347, Sept. 1995.

[138] J. Yuan, Z. Li, W. Yu, and B. Li, "A cross-layer optimization framework for multihop multicast in wireless mesh networks," *IEEE J. Select. Areas Commun.*, vol. 24, no. 11, pp. 2092–2103, Nov. 2006.

[139] J. Zander, "Distributed cochannel control in cellular radio systems," *IEEE Trans. Veh. Technol.*, vol. 41, no. 3, pp. 305–311, Aug. 1992.

[140] ——, "Performance of optimum transmitter power control in cellular radio systems," *IEEE Trans. Veh. Technol.*, vol. 41, no. 1, pp. 57–62, Feb. 1992.

Index

List of Publications

International Journals

1. G. Bacci, M. Luise, H. V. Poor, and A. M. Tulino, "Energy-efficient power control in impulse radio UWB wireless networks," *IEEE J. Select. Topics Signal Processing*, vol. 1, no. 3, pp. 508–520, Oct. 2007.

2. G. Bacci, M. Luise, and H. V. Poor, "Energy-efficient power control is (almost) equivalent for DS-CDMA and TH-UWB," *IEE Electronics Letters*, vol. 44, no. 8, pp. 555–557, 10th Apr. 2008.

3. G. Bacci, M. Luise, and H. V. Poor, "Game theory and power control in ultrawideband networks," *Physical Communication*, vol. 1, no. 1, pp. 21–39, 1st Quarter 2008.

4. G. Bacci, M. Luise, and H. V. Poor, "Performance of rake receivers in IR UWB networks using energy-efficient power control," *IEEE Trans. Wireless Commun.*, to appear.

International Conferences

5. G. Bacci, F. Principe, M. Luise, M. Casucci, and M.C. Terzi, "SOFT-REC: A GPS real-time software receiver with EGNOS augmentation," in *Proc. ESA Workshop on EGNOS Performance and Applications*, Gdynia, Poland, Oct. 2005. (best paper award of the plenary session "Applications and Tools - p. 2")

6. G. Bacci and M. Luise, "A new set of spreading sequences that improves time-delay estimation in satellite positioning," in *Proc. IST Mobile & Wireless Commun. Summit*, Mykonos, Greece, June 2006.

7. G. Bacci and M. Luise, "Minimizing the delay estimation error of a spread spectrum signal for satellite positioning," in *Proc. European Signal Processing Conference (EUSIPCO)*, Florence, Italy, Sept. 2006.

8. G. Bacci, M. Luise, and F. Zanier, "Signal-in-space design criteria for next generation satellite positioning," in *Proc. ESA Int. Workshop on Signal Processing for Space Communications (SPSC)*, Noordwijk, The Netherlands, Sept. 2006.

9. F. Zanier, G. Bacci, and M. Luise, "Nonbinary bandlimited signature waveforms for spread spectrum signals with application to satellite positioning," in *Proc. ESA Workshop on Satellite Navigation User Equipment Technologies (NAVITEC)*, Noordwijk, The Netherlands, Dec. 2006.

10. G. Bacci, M. Luise, and H. V. Poor, "Game-theoretic power control in impulse radio UWB wireless networks," in *Proc. European Wireless Conference*, Paris, France, Apr. 2007.

11. G. Bacci, M. Luise, and H. V. Poor, "Game-theoretic analysis of energy efficiency in multiuser impulse radio systems," *IEEE Communication Theory Workshop (CTW)*, Sedona, AZ, United States, May 2007 (invited talk).

12. F. Zanier, G. Bacci, and M. Luise, "Non-binary spread spectrum signals with good delay-tracking features for satellite positioning," in *Proc. Int. Waveform Diversity and Design Conference (WDD)*, Pisa, Italy, June 2007. (best student paper award)

13. G. Bacci, M. Luise, and H. V. Poor, "Large system analysis of game-theoretic power control in UWB wireless networks with rake receivers," in *Proc. IEEE Int. Workshop on Signal Processing Advances for Wireless Communications (SPAWC)*, Helsinki, Finland, June 2007.

14. G. Bacci, M. Luise, and H. V. Poor, "Performance comparison of energy-efficient power control for CDMA and multiuser UWB networks," in *Proc. IST Mobile & Wireless Commun. Summit*, Budapest, Hungary, July 2007.

15. G. Bacci, M. Luise, and H. V. Poor, "Game theory and resource allocation in wireless communications," in *Proc. Joint Workshop on Coding and Communications (JWCC)*, Dürnstein, Austria, Oct. 2007 (invited paper).

16. V. Pellegrini, G. Bacci, and M. Luise, "SOFT-DVB: A fully-software GNURadio-based ETSI DVB-T modulator," in *Proc. Karlsruhe Workshop on Software Radios (WSR)*, Karlsruhe, Germany, Mar. 2008.

17. G. Bacci, *et al.*, "SORGENS: A satellite payload for future navigation and communication missions," in *Proc. European Navigation Conference (ENC-GNSS)*, Toulouse, France, Apr. 2008.

18. F. Zanier, G. Bacci, M. Luise, and M. Crisci, "Multipath resistance for non-binary DS/SS signals with good delay-tracking features for satellite positioning," in *Proc. European Navigation Conference (ENC-GNSS)*, Toulouse, France, Apr. 2008.

National Conferences

19. G. Bacci, M. Luise, and H. V. Poor, "Performance of noncooperative power control techniques for UWB wireless networks," in *Riunione Annuale GTTI*, Rome, Italy, June 2007.